NASA CONTRACTOR REPORT

NASA CR-1210

AN APPLICATION OF SIMILITUDE TO MODEL DESIGN OF A SOIL-PROJECTILE SYSTEM

by Katsuyuki Awoshika and William R. Cox

Prepared by
THE UNIVERSITY OF TEXAS AT AUSTIN
Austin, Texas
for Langley Research Center

NATIONAL AERONAUTICS AND SPACE ADMINISTRATION • WASHINGTON, D. C. • NOVEMBER 1968

NASA CR-1210

AN APPLICATION OF SIMILITUDE TO MODEL DESIGN OF A SOIL-PROJECTILE SYSTEM

By Katsuyuki Awoshika and William R. Cox

Prepared under Grant No. NsG-604 by
THE UNIVERSITY OF TEXAS AT AUSTIN
Austin, Texas

for Langley Research Center

NATIONAL AERONAUTICS AND SPACE ADMINISTRATION

For sale by the Clearinghouse for Federal Scientific and Technical Information
Springfield, Virginia 22151 – CFSTI price $3.00

PREFACE

The research work described in this report was conducted at The University of Texas under sponsorship of Grant NsG-604 from the National Aeronautics and Space Administration, Langley Research Center, Hampton, Virginia. Mr. M. E. Hathaway of Langley's Space Structures Branch, Impacting Structures Section, was technical monitor for the Grant. This is one of several reports which have been issued under sponsorship of Grant NsG-604.

The study was done under the direction of Dr. William R. Cox, Assistant Professor of the Department of Civil Engineering. Dr. Carl W. Morgan, Associate Professor of the Department of Civil Engineering, reviewed the manuscript. Mr. Paul A. Hustad, graduate student, and Mr. Olen L. Hudson, Technical Staff Assistant, made significant contributions to the field testing.

ABSTRACT

A model design by means of similitude, or dimensional analysis, was made for the simulation of a space capsule landing on soils. In order to examine the validity of the model design for sands, a series of cone model tests was carried out on Ottawa Sand and Colorado River Sand. The weights of cone models were 43.0 and 129.5 pounds. The impact velocity of models was in the relatively low range of 10 to 23 fps. The validity was checked by examining the agreement of the measured variables from one of the models with the prediction of variables from the other model. The results were satisfactory.

A model design law is discussed for clayey soils impacted with projectiles consisting of a circular plate, a wedge, and a sphere. The application of this model design law to vertical impact tests of a circular plate, a cone and a sphere on a clay was examined.

TABLE OF CONTENTS

SYMBOLS AND NOTATIONS

a	Maximum acceleration on a projectile, g
$a(t)$	Acceleration record from an accelerometer
c	Cohesion of a soil, psi
d	Penetration depth of a projectile, inch
D_{10}	Effective diameter of soil particles, inch
E	Bulk modulus of a soil, psi
F	Force
g	Gravitational acceleration, ft/sec^2
L	Length
ℓ_1	First characteristic length, inch
ℓ_2	Second characteristic length, inch
m	Subscript that signifies model
m	Mass of a projectile, slug
n	Length scale
p	Subscript that signifies prototype
S	Degree of saturation of a soil
t	Rise time of impact, msec
T	Time
v	Impact velocity of a projectile, fps
w	Water content, percent
α	Distortion factor
δ	Prediction factor
δ_1	Prediction factor for maximum acceleration
δ_2	Prediction factor for penetration
θ	Apex angle of a cone or a wedge, degree

λ_a	Scale factor for acceleration
λ_d	Scale factor for penetration
λ_g	Scale factor for gravitational acceleration
λ_ℓ	Length scale
λ_m	Scale factor for mass
λ_t	Scale factor for time
λ_v	Scale factor for velocity
μ	Frictional factor between a soil and a projectile
π	π term
ρ	Mass density of a soil, slug/ft^3
ϕ	Internal angle of friction of a soil, degree

LIST OF FIGURES

LIST OF TABLES

CHAPTER I

INTRODUCTION

1.1 GENERAL

The system of space capsules impacting earth constitutes one region in a large series of projectile-target systems. The fundamental interaction mechanism between the projectile and the soil target is dependent on the initial and boundary conditions. For instance, the phenomenon ranges from hyper-velocity impact which results in thermal effects and crater formation in soil to low velocity impact which results in elastic displacement of soil. Also, the mechanism is affected greatly by the geometric shape of the projectile. These facts suggest that it is extremely difficult, if not impossible, to set up one general rule applicable to every phenomenon. It is a more practical approach to limit the problem within the range of immediate attention.

In an attempt to develop proper prediction methods for the behavior of space capsules impacting on soil, a series of model tests have been carried out at The University of Texas.

Reese et al[16] carried out vertical drop tests of spherical models on partially saturated sandy clay. In this study, the general behavior of projectiles impacting soils was brought to light. As a prediction means, the application of similitude to modeling was tried. A set of experimental equations expressing the modulus of soil and the maximum force was derived to predict the prototype behavior.

Poor[15] investigated the dynamic response of plates, spheres, and cones during vertical impact on a sandy clay. Poor derived empirical formulas of the modulus of deformation of soil from force-deformation relationships. Using this modulus of deformation, the behavior of a prototype was predicted by extrapolation.

Reichmuth[17] studied inclined impact of wedges, cylinders and spheres on sands and clay. Reichmuth proposed three methods for predicting impact response. The first method uses a scaled model for the direct measurement of acceleration. The second method employs empirical predictions consisting of pertinent primary variables. The third method is based on a three-phase earth-materials diagram for the immediate determination of dynamic response.

Objectives

The present study endeavors to establish, by means of the theory of similitude, or dimensional analysis, a model law for impact of rigid bodies impacting on sands and clay. The model designed by this law should predict the prototype behavior with permissible error. The validity of the model law for sand is checked by using a two-models system in which one model is regarded as the prototype of the other model. It is also a main purpose of this study to explore difficulties in the modeling of soils. The study was also extended to clay. The feasibility of modeling by similitude was checked by making use of model tests.

Scope of Study

The scope of this study is limited to vertical impact of rigid projectiles on typical soils. The impact results in penetration of the projectile into the soil. The penetration, however, is not so great as to bury the projectiles. The vertical impact tests of cones, which were used to check the validity of model law for sand, were carried out for dry-dense, dry-loose and saturated-dense states of Ottawa Sand and Colorado River Sand. The impact velocity of this test ranged from 10 to 23 fps.

1.2 SOILS AS TARGET MATERIAL

Phenomenology

It is important to emphasize the need for an accurate definition of the physical system in order to develop a correct dimensional analysis. The modeling of soils for problems in soil dynamics is challenging because soils in nature have large differences in physical and chemical properties. Moreover, it is difficult to determine for each soil which physical properties are significant in soil dynamics. At one range of impact velocities one group of soil properties may be significant whereas at a different range in impact velocities another group of soil properties may become significant.

The varieties of soils which are found on the earth's surface may range between those which resemble a solid rock to those which resemble a viscous fluid. The real soil is neither homogenous nor isotropic. In order to make a theoretical treatment of this material, some idealization and generalization are desirable.

A soil may be regarded as a material of three phases: solid, air and water. The strength and modulus of deformation of soil depend on:

1. type, shape, and distribution of the solid particles,
2. structural arrangement of the solid particles,
3. chemical properties of the solid particles,
4. air and water content,
5. mass density,
6. original confining pressure,
7. loading rate,
8. stresses caused by the loading element, and
9. size of loading element.

The system of projectile and soil target can be classified into three groups:

A. Non-Penetrating Projectile

The projectile does not penetrate the surface. It may rebound from the surface or crash. The impact of a relatively soft projectile on solid rocks may correspond to this case. This group is not examined in this study.

B. Penetrating Projectile

If the projectile is rigid compared with the soil strength, then it will penetrate the soil by shearing, pulverizing and compressing the soil. A certain amount of the energy of a projectile will be lost to generation of heat, generation of sound waves, and the generation of two radial and two surface waves in the soil body.

One of the body waves that oscillates in the radial direction is the compressive wave and the other is the shear wave. One of the two surface waves is the Love wave or the surface shear wave, in which the particles of soil move in a path parallel to the surface of the earth and at right angles to the direction of propogation. The second surface wave is the Rayleigh wave which causes the ripple movement of the earth surface by its eliptical movement with its long axis perpendicular to the earth surface.

The cubical compressibility of water is 3.4×10^{-6} sq. in. per lb. The compressibility of soil grains is of the order 1×10^{-7} to 2×10^{-7} sq. in. per lb. Both water and soil grains may be regarded as incompressible. The soil structure of dry and half-saturated soil is compressible. Saturated soils are essentially incompressible during rapid loading, since the water does not have enough time to drain out. Pulverization is expected to occur during projectile entry into soils composed of large particles such as gravel,

size range 200 to 2 mm and sand, size range 2 to 0.06 mm. The particle size of silt ranges from 0.06 mm to 0.002 mm and clay particle sizes are smaller than 0.002 mm. It may be assumed that there is no pulverization in silt and clay.

The shock of impact in sand may cause dilatancy. If its density is greater than the critical density, its volume increases upon impact, and, if its density is smaller than the critical density, then its volume decreases. Critical density is defined as a transitional density at which there is no volume change of sand during shear. It is also assumed that waves generated by the impact will change the soil structure, especially of loose unsaturated sand.

It may be assumed that the penetration mechanism is mainly dependent on the shear strength of soils. The shear strength of soil is greatly influenced by water content and soils found in nature have, almost without exception, some water. Therefore, the study of saturated soils, as the extreme case of water content, is as important as the study of dry soils.

C. Impact in Water

Impact in water is another boundary limit of the projectile-soil target problem. It is associated with such soils as newly formed and highly saturated alluvial soils. Upon impact a projectile is subjected to the combined effects of compression wave forces due to the incompressibility and the viscosity of the water. The compression wave is a function of mass density of water. A projectile is first met with deceleration after impact until the projectile reaches the constant terminal velocity. The most important indexes of this case are the Reynolds number and the Froude number.

1.3 MODEL DESIGN LAW

1.3.1 General

The theory of similitude, on which model design and analysis are based, is developed by dimensional analysis. Dimensional analysis is the science of characteristic generalized variables that are involved in a physical phenomenon and is the method of deriving and applying these variables by means of dimensional relationships existing among the pertinent variables.

According to Murphy[12] dimensional analysis is based on the following two axioms:

Axiom 1. Absolute numerical equality of quantities may exist only when the quantities are similar qualitatively.

Axiom 2. The ratio of the magnitudes of two like quantities is independent of the units used in their measurements, provided that the same units are used for evaluating each.

The theoretical significance of model design based on the similitude is given by Gukhman[6] as follows. Let us consider the solution of an equation

$$F(x_1, x_2, \ldots, x_n) = 0 \tag{1.1}$$

where F denotes a function of any arbitrary type, and $x_1, x_2, \ldots, x_n$ are the independent variables, unknown variables and parameters that describe the problem.

Now let us carry out similar transformation of all the quantities by multiplying each one of them with different constants k_i. If the equation is to remain unchanged,

$$F(k_1x_1, k_2x_2, \ldots, k_nx_n) = 0. \tag{1.2}$$

Since the constants k_i are independent of quantities x_i, the necessary condition for satisfying both Eqs 1.1 and 1.2 is,

$$F(k_1x_1, k_2x_2, \ldots, k_nx_n) = \phi(k_1, k_2, \ldots, k_n) \times F(x_1, x_2, \ldots, x_n). \qquad (1.3)$$

Equation 1.3 indicates that the function F possesses the special property that a similar transformation of the individual variables leads to a similar transformation of the function as a whole. That is to say the function F is homogeneous.

Then the form of function F is limited to a special form.

Denoting $x_i' = k_i x_i$, Eq 1.3 is expressed in a contracted form,

$$F\left[x_i'\right] = \phi\left[k_i\right] F\left[x_i\right]$$

where $[\ ]$ denotes "all of x_i".

Differentiating the above equation with respect to one of the k_i, for example, with respect to k_1,

$$\frac{\partial F\left[x_i'\right]}{\partial k_1} = \frac{\partial \phi}{\partial k_1} F\left[x_i\right].$$

However,

$$\frac{\partial F\left[x_i'\right]}{\partial k_1} = \frac{\partial F\left[x_i'\right]}{\partial x_1'} \cdot \frac{\partial x_1'}{\partial k_1} = \frac{\partial F\left[x_i'\right]}{\partial x_1'} \cdot x_1.$$

Therefore,

$$\frac{\partial F\left[x_i'\right]}{\partial x_1'} x_1 = \frac{\partial \phi}{\partial k_1} F\left[x_i\right].$$

All these relationships are valid for any values of the factors k_i. The previous equation then assumes the form,

$$x_1 \frac{\partial F\left[x_i\right]}{\partial x_1} = F\left[x_i\right] \left| \frac{\partial \phi}{\partial k_1} \right|_{\left[k_i\right]}.$$

But

$$\left| \frac{\partial \phi}{\partial k_1} \right|_{\left[k_i\right]} = a_1,$$

where a_1 is some constant. Substituting this value in the previous equation,

$$x_1 \frac{\partial F}{\partial x_1} = a_1 F$$

or

$$\frac{1}{F} \frac{\partial F}{\partial x_1} = \frac{a_1}{x_1}$$

$$F = C_1 x_1^{a_1} \tag{1.4}$$

Here C_1 is a quantity which depends on all the remaining variables except x_1.

By repeating this treatment for all the variables in turn, we finally find

$$F = C_1 x_1^{a_1} x_2^{a_2} \ldots\ldots x_n^{a_n}, \tag{1.5}$$

where C is a constant.

Thus the function F has to be represented by a power group, which is a too stringent limitation to use for any analytical work.

The introduction of power groups as the new variables, however, enables the similar transformation without any restrictions to the structure of the function F.

Equation 1.3 is unconditionally satisfied, if $k_1 = k_2 = \ldots = k_n = 1$. This is a quite trivial case, since it merely signifies two identical phenomena. Nevertheless this condition plays an important role for the new variables.

Let us form new variables P_j as a homogeneous function of variables x_i,

$$P(x_i) = C\, x_1^{a_1} x_2^{a_2} \ldots x_n^{a_n}. \tag{1.6}$$

Carrying out a similar transformation of the variables x_i, the new transformation factors for the variables P_j, K_j is constructed,

$$\left.\begin{aligned} P_j(k_i x_i) &= C\,(k_1^{a_1} k_2^{a_2} \ldots k_n^{a_n})\, x_1^{a_1} x_2^{a_2} \ldots x_n^{a_n} \\ K_j &= k_1^{a_1} k_2^{a_2} \ldots k_n^{a_n}, \end{aligned}\right\} \tag{1.7}$$

where K_j are also any arbitrary constants.

Using each of the power groups contained in the function, Eq 1.1 is rewritten,

$$F(x_1, x_2, \ldots, x_n) = P_0\, \phi(P_1, P_2, \ldots, P_r), \tag{1.8}$$

where P_0 is the common part of P_j. Naturally, in the general case the number of r is less than n. The nontrivial solution of $F(x_i) = 0$ is reduced to the solution of

$$\phi(P_1, P_2, \ldots, P_r) = 0. \tag{1.9}$$

The necessary and sufficient condition of invariant equation, $K_j = 1$, is no more trivial.

The dimensional way of deriving the power terms out of primary variables is none other than the Buckingham π Theorem.

1.3.2 Buckingham π Theorem

Buckingham π Theorem is summarized by the statement that the number of dimensionless products in a complete set is equal to the total number of variables minus the number of fundamental dimensions in the problem, or as it was put more rigorously by Langhaar[10], the number of dimensionless products in a complete set is equal to the total number of variables minus the maximum number of these variables that will not form a dimensionless product. That is, if a phenomenon involving n physical quantities, $x_1, x_2, \ldots, x_n$, is expressed by an equation,

$$F(x_1, x_2, \ldots, x_n) = 0 \tag{1.10}$$

and the number of fundamental quantities constituting these n variables is m, then the above equation is transformed to,

$$\phi(\pi_1, \pi_2, \ldots, \pi_{n-m}) = 0, \tag{1.11}$$

where $\pi_1, \pi_2, \ldots, \pi_{n-m}$ are the independent dimensionless products consisting of less than $m + 1$ variables out of n. π terms are generally expressed as,

$$\pi_1 (x_1, x_2, \ldots, x_m, x_{m+1})$$

$$\pi_2 (x_1, x_2, \ldots, x_m, x_{m+2})$$

. . .

$$\ldots$$

$$\pi_{n-m}\,(x_1, x_2, \ldots, x_m, x_n).$$

Other π terms may be obtained by combining the above π terms.

Solving the last equation for the π terms yields

$$\left.\begin{aligned} \pi_1 &= \theta_1\,(\pi_2, \pi_3, \ldots, \pi_{n-m}) \\ \pi_2 &= \theta_2\,(\pi_1, \pi_3, \pi_4, \ldots, \pi_{n-m}) \\ &\ldots\ldots \\ \pi_{n-m} &= \theta_{n-m}\,(\pi_1, \pi_2, \ldots, \pi_{n-m+1}). \end{aligned}\right\} \quad (1.12)$$

Since these are the general relationships applicable to an array of combinations for a phenomenon, these are applied to both the prototype and its model:

$$\left.\begin{aligned} \pi_{1p} &= \pi_{1m} \\ \pi_{2p} &= \pi_{pm} \\ &\ldots\ldots \\ \pi_{(n-m)p} &= \pi_{(n-m)m} \end{aligned}\right\} \quad (1.13)$$

where suffix p refers to prototype and m to model. These equations are used both for specifying the design conditions and test methods of models and for predicting the behavior of prototypes.

1.3.3 Calculation of π Terms

Any dimensionless product, π, of n variables, x_i, has the form,

$$\pi = x_1^{\alpha}\, x_2^{\beta}\, x_3^{\gamma} \ldots x_n^{\nu}, \quad (1.14)$$

where α, β, γ, ..., ν are exponents.

Dimensionless products π are reduced to the solution of the linear algebraic equations,

$$\left.\begin{aligned} &\alpha\,\alpha_1 + \beta\,\beta_1 + \gamma\,\gamma_1 + \ldots + \nu\,\nu_1 = 0 \\ &\alpha\,\alpha_2 + \beta\,\beta_2 + \gamma\,\gamma_2 + \ldots + \nu\,\nu_2 = 0 \\ &\qquad\ldots\ldots \qquad\qquad \ldots\ldots \\ &\alpha\,\alpha_m + \beta\,\beta_m + \gamma\,\gamma_m + \ldots + \nu\,\nu_m = 0 \end{aligned}\right\} \quad (1.15)$$

where m is the number of fundamental quantities. There are m equations each containing n terms at most.

The matrix of the coefficients is

$$\begin{pmatrix} \alpha_1 & \beta_1 & \gamma_1 & \ldots & \nu_1 \\ \alpha_2 & \beta_2 & \gamma_2 & \ldots & \nu_2 \\ \cdot & & & & \cdot \\ \cdot & & & & \cdot \\ \cdot & & & & \cdot \\ \alpha_m & \beta_m & \gamma_m & \ldots & \nu_m \end{pmatrix}$$

If the rank of this matrix is m, then the values of $n - m$ unknowns may be assigned arbitrarily and the others will be uniquely determined. Hence there will be $n - m$ independent sets of solutions to Eq 1.15. Then these determine the products $\pi_1, \pi_2, \pi_3, \ldots, \pi_{n-m}$. If the rank of the matrix is $m - 1$, then the number of dimensionless products π will be $n - m + 1$.

CHAPTER II

MODEL DESIGN BY DYNAMIC SIMILITUDE

2.1 GENERAL

In order to achieve complete similitude, the model must be constructed and tested in such a way as to comply with the conditions of

a. Geometric similarity. Constant ratio between all corresponding lengths in model and prototype.

b. Mechanical similarity. Proportionality of weight and density between the two systems.

c. Kinematic similarity. Proportionality between the two systems in regard to all corresponding time and time intervals.

d. Dynamic similarity. Proportionality of all the forces in the system.

Considering these restrictions, it is reasonable to start the study with the simplest system. A more complex and physically realistic system can be investigated with a little modification once a satisfactory model design method is developed for a relatively simple system.

For the sake of simplicity and avoiding complex factors, a cone was selected as a model of an impacting body on soil targets. A cone has the advantage of making a model of any length scale out of one cone so long as its penetration does not exceed its height. The apex angle of the cone was arbitrarily chosen as 60 degrees. This acute angle was found out later to cause difficulty in getting exact vertical penetration. The ratio of weight or mass of two models was chosen approximately 1 to 3. It is desirable to get as large mass ratio as possible to get a significant length scale. As it is stated later, mass scale of 3 corresponds to 1.44 length scale.

The models were dropped vertically, although the actual impact of the prototype may have up to 20 or 30 degrees of tilting of the incidence angle from the vertical.

The correlation between the dynamic behavior of soils subjected to impact of a projectile and the conventionally determined static properties of soils has not yet come to light. This leads to the immediate difficulty of selecting the proper properties of soils as test conditions. For this reason it seems to be justifiable to use the identical soil for both the prototype and the model.

The greatest advantage of using sand lies in the relative easiness of preparing and reproducing the homogeneous and controlled state. The necessary amount of sand can be carried to any place where it is most convenient to do the tests. Further, according to Whitman[23], there is no effect of strain rate on the angle of internal friction of sand. This suggests the possibility of application of static sand properties to its dynamic behavior. For these reasons sands were chosen as target material.

2.2 PERTINENT VARIABLES

Choosing the correct and sufficient number of variables is the most critical phase of dimensional analysis. There should be as few variables as possible to avoid nonessential complexity, and yet there must be sufficient number of variables to represent the phenomenon. The infallible choice of variables depends primarily on the clear physical concept of the phenomenon, which may be attained by deep insight or experiences. This is especially true in soil dynamics, where the properties of material is not easy to define and determine.

2.2.1 Interaction Mechanism Between Projectile and Soil

It is duly assumed that the dynamic penetration of a rigid body into soil also follows the movement pattern similar to that of static penetration. The mechanism of static penetration is often approximated in soil mechanics by Prandtl's theory. Prandtl's theory considers plastic equilibrium in describing the penetration of hard bodies into another softer, homogeneous, anisotropic material. In his analysis of the penetration problem, Prandtl assumed a shape of rupture surface consisted of arcs of logarithmic spirals and lines tangent to the spirals. The ultimate static bearing capacity of the hard body is obtained in terms of the angle of internal friction and cohesion of the softer body and the size or width of the hard body.

Observation of model impact tests on sands suggests the occurrence of a mechanism similar to Prandtl's mechanism. A circular heaving of the sand surface was observed extending a cone diameter in the horizontal direction at the ground level. In the case of dry sand, splashing of sand was seen which on a slow motion movie looked similar to the splashing of water. The dynamic penetration brings into play other effects than the plastic equilibrium between the static forces. When the impact velocity is low, the problem might be dealt with by a modification of static theory. As the impact velocity increases, the effect of mass of soil within the moving soil wedge becomes more apparent, and consequently the strain-rate-effect on soil strength may become greater. Even the basic material property of soil strength may change its character at still higher impact velocities. For the time being, it is convenient to treat the dynamic soil strength in terms of static soil strength. The dynamic strength of a soil is then dealt with by the concept of strain-rate-effect.

The strain-rate-effect on the shear strength of a soil must be dependent on the constitutive properties of soil and the boundary conditions of the system. The constitutive properties that affect the shear strength of a soil include: (a) particle type, size and shape, (b) grain size distribution and degree of cementation, (c) void ratio, (d) mass density, (e) water content, and (f) drainage rate. Normally a soil bed in nature approaches a semi-infinite body with horizontal surface. The sand bed used in this test was bounded by three hard clay walls. The test sand bed can be regarded as semi-infinite if the effect of propogation of shock waves on soil strength is not significant. The distance from the point of impact to the nearest boundary was at least more than two times the maximum penetration. The extent of area of heaving of sand due to impact was limited to about as much as the penetration depth from the edge of the cavity formed by the penetration of a projectile.

The surface condition of a model must also affect the dynamic penetration process[19]. The magnitude of frictional force between the metal surface of a model and the soil is one of the influential factors of forming the shape of soil wedge upon impact.

To sum up, the movement of a model during impact is expressed by a general equation of motion

$$m \frac{d^2x}{dt^2} + mg = F\ (x,\ m,\ v,\ \theta,\ \mu,\ c,\ \phi,\ \rho,\ D_{10},\ E,\ S,\ \ldots.)$$

where F is the reaction of soil bed and function of such various parameters as penetration depth x, mass of projectile m, impact velocity v, factor of geometric shape θ, factor of friction between projectile and soil μ, cohesion of soil c, angle of internal friction of soil ϕ, mass density of

soil ρ, effective grain size of soil D_{10}*, bulk modulus of soil E, degree of saturation of soil S, and other pertinent soil properties.

2.2.2 Summary of Pertinent Variables

The following properties of a soil are assumed to have immediate effect on the soil-projectile interaction process. The degree of contribution of each variable to the phenomenon may vary from case to case.

Variables	Symbol	Unit	Dimension
1. Cohesion of a soil	c	psi	FL^{-2}
2. Angle of internal friction of a soil	ϕ	degree	none
3. Effective size of soil particles	D_{10}	in.	L
4. Wet mass density of a soil	ρ	$slug/ft^3$	$FL^{-4}T^2$
5. Bulk modulus of a soil	E	psi	FL^{-2}
6. Degree of saturation of a soil	S	percent	none

The variables that define the geometrical, dynamic, and operational conditions of a cone model are,

Variables	Symbol	Unit	Dimension
7. Apex angle of a cone	θ	degree	none
8. Penetration depth of a cone	d	in.	L
9. Mass of a cone	m	slug	$FL^{-1}T^2$
10. Impact velocity of a cone	v	fps	LT^{-1}
11. Maximum acceleration during impact	a	ft/sec^2	LT^{-2}
12. Rise time of impact	t	msec	T
13. Gravitational acceleration	g	ft/sec^2	LT^{-2}
14. Factor of friction of cone surface	μ	none	none

*D_{10} is the effective diameter of soil particles, which means 10 percent of the soil particles are finer than this size.

The model is considered a rigid body and its elastic properties are neglected.

2.3 DERIVATION OF π TERMS

Let us assume that the soil projectile interaction is expressed by a function in terms of variables in the preceding section,

$$f\ (c,\ \phi,\ D_{10},\ \rho,\ E,\ S,\ \theta,\ d,\ m,\ v,\ a,\ t,\ g,\ \mu) = 0 \qquad (2.1)$$

Among these variables ϕ, S, θ, and μ are dimensionless. D_{10} and d have the same dimension, then one of the dimensionless products can be $\frac{D_{10}}{d}$. a and g also have the same dimension, therefore a dimensionless variable $\frac{a}{g}$ is made. Likewise c and E have the same dimension and a dimensionless product $\frac{E}{c}$ is formed. Excluding a, ϕ, S, θ, D_{10}, and E, the rest of the dimensional products are expressed in a general form,

$$\pi = c^{k_1}\ \rho^{k_2}\ d^{k_3}\ m^{k_4}\ v^{k_5}\ g^{k_6}\ t^{k_7}$$

$$= (FL^{-2})^{k_1}\ (FL^{-4}T^2)^{k_2}\ (L)^{k_3}\ (FL^{-1}T^2)^{k_4}\ (LT^{-1})^{k_5}\ (LT^{-2})^{k_6}\ (T)^{k_7}$$

This expression is resolved into three component auxiliary equations with respect to three basic dimensions.

$$\left.\begin{array}{ll} F & 0 = k_1 + k_2 + k_4 \\ L & 0 = -2k_1\ -4k_2 + k_3 - k_4 + k_5 + k_6 \\ T & 0 = 2k_2 + 2k_4 - k_5 - 2k_6 + k_7 \end{array}\right\} \qquad (2.2)$$

The dimensional matrix made of coefficients of the above equations is,

$$\begin{array}{ccccccc} k_1 & k_2 & k_3 & k_4 & k_5 & k_6 & k_7 \\ \left[\begin{array}{ccccccc} 1 & 1 & 0 & 1 & 0 & 0 & 0 \\ -2 & -4 & 1 & -1 & 1 & 1 & 0 \\ 0 & 2 & 0 & 2 & -1 & -2 & 1 \end{array}\right]. \end{array}$$

The determinant of the first three column is,

$$\begin{vmatrix} 1 & 1 & 0 \\ -2 & -4 & 1 \\ 0 & 2 & 0 \end{vmatrix} = -2 \ (\neq 0)$$

Then this matrix is rank 3, and the number of dimensionless products is 7 - 3 = 4. There are seven unknowns in Eq 2.2 and there are three equations, so any four unknowns can be assigned any arbitrary value to determine the rest of the three unknowns.

(1) If $k_1 = 1$, $k_3 = k_6 = k_7 = 0$

$k_2 = -1$, $k_4 = 0$, and $k_5 = -2$.

Then

$$\pi_1 = \frac{c}{\rho v^2}$$

(2) If $k_3 = 1$, $k_1 = k_6 = k_7 = 0$

$k_2 = 1/3$, $k_4 = -1/3$, and $k_5 = 0$.

Then

$$\pi_2 = \left(\frac{\rho}{m}\right)^{1/3} d.$$

(3) If $k_6 = 1$, $k_1 = k_3 = k_7 = 0$,

$k_2 = -1/3$, $k_4 = 1/3$, and $k_5 = -2$.

Then

$$\pi_3 = \left(\frac{m}{\rho} \right)^{1/3} \frac{g}{v^2}.$$

(4) If $k_7 = 1$, $k_1 = k_3 = k_6 = 0$,

$k_2 = 1/3$, $k_4 = -1/3$, and $k_5 = 1$.

Then

$$\pi_4 = \left(\frac{\rho}{m} \right)^{1/3} vt.$$

(5) Combining π_2 and π_3,

$$\pi_5 = \frac{gd}{v^2}.$$

(6) Combining π_3 and π_4,

$$\pi_6 = \frac{gt}{v}.$$

Using π_1, π_2, π_5, and π_6, Eq 2.1 is rewritten,

$$f \left(\frac{c}{\rho v^2}, \left(\frac{\rho}{m} \right)^{1/3} d, \frac{gd}{v^2}, \frac{gt}{v}, \frac{D_{10}}{d}, \frac{a}{g}, \frac{E}{c}, \phi, S, \theta \right) = 0 \qquad (2.3)$$

The term including the bulk modulus E is neglected on the assumption that elastic behavior of soil during impact of a projectile has little effect on the response of the projectile. It is further assumed that the particle size of a soil, the effective size of soil particle D_{10} and the friction between the projectile surface and soil may be neglected.

Then Eq 2.3 is simplified to the form,

$$f\left(\frac{c}{\rho v^2}\left(\frac{\rho}{m}\right)^{1/3} d, \frac{gd}{v^2}, \frac{gt}{v}, \frac{a}{g}, \phi, S, \theta\right) = 0 \qquad (2.4)$$

2.4 MODEL DESIGN FOR VARIOUS GEOMETRIC SHAPES OF PROJECTILE

The conceivable geometric shapes of a projectile are a circular or rectangular flat plate, a wedge, a sphere and a cone. The introduction of characteristic length will enable the model design of a projectile of various shapes. The characteristic lengths of a plate are its width and its length or its radius. The characteristic length of a wedge is its width. The characteristic length of a sphere is its radius. A cone does not have a characteristic length that represents its shape, so long as the penetration does not exceed the cone height.

The characteristic length, ℓ_1, and the penetration depth, d, make a dimensionless variable, $\frac{d}{\ell_1}$. If the number of characteristic length is more than two, the ratios between them make new dimensionless variables. For instance, characteristic lengths ℓ_1 and ℓ_2 make a dimensionless variable, $\frac{\ell_2}{\ell_1}$.

The equation that represents the soil-projectile phenomenon in general form is developed from Eq 2.4.

$$f\left(\frac{c}{\rho v^2}, \left(\frac{\rho}{m}\right)^{1/3} d, \frac{gd}{v^2}, \frac{gt}{v}, \frac{a}{g}, \frac{d}{\ell_1}, \frac{\ell_2}{\ell_1}, \phi, S, \theta\right) = 0 \qquad (2.5)$$

where

ℓ_1 is the first characteristic length, which is

the width of a rectangular plate,

the radius of a circular plate,

the width of a wedge, or

the radius of a sphere,

ℓ_2 is the second characteristic length, which is

the length of a plate, and

θ is the apex angle of a wedge or a cone.

The terms $\frac{d}{\ell_1}$ and $\frac{\ell_2}{\ell_1}$ are neglected for a cone.

The terms $\frac{\ell_2}{\ell_1}$ and θ are neglected for a sphere and a circular plate.

A plate does not require the term of θ. Depending on the nature of the soil, either the angle of internal friction of a soil, ϕ, or the term including the cohesion of a soil, $\frac{c}{\rho v^2}$, may be excluded from the Eq 2.5. As a matter of course the new variables, ℓ_1 and ℓ_2, give the design condition of a model. That is,

$$\frac{\ell_{1p}}{\ell_{1m}} = n \qquad \text{and}$$

$$\frac{\left(\frac{\ell_2}{\ell_1}\right)_p}{\left(\frac{\ell_2}{\ell_1}\right)_m} = 1, \qquad (2.6)$$

where n is the length scale.

2.5 SCALE FACTORS

The major condition or restriction to the model design is the use of the same soil for both the prototype and its model. Another condition is the assumption of the same maximum acceleration on the prototype and the model.

The model designs for the sand and the clay present different features due to the difference of their characteristics. In sand the cohesion is neglected. Hence, the term, $\frac{c}{\rho v^2}$, which contains the cohesion, drops out of

the design condition. On the other hand, the angle of internal friction, ϕ, is omitted in clays.

2.5.1 Sand

Neglecting the term, $\frac{c}{\rho v^2}$, from Eq 2.4, the equation expressing the impact of a cone on a sand is written as Eq 2.7,

$$f\left(\left(\frac{\rho}{m}\right)^{1/3} d, \frac{gd}{v^2}, \frac{gt}{v}, \frac{a}{g}, \phi, S, \theta\right) = 0 \qquad (2.7)$$

It is convenient to establish the model system on a proper length scale. The rest of the scale factors can be derived in terms of the length scale. Let the length scale be,

$$\lambda_\ell = \frac{\text{length in prototype}}{\text{length in model}} = \frac{\ell_p}{\ell_m} = n,$$

where p refers to prototype and m to model. The scale factor for penetration depth is the length scale itself,

$$\lambda_d = \frac{d_p}{d_m} = n$$

The time scale is obtained from the condition of the identical gravitational acceleration,

$$g_p = g_m$$

$$\left(\frac{\ell}{t^2}\right)_p = \left(\frac{\ell}{t^2}\right)_m$$

$$\lambda t = \frac{t_p}{t_m} = \left(\frac{\ell_p}{\ell_m}\right)^{1/2} = \sqrt{n}$$

The condition of the identical gravitational acceleration is only applicable on earth. On another planet, the gravitational acceleration on that particular planet of interest must be the prototype gravitational acceleration g_p.

The dimensionless variable $\frac{gt}{v}$ gives the scale factor of impact velocity,

$$\left(\frac{gt}{v}\right)_p = \left(\frac{gt}{v}\right)_m$$

$$\lambda_v = \frac{v_p}{v_m} = \frac{g_p}{g_m} \cdot \frac{t_p}{t_m} = 1 \cdot \sqrt{n} = \sqrt{n}$$

The dimensionless variable $\left(\frac{\rho}{m}\right)^{1/3} d$ gives the scale factor of the mass of model.

$$\left(\left(\frac{\rho}{m}\right)^{1/3} d\right)_p = \left(\left(\frac{\rho}{m}\right)^{1/3} d\right)_m$$

$$\lambda_m = \frac{m_p}{m_m} = \frac{\rho_p}{\rho_m} \cdot \left(\frac{d_p}{d_m}\right)^3 = 1 \cdot n^3 = n^3,$$

since the mass density of soil is the same for both the prototype and the model.

The design conditions for the internal angle of friction of a soil, ϕ, the degree of saturation of a soil, S, and the apex angle of a cone, θ, are automatically satisfied,

$$\phi_p = \phi_m,$$

$$S_p = S_m,$$

and $$\theta_p = \theta_m.$$

Two weights of cone models were used, one of 129.5 lbs, and the other of 43.0 lbs. Taking the heavy model for the prototype, the scale factor for the mass of a cone projectile is obtained,

$$\lambda_m = n^3 = \frac{m_p}{m_m} = \frac{129.5g}{43.0g} = 3.01.$$

Hence

$$n = 1.44,$$

and

$$\sqrt{n} = 1.20 .$$

The relationships between the primary variables of the prototype, the heavy cone, and its model, the light cone, is summarized as follows.

Variables	Scale Factor	Prototype	Model
Angle of internal friction of a soil, ϕ	1		
Mass density of a soil, ρ	1		
Degree of saturation of a soil, S	1		
Apex angle of a cone, θ	1	60°	60°
Penetration depth of a model, d	n = 1.44		
Mass of a model, m	n^3 = 3.01	129.5 lbs	43.0 lbs
Impact velocity of a model, v	$\sqrt{n}$ = 1.20		
Max. acceleration of a model, a	1		
Gravitational acceleration, g	1		
Rise time of impact, t	$\sqrt{n}$ = 1.20		

2.5.2 Clay

Cone

The impact of a cone on a clay is expressed by Eq 2.8 which is obtained by neglecting the term of angle of internal friction in Eq 2.4.

$$f\left(\frac{c}{\rho v^2}, \left(\frac{\rho}{m}\right)^{1/3} d, \frac{gd}{v^2}, \frac{gt}{v}, \frac{a}{g}, S, \theta\right) = 0 \qquad (2.8)$$

From the test condition, the following relations are satisfied,

Degree of saturation of a soil: $S_p = S_m$

Apex angle of a cone: $\theta_p = \theta_m$

Since the same gravitational acceleration is working on both the prototype and its model,

$$g_p = g_m,$$

so that

$$\lambda_a = \lambda_g = 1. \qquad (2.9)$$

Assuming the basic length scale $\lambda_\ell = n$, the term $\frac{gd}{v^2}$ gives the scale factor for the velocity,

$$\lambda_v = \frac{v_p}{v_m} = \left(\frac{g_p}{g_m}\right)^{1/2} \cdot \left(\frac{d_p}{d_m}\right)^{1/2} = \sqrt{1} \cdot \sqrt{n} = \sqrt{n}\ . \qquad (2.10)$$

The term $\frac{gt}{v}$ gives the time scale,

$$\lambda_t = \frac{v_p}{v_m} \cdot \frac{g_m}{g_p} = \sqrt{n} \cdot 1 = \sqrt{n} \qquad (2.11)$$

The scale factor of the mass of model is derived from the term $\left(\frac{\rho}{m}\right)^{1/3} d$

$$\lambda_m = \frac{m_p}{m_m} = \frac{\rho_p}{\rho_m} \cdot \left(\frac{d_p}{d_m}\right)^3 = 1 \cdot n^3 = n^3\ . \qquad (2.12)$$

All the scaled factors are summarized as follows.

Variables	Scale Factor
Cohesion of a soil, c	1
Wet mass density of a soil, ρ	1
Degree of saturation of a soil, S	1
Apex angle of a cone, θ	1
Penetration depth of a cone, d	n
Mass of a model, m	n^3
Impact velocity of a cone, v	$\sqrt{n}$
Max. acceleration of a cone, a	1
Rise time of impact, t	$\sqrt{n}$

Hereupon, the dimensionless product $\frac{c}{\rho v^2}$ does not satisfy the model law,

$$\left(\frac{c}{\rho v^2}\right)_p = \frac{(\lambda_c\ c_m)}{(\lambda_\rho\ \rho_m) \cdot (\lambda_v\ v_m)^2}$$

$$= \frac{(1 \cdot c_m)}{(1 \cdot \rho_m \cdot (\sqrt{n}\ v_m)^2}$$

$$= \frac{1}{n} \cdot \left(\frac{c_m}{\rho_m\ v_m^2}\right) \left(\neq \left(\frac{c}{\rho v^2}\right)_m \right) . \qquad (2.13)$$

If either the cohesion of a soil, c, or the mass density of a soil can be varied this distortion is avoided. If it is unavoidable, there are two general solutions to this. The one is the experimental way to derive the prediction factor. The other is the theoretical way to compensate the distortion of a dimensionless parameter by adjusting the distortion factors in such a way that the prediction factor becomes unity. The latter method

requires the full knowledge of the equation that expresses the phenomenon to derive the equation of prediction factor and also the free choice of distortion factor of a dimensionless variable, which is not realistic to the present case.

The prediction factor is defined in a general way,

$$\delta = \frac{\pi_{1p}}{\pi_{1m}} = \frac{f\ (\pi_{2p},\ \pi_{3p},\ \ldots,\ \pi_{sp})}{f\ (\alpha\ \pi_{2m},\ \pi_{3m},\ \ldots,\ \pi_{sm}} , \tag{2.14}$$

where δ is the prediction factor and α is the distortion factor of a dimensionless variable π_2.

If the maximum acceleration is of interest, Eq 2.8 is rewritten in the form,

$$\frac{a}{g} = f\left(\frac{c}{\rho v^2},\ \left(\frac{\rho}{m}\right)^{1/3} d,\ \frac{gd}{v^2},\ \frac{gt}{v},\ S,\ \theta\right) = 0 \tag{2.15}$$

and the prediction factor for the π term $\frac{a}{g}$ is

$$\delta = \frac{\left(\frac{a}{g}\right)_p}{\left(\frac{a}{g}\right)_m} = \frac{f\left(\left(\frac{c}{\rho v^2}\right)_p,\ \left(\frac{\rho}{m}\right)_p,\ \ldots\ \theta_p\right)}{f\left(\alpha\left(\frac{c}{\rho v^2}\right)_m,\ \left(\frac{\rho}{m}\right)_m,\ \ldots,\ \theta_m\right)} . \tag{2.16}$$

CHAPTER III

TEST ON SANDS

3.1 GENERAL

The aim of the series of impact tests on sand was to verify the feasibility of modeling the response of an impacting cone. An examination was made of the agreement of predicting behavior of a prototype from experiments with a model. This was done for two different states in each of two sands.

3.2 TEST EQUIPMENT

3.2.1 Launching Device

The launching device designed by Reichmuth[17] was used in this experiment (Fig. 3.1).

The launching device consists of a set of aluminum framing mounted on a pickup truck, a nitrogen thrust system, a wagon that carries the model, and a braking system.

The main part of the framing is a pair of rails made of 14 ft long, 1-1/2 x 2 in. rectangular aluminum tubes. The model is carried by a wagon which rolls down the track formed by these two rails. The top ends of the rails are attached by hinges to a pair of 14 ft long aluminum I beams set upright on a pickup. These hinges can slide along the I beams to position the rails at any angle from vertical to horizontal.

The thrust system at the upper end of the rails is operated by 500 psi high pressure nitrogen. It consists of two pistons with gas to actuate the pistons regulated by a valve to give desired velocity to the model. In the series of tests described in this report the thrust system was not used,

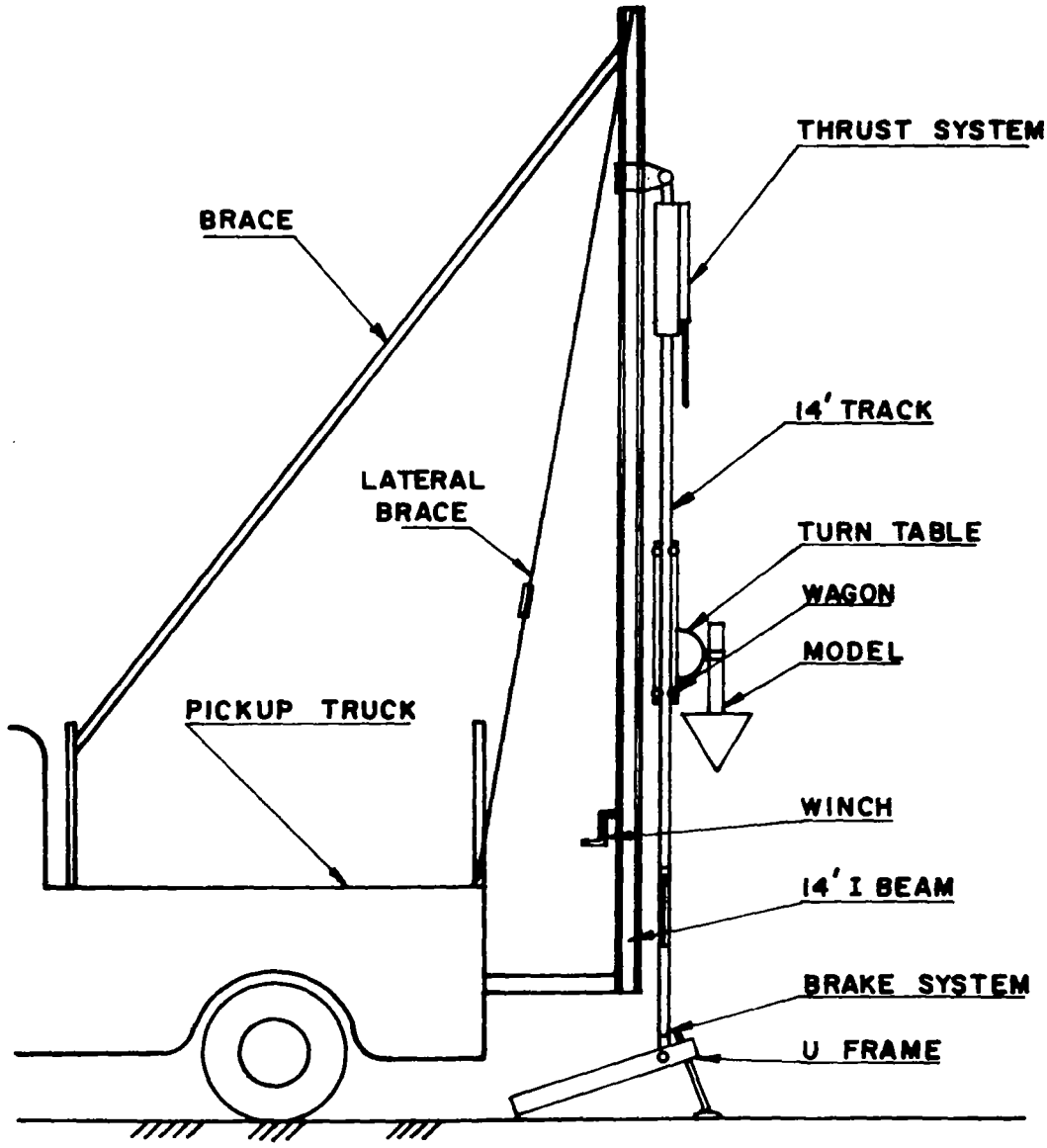

FIG.3.1 LAUNCHING DEVICE SETUP

since the initial velocity was obtained by free fall. The maximum velocity obtained by free fall was 30 fps.

The braking system also consists of two pistons pressured by nitrogen at 10 percent of thrusting pressure or 25 psi, whichever is more.

The wagon holds the model at desired trim angle until model release about 10 inches above the target soil. Before release the wagon is connected to a yoke by a pair of jaws which are released by a solenoid. The yoke may be fastened to any position along the rails to give the desired impact velocity to the model. The jaws of the wagon which hold the model are released also by a solenoid triggered by a cam operated microswitch mounted on the wagon. The cam is attached to one of the rails.

3.2.2 Measuring Instruments

Electrical equipments were used to record the acceleration-time history of the model during impact and the model speed immediately before impact. All electrical equipments used are identical with those used by Reichmuth.

Accelerometers

Two small and lightweight tri-axis accelerometers of Type 4-204 made by Consolidated Electrodynamics were built in the mast of the model along its axis. Each of three accelerometer moduli consists of a four-active-arm, spring type unbonded strain gage element and a seismic mass damped by the shear action of a viscous fluid. The maximum acceleration ranges were 250 g's for both vertical and rotational direction and 100 g's for transverse direction. The accelerometer modules for vertical and rotational directions were calibrated for 200 g's. This calibrated value was about 10 times of the working range. The full range output for all three axes was approximately

40 millivolts at the rated excitation of 5 volts DC. The natural frequency of each accelerometer modules ranged between 1300 and 1600 cycles per second.

In order to avoid the disturbance on record due to the natural frequency of the accelerometer, symmetrical "parallel T" filter circuits having a theoretical infinite attenuation at a frequency of 1540 cycles per second were added to the vertical and rotational accelerometers. The frequencies of impact impulse ranged between 20 and 30 cycles per second.

A type 565 dual beam Tektronix oscilloscope having two type 3A3 dual trace differential vertical amplifiers was used to record the acceleration-time curve. A Tektronix Type C12 camera took instantaneous 3-1/4 x 4-1/4 in. Polaroid pictures of oscilloscope screen images.

A one and a half KVA generator driven by a gasoline engine was used to supply 110 volts AC power for the oscilloscopes and DC power for the accelerometers. A Harrison Labs Model 6204A rectifier was employed for rectifying and transforming of the 5 volts DC power for the accelerators. This voltage was regulated manually by the operator before each test.

Velocity Detector

The model velocity was obtained by measuring the speed of the wagon immediately before model release. The point of velocity measurement was about two feet above the target sand bed.

The velocity detector consists of an oscilloscope triggering circuit and a series parallel circuit having four music-wire contacts at two in. intervals that are opened in succession by an outrigger protruding from the falling wagon.

A type 502A dual beam Tektronix oscilloscope gives the voltage steps and time relation. The oscilloscope screen image was also recorded on a 3-1/4 x 4-1/4 in. Polaroid film.

3.2.3 Models

The monolithic aluminum cone was formed by casting (Figs. 3.2 and 3.3). The cone is 12 in. high and has an apex angle of 60 degrees. Its wall and cross ribs have 1/2 in. thickness. In the center of the cone a 3 x 3 in. mast was fixed inside a bracket formed by 1/2 in. thick aluminum plates. The mast consists of two pieces of 3 x 1.5 in. solid aluminum bar in which two accelerometers are encased. At the upper part of the mast there are two grooves for the jaws of the release mechanism. The light cone weighs 43.0 lbs. In order to obtain a heavy cone, two steel discs of 1 and 2 in. thickness were added on the base of the cone. The heavy model weighs 129.5 lbs.

3.3 SAND BEDS

Two widely different types of sands were tested in dry-loose, dry-dense and saturated-dense states. The one type of sand is a standard Ottawa Sand and the other is a Colorado River Sand obtained locally in Austin, Texas.

The Ottawa Sand is a poorly graded, fine, white sand consisting of round particles of silica. Referring to the work of Reichmuth[17], the maximum void ratio was 1.12, the minimum void ratio was 0.577 and the specific gravity was 2.654. Its grain size distribution is shown in Fig. 3.4.

The Colorado River sand is a well graded light brown sand comprised of subangular particles of quartz with some limestone and feldspar. The maximum diameter reaches about 1/4 in. Its physical properties were also determined in the previous study. The maximum void ratio was 0.80 and the minimum void ratio was 0.39. The specific gravity was 2.644. The grain size distribution is shown in Fig. 3.4.

The tests were carried out at the Balcones Research Center of The University of Texas. The test site was sheltered by an abandoned reinforced

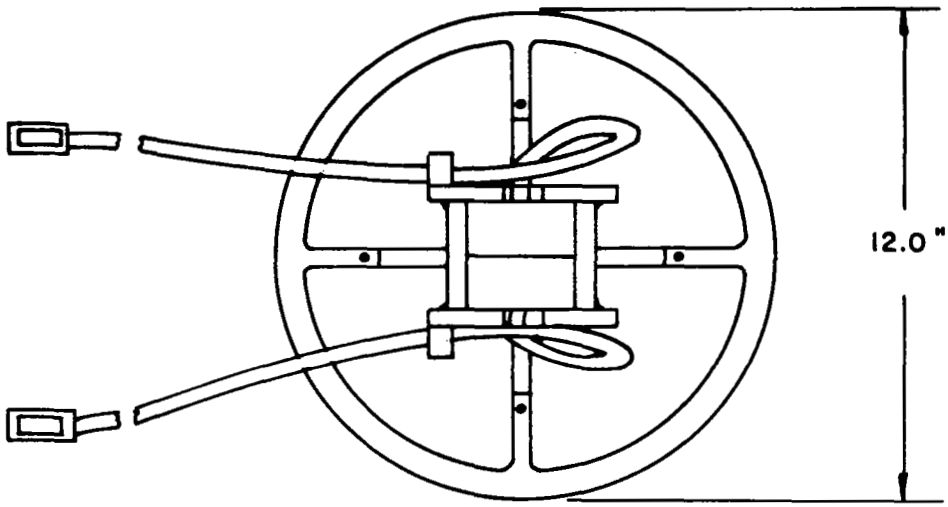

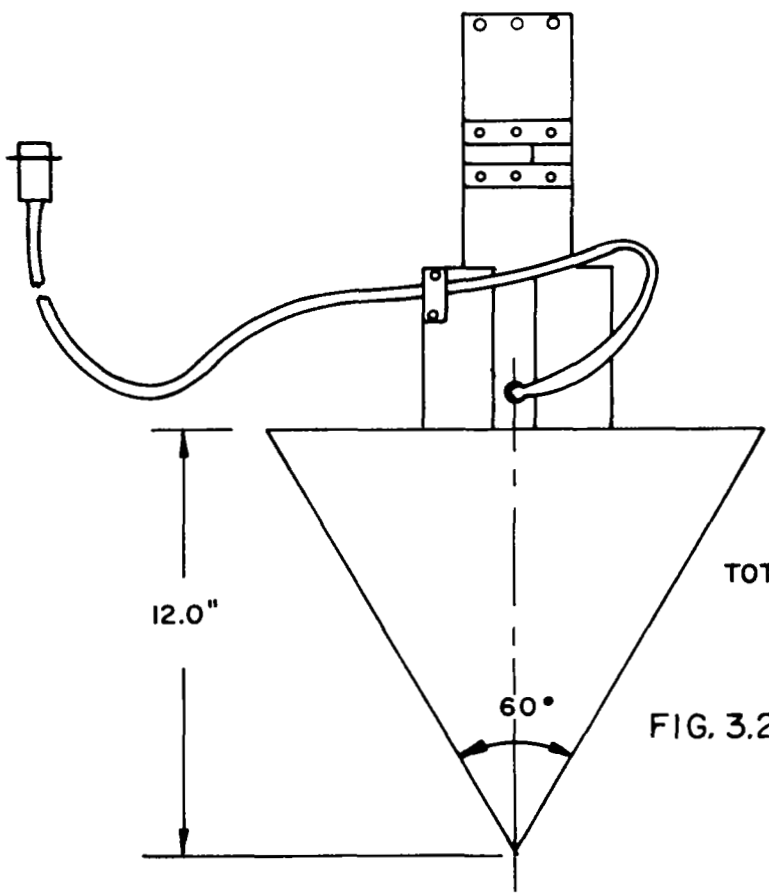

TOTAL WEIGHT 43.0 LBS.

FIG. 3.2 LIGHT CONE (MODEL)

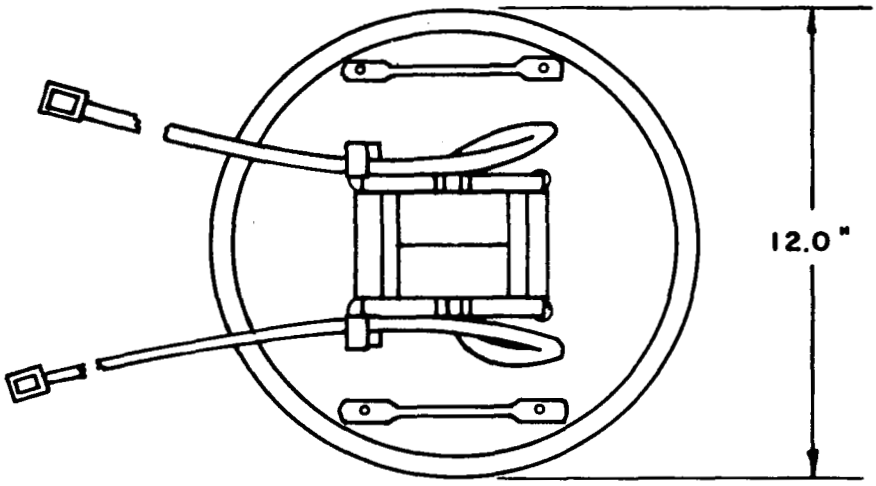

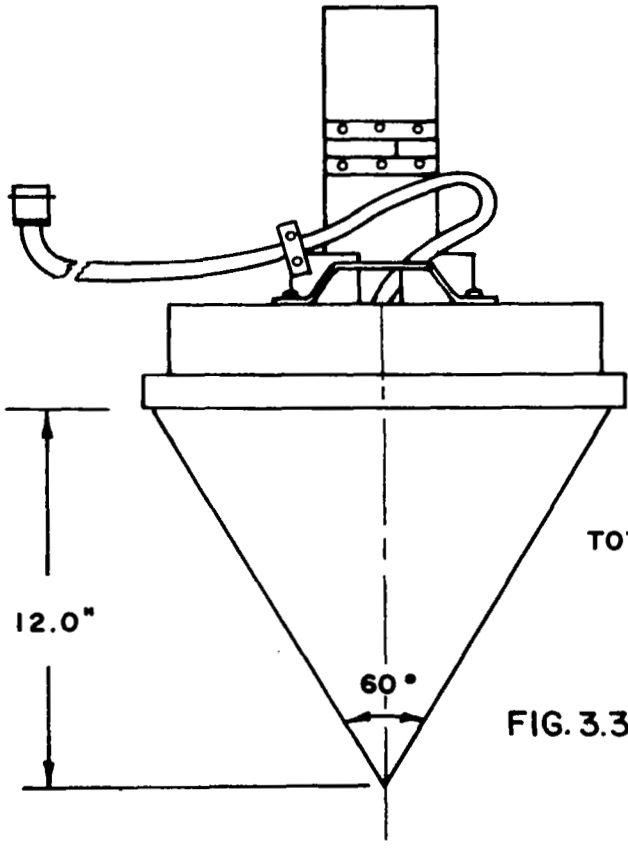

TOTAL WEIGHT 129.5 LBS.

FIG. 3.3 HEAVY CONE (PROTOTYPE)

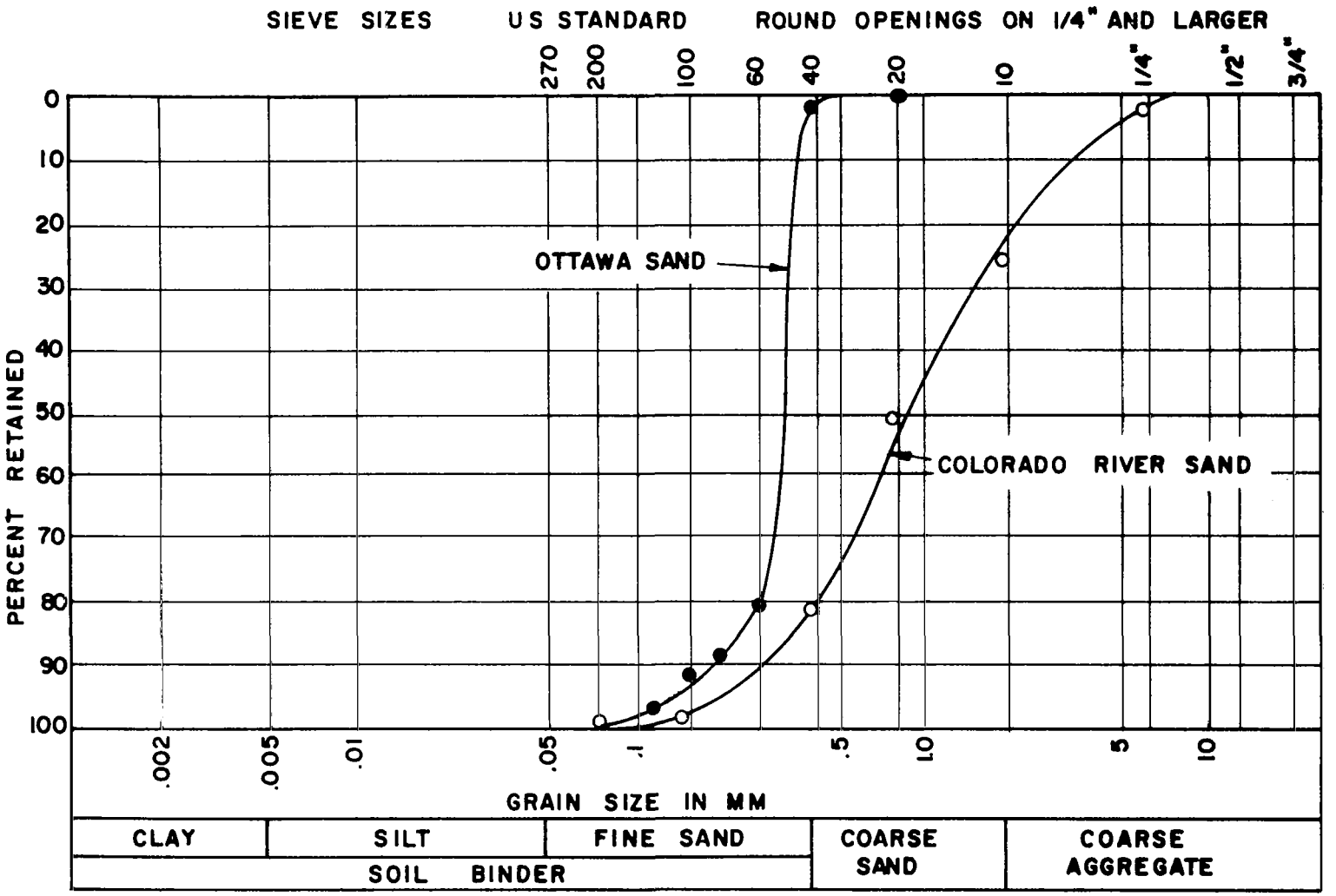

FIG. 3.4 GRAIN SIZE DISTRIBUTION

concrete industrial building. A pit for the sand bed of 3.5 ft width, 5 ft length and 4 ft depth was dug in the firm clayey ground. Before filling with sand, the pit was lined with a sheet of plastic film to make it watertight. First, dry Ottawa Sand was tested both in dense and loose state. Then it was submerged with water and tests were run on saturated-dense Ottawa Sand. The saturated Ottawa Sand was removed from the pit and tests were repeated for Colorado River Sand in dry-loose, dry-dense, and saturated-loose conditions.

The loose states of sands were prepared by turning sands with a shovel to the depth of about one and a half ft below the surface before each test. The average dry and wet density and void ratio of loose sands are as follows.

	Dry-Loose Ottawa Sand	Dry-Loose Colorado River Sand
Dry Density (pcf)	88	95
Wet Density (pcf)	90	96
Water Content (percent)	1.3	1.7
Void Ratio	0.87	0.75

The dry density is defined as the density of an oven-dried sample. The wet density is defined as the density of the sand in situ with hygroscopic moisture.

Dense sands were obtained by tamping. They were first tamped by foot for a few minutes. Then a 10 x 7 in. concrete block weighing about 20 lbs was dropped from about 1 ft height onto the surface of the sand bed for several minutes. The area of compaction was about 2 x 2 ft. The average dry and wet density and the void ratio of dense sands were measured as follows.

	Dry-Dense Ottawa Sand	Dry-Dense Colorado River Sand
Dry Density (pcf)	103	104
Wet Density (pcf)	104	106
Water Content (percent)	1.1	1.5
Void Ratio	0.61	0.59

The saturation of the sand resulted in a further compaction from the dry-dense state. Although the sands were flooded before each test, the impact of a model caused almost instantaneous dissipation of water from the sand bed surface and it was necessary to add more water before each test to maintain saturation. The average density and void ratio of saturated sands were as follows:

	Saturated-Dense Ottawa Sand	Saturated-Dense Colorado River Sand
Dry Density (pcf)	114	113
Wet Density (pcf)	136	131
Water Content (percent)	19.3	16.0
Void Ratio	0.45	0.47

Immediately after each test a sample of the sand was taken by a 1-15/16 in. inner diameter, 1-9/16 in. height and 1/32 in. wall thickness brass ring. The sand sample was used to determine the water content and the density or void ratio. The ring was pushed into the undisturbed part of the sand bed and was dug out after a plate had been pushed into the soil at the bottom. The sand at the top of the ring was leveled with a straight edge and the weight of the sand and the ring was measured immediately at the test site. Figures 3.5 and 3.6 show the distribution of density measurements.

The variation of density in the vertical direction of the sand bed was also observed. Density measurements were taken at three depths, once

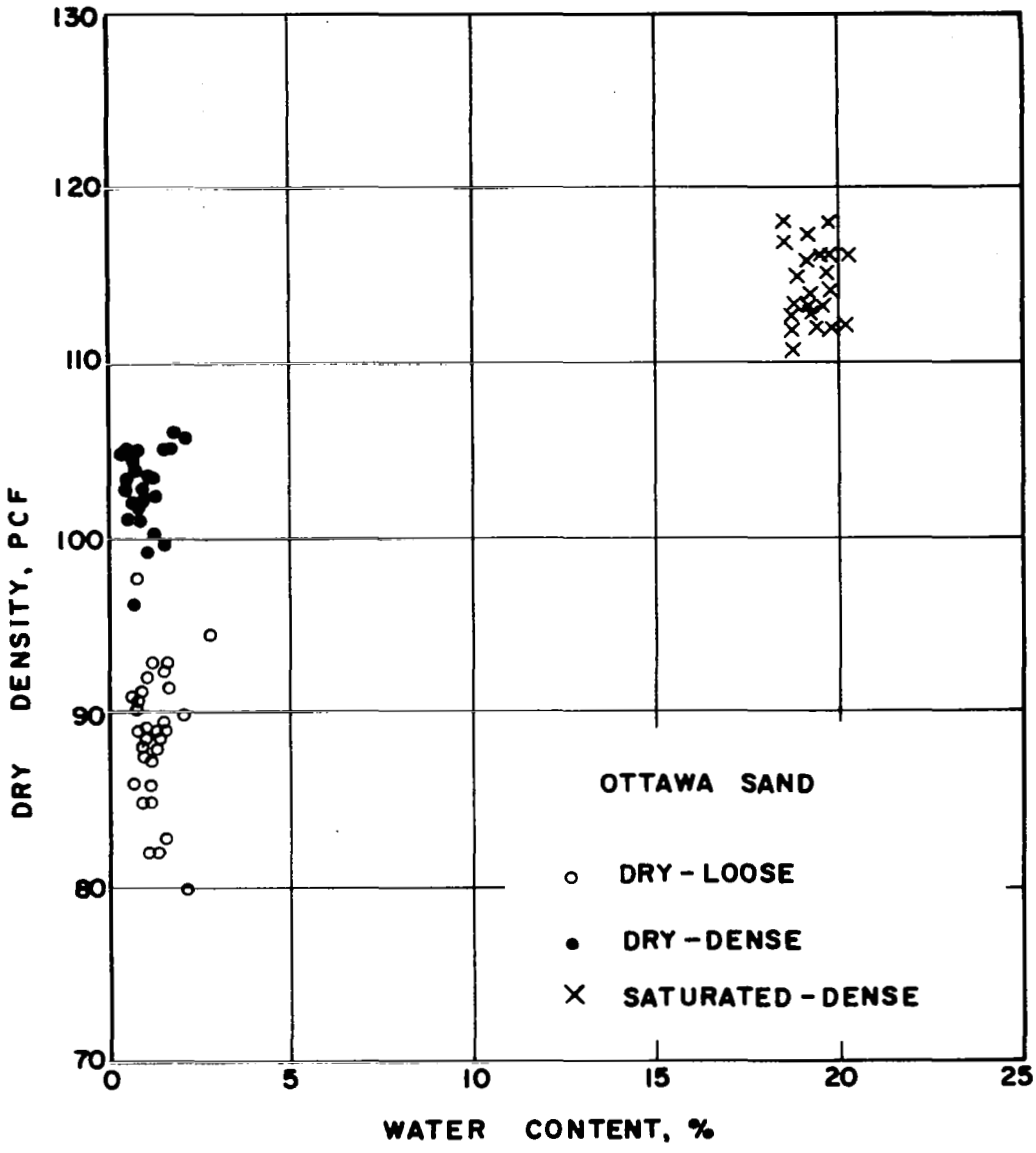

FIG. 3.5 DENSITY MEASUREMENTS, OTTAWA SAND

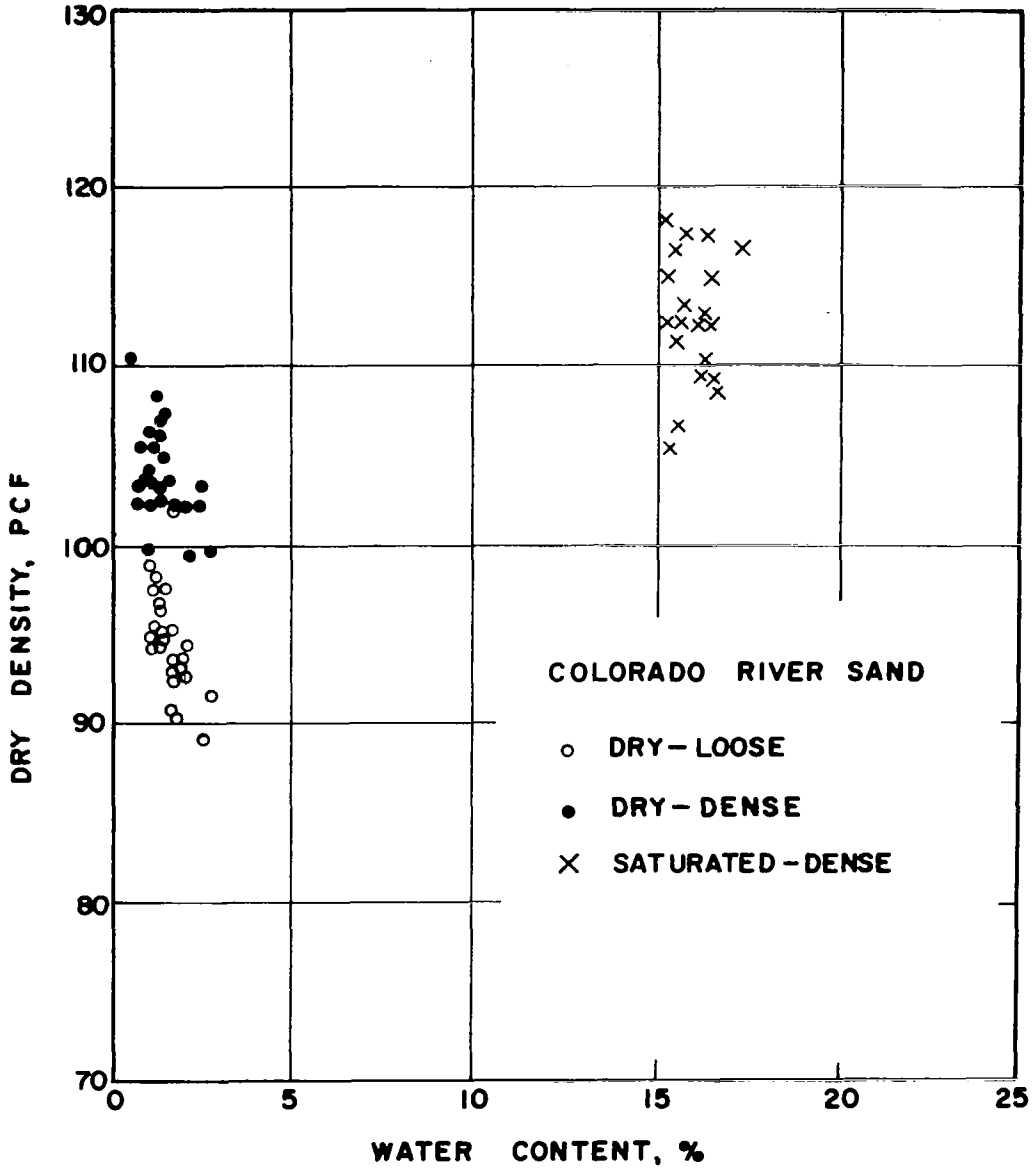

FIG. 3.6 DENSITY MEASUREMENTS, COLORADO RIVER SAND

for the loose-dry Ottawa Sand and once for the dense-dry Colorado River Sand. Test results showed that sand beds were fairly uniform to a depth of about one ft below the surface. Below one ft, the state of sand was not affected by each treatment and remained always at the same density of about 95 pcf.

Although there was a small variation in density measurements as shown in Figs. 3.5 and 3.6, the responses of the models were classified into three distinct groups, namely, dry-loose, dry-dense, and saturated-dense sands.

In spite of the fact that there was local nonuniformity of density of the sand bed, as a whole the sand beds still maintained the desired characteristics of each state of sand. The local nonuniformity of sand might be attributed to the forming of clods by moisture in sand and the insufficient raking of the disturbed sand bed. It is also to be pointed out that the reliability of sampling with relatively small rings is in question.

3.4 TEST PROCEDURE

3.4.1 Drop Test

The same test procedures were repeated for Ottawa Sand and Colorado River Sand in dry-loose, dry-dense and saturated-dense states. For each state of sands both the light and heavy cones were dropped from varying height to achieve five different impact velocities, that is 10, 14, 17, 19 and 23 ft per second. The same tests were repeated at least twice to check the error. Altogether 149 tests were conducted from July 10, 1967 to August 10, 1967. In each test the following records were taken.

1. Drop height and nominal velocity.
2. Vertical free fall distance from the last pin of velocity detector.
3. Time bases and sensitivities of two oscilloscopes.
4. Penetration depth.
5. Acceleration time history by an oscilloscope.

6. Step impulses from velocity detector.

3.4.2 Data Processing

The 3-1/4 x 4-1/4 in. pictures of acceleration and velocity record are too small for accurate interpretation. The contact transparencies were reproduced for use in an overhead projector. The pictures were projected on 11 x 17 in. graph paper and the enlarged records were drawn of acceleration curves and velocity step. The total course of acceleration was then divided into nearly 25 equal time intervals to read the time and acceleration. All the data were punched on computer cards for subsequent calculations by an electronic computer. First the acceleration-time relations were plotted by the computer for the immediate check of errors in input data. Varying velocity and penetration of a model during impact were obtained by numerical integration of the acceleration curve, once for the velocity and twice for the penetration. The numerical integration was done by using the trapezoidal rule for the second point, Simpson's 1/3 formula for the third point and Simpson's 3/8 formula for the following points.

3.5 ERROR CHECK

The direct measurements were compared with the calculations of velocity and penetration of a model. The errors which were observed in the comparisons may be attributed to several factors. It was observed during the fall of the wagon that the track moved upwards even though several sand bags each weighing 100 lbs were resting on the U frame. It was also observed that the track, made of two aluminum rectangular tubes, swung back and forth. The models at rest after impact usually tilted a few degrees forward or backward. It was sometimes necessary to lean the track up to 5 degrees backwards to get the vertical penetration of a model.

3.5.1 Impact Velocity

The time from the triggering of the oscilloscopes to the moment of initiation of impact was calculated in two ways to check the impact velocity.

The distance between the first triggering point and the sand surface was measured before each test. The travel time was calculated by dividing this distance by the measured velocity.

The traveling time was also obtained by adding the delay time of the oscilloscope to the lag time of acceleration read on a photo record.

These two differently obtained times check the change in traveling distance. For instance, one in. change in distance results in 4.2 msec difference at 20 fps. Total traveling time is 71 msec for 17 in. travel and 20 fps. They also check the change in relative velocity between the track and the model. If the track was moving upward at 1 fps, the traveling time for 17 in. travel at 21 fps relative velocity is calculated to be 67.5 msec, which is 3.5 msec less than the actual time. There is no way to separate the effects of upward displacement and the movement of track.

The test results showed that the check time calculated from the measured velocity was normally about 10 msec smaller than the other. It can be attributed either to the few in. upward displacement of the track or to the 2-3 fps upward movement of the track. If the check time difference is solely due to the displacement of the track, the measured velocity does not need correction. If it is caused by the movement of the track the measured velocity must be corrected accordingly. According to the visual observation, the track jumped a few in. upward. It may be certain that both the displacement and the movement of the track affected the check time. Therefore, the average of the directly measured velocity and the velocity calculated from the delay and lag time was taken to use in the whole subsequent analysis.

3.5.2 Acceleration Curve

Newton's law says that the momentum change is equal to the impulse,

$$mdv = Fdt, \tag{3.1}$$

where m is the mass of a cone, dv is the change in velocity, F is the force from the soil on a cone and dt is time.

For the case of a body in free-fall impacting on soil the directions of the force F in Eq 3.1 is taken as negative when it is opposing the direction of impact velocity; therefore,

$$mdv = -Fdt. \tag{3.2}$$

Taking the integral of Eq 3.2 from the start to the end of the impact,

$$\int_1^2 m\,dv = -\int_1^2 F\,dt$$

$$= -\int_1^2 m\,a(t)\,dt$$

$$\int_1^2 dv = -\int_1^2 a(t)\,dt$$

$$v_2 - v_1 = -\int_1^2 a(t)\,dt. \tag{3.3}$$

CR-1210

This relationship reduces to an expression for calculating the velocity from an acceleration curve if the initial velocity, v_1, is known.

A correction of the measured acceleration a(t) is necessary, when the terminal velocity calculated from the acceleration record, a(t), by using Eq 3.3 does not agree with the real terminal velocity of the phenomenon which in this study is zero.

The ideal acceleration, velocity and penetration vs. time relations are represented by Fig. 3.7. In the acceleration curve the zero line is taken as gravitational acceleration. A typical acceleration curve obtained from field data is shown by a solid line in Fig. 3.8(a). An integration of this curve with respect to time yields velocity and this is shown by a solid line in Fig. 3.8(b) and it can be seen that this velocity does not come to zero. In order to bring the terminal velocity zero, the acceleration record has to be corrected.

Some of the acceleration records were incomplete and missed the last portion of the curve which was necessary to calculate the terminal velocity. Since the difference between the calculated terminal velocity and minimum velocity is small, the minimum velocity was used for the correction of acceleration record. The minimum velocity was calculated for each test and a correction factor was determined to bring the minimum velocity to zero.

Taking the minimum velocity as zero is still underestimating the acceleration. However, as a result of the correction, the scattering of acceleration record was improved.

After the test, in an effort to find the cause of deviation of acceleration, every part of the electrical equipment was checked for its function and effect on the acceleration measurement, but no defect was found there. Finally, another series of tests with a smaller sphere model was

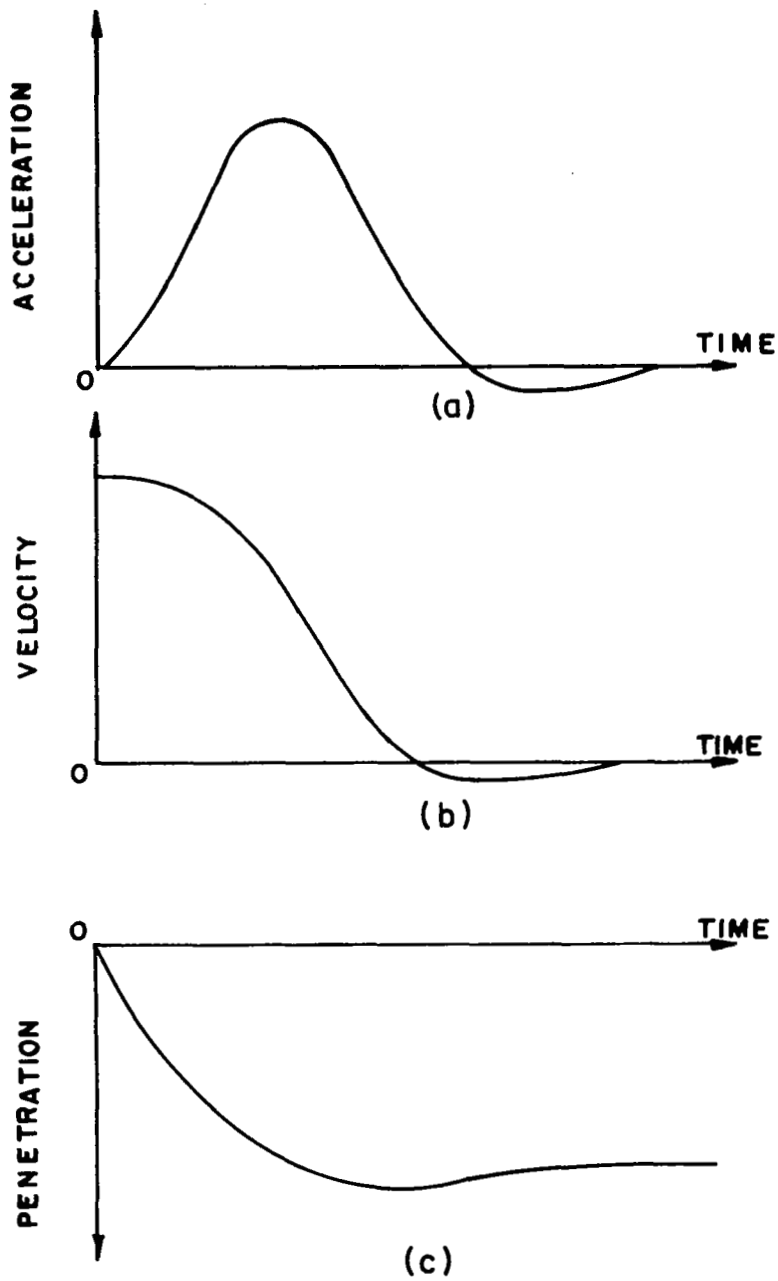

FIG. 3.7 IDEALIZED ACCELERATION, VELOCITY AND PENETRATION VS. TIME RELATIONS

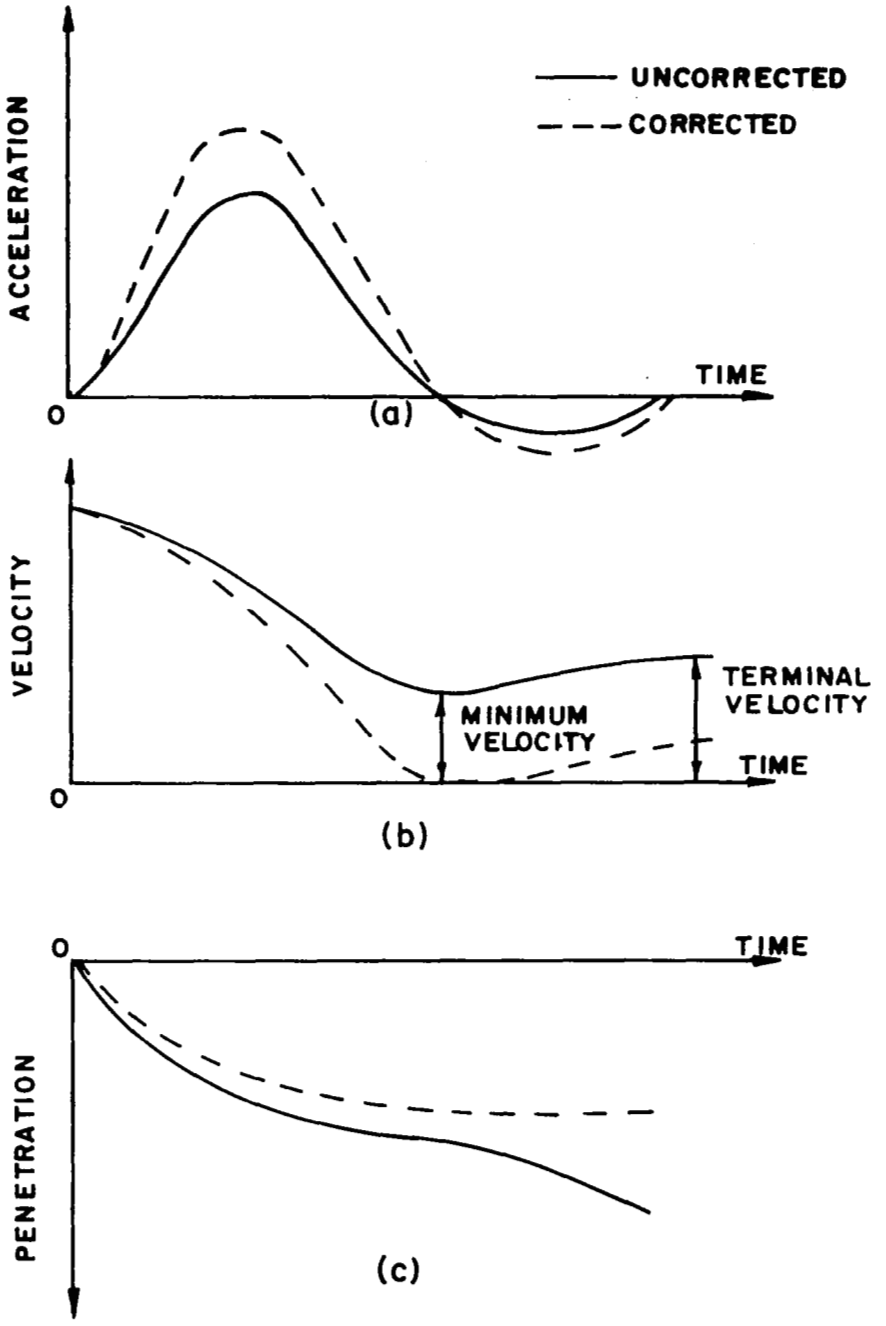

FIG. 3.8 TYPICAL INTEGRATION OF ACCELERATION CURVE

carried out in the laboratory to check the function of accelerometers. Acceleration records again showed some random deviation. One reasoning to this unsteady measurement is that the working range of the accelerometer was too small for its maximum capacity. The maximum acceleration measured was 40 g, whereas the maximum capacity of the accelerometer was 250 g. Another cause may be due to the invalidness of assuming a rigid body of the model.

3.6 TEST RESULTS AND ANALYSIS

3.6.1 Test Records

All the test results are tabulated in Appendix I. In Table I-A through I-F in Appendix I, the maximum forces and maximum accelerations are corrected as discussed in Section 3.5.2. The correction factors are also listed in these tables.

Typical shapes of acceleration vs. time curves are shown in Fig. 3.9. In Fig. 3.9 examples are shown for the heavy cone and the light cone impacting at 23 fps nominal velocity into the dry-loose, dry-dense and saturated state of Colorado River Sand. The curves approach a triangular shape. The triangular shapes for the loose sand test have the lowest height and the broadest base. The saturated sand test gives triangular shapes with the tallest height and the narrowest base. The dry-dense sand test comes in between.

Figures 3.10 through 3.15 show the relations of impact velocity versus penetration depth for different states of sands. The static penetration corresponding to zero impact velocity was obtained by placing the cone model slowly on the sand surface and allowing the cone to penetrate under its own weight. Penetration increases almost linearly with impact velocity. The behavior of a heavy cone in loose sands is different from others. Figure 3.10 and Fig. 3.13 show that the penetration of a heavy cone did not increase

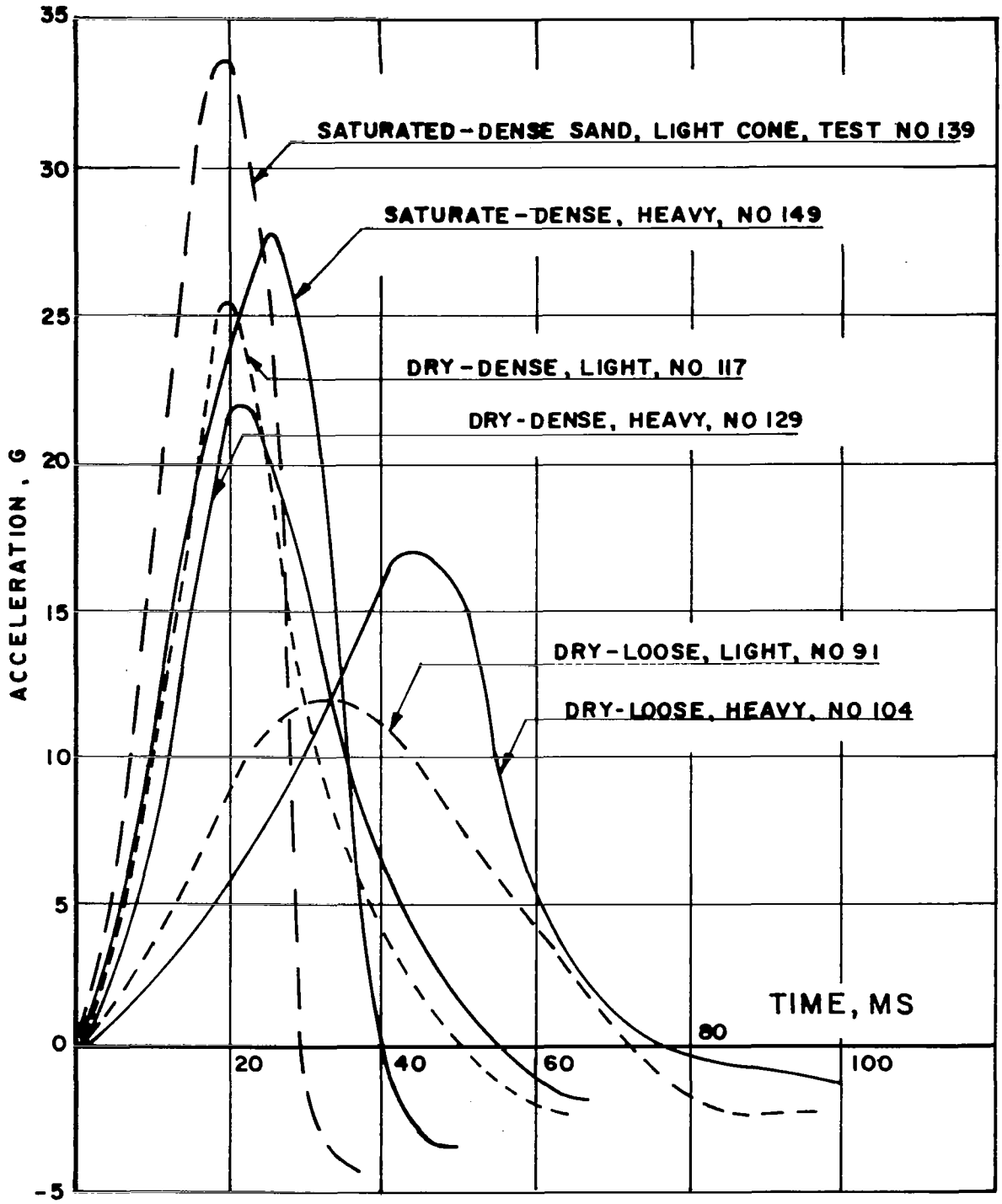

FIG. 3.9 ACCELERATION CURVES FOR COLORADO RIVER SAND AT 23 FPS NOMINAL IMPACT VELOCITY

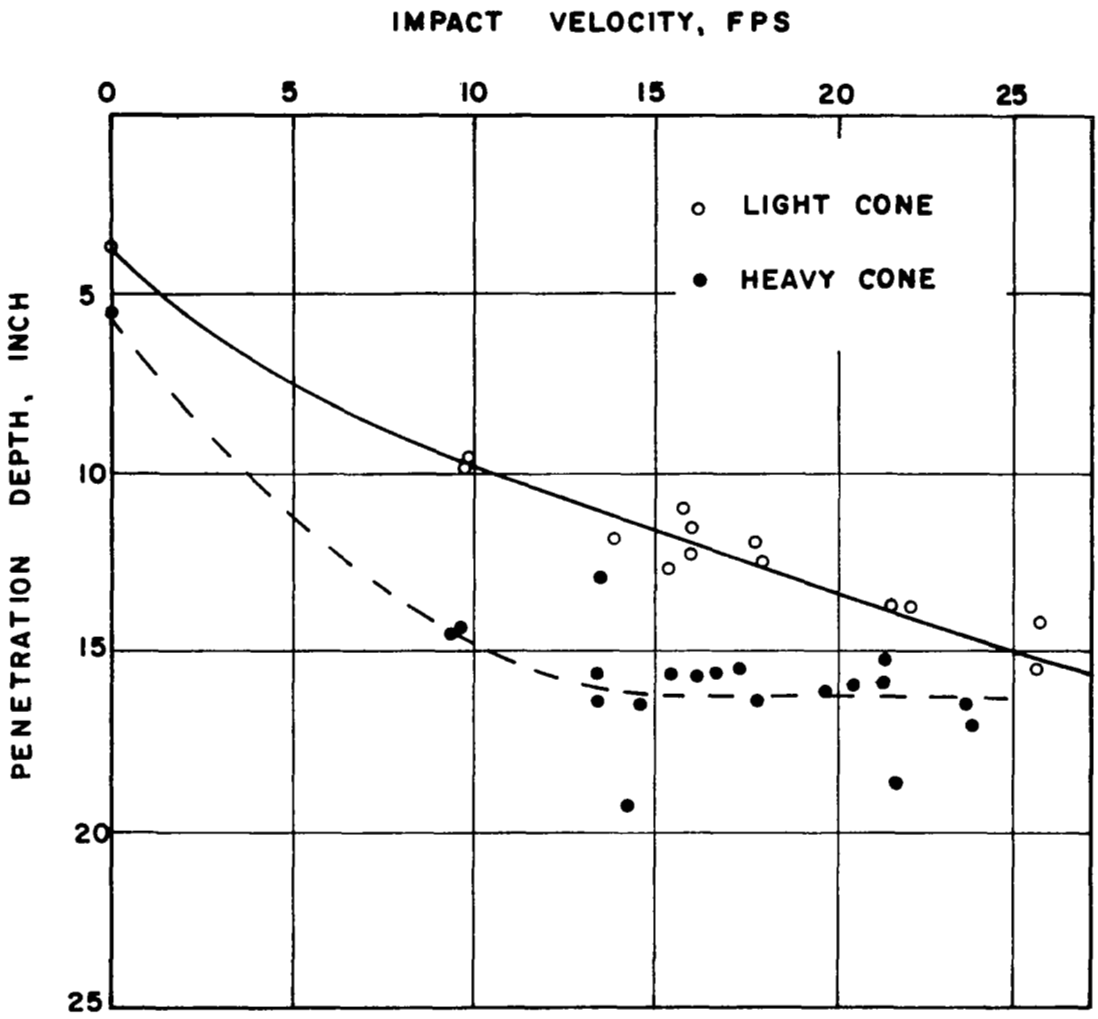

FIG. 3.10 PENETRATION VS. IMPACT VELOCITY
DRY-LOOSE OTTAWA SAND

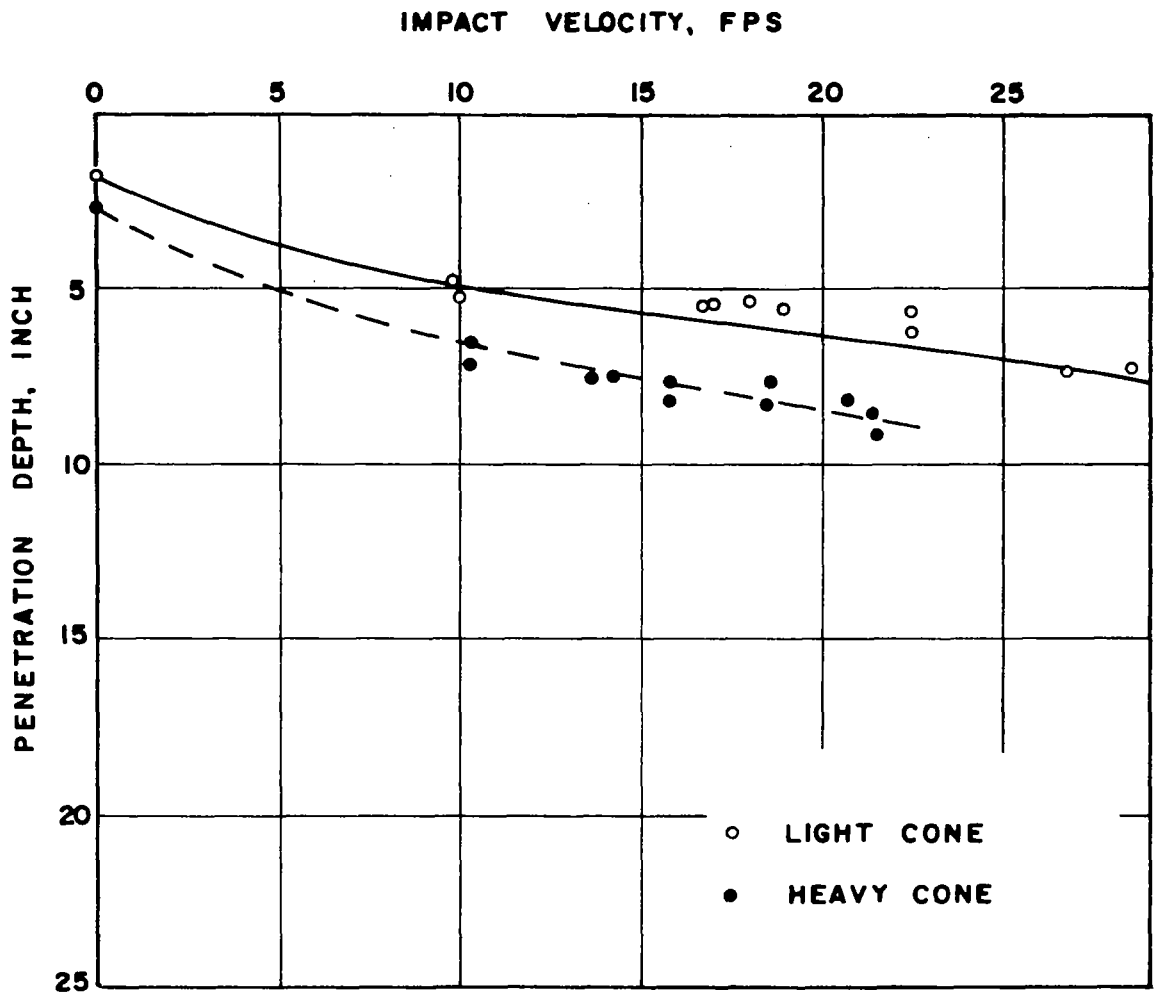

FIG. 3.11 PENETRATION VS. IMPACT VELOCITY
DRY-DENSE OTTAWA SAND

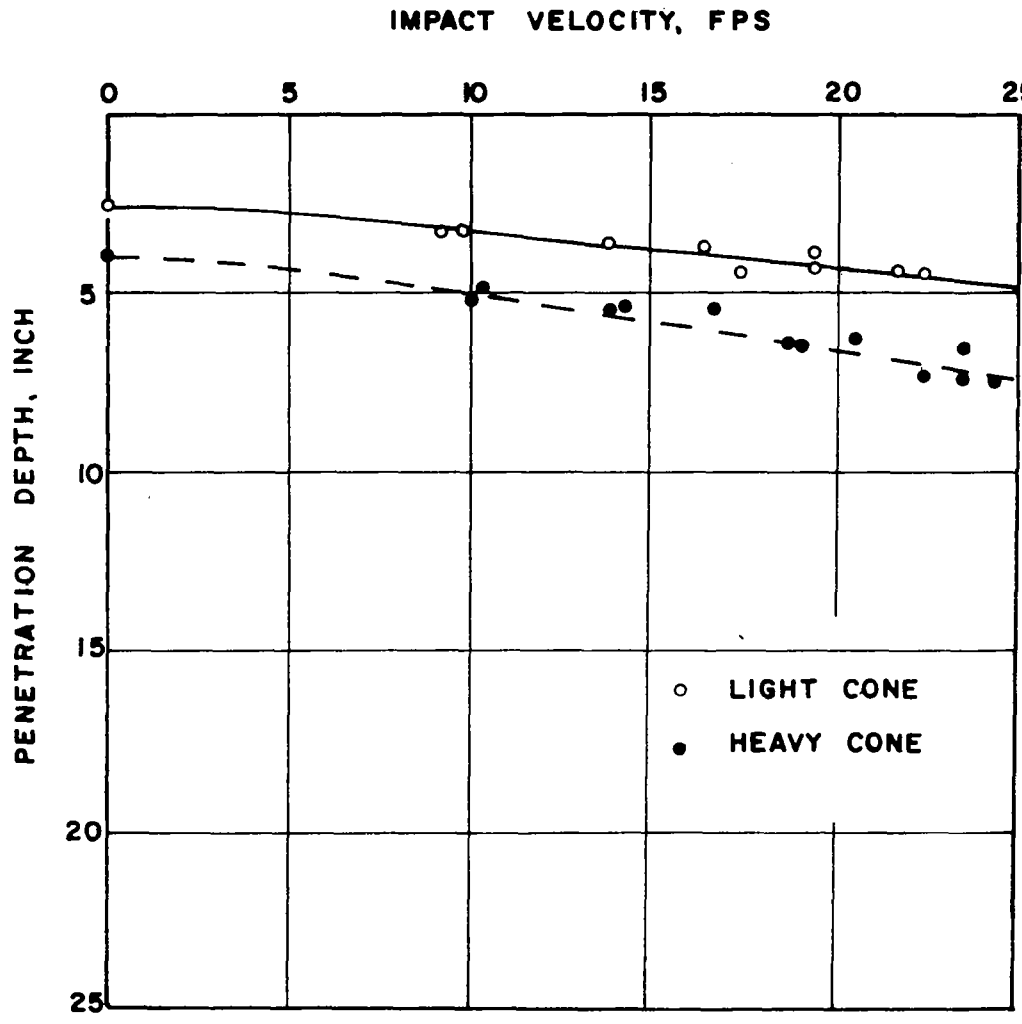

FIG. 3.12 PENETRATION VS. IMPACT VELOCITY SATURATED-DENSE OTTAWA SAND

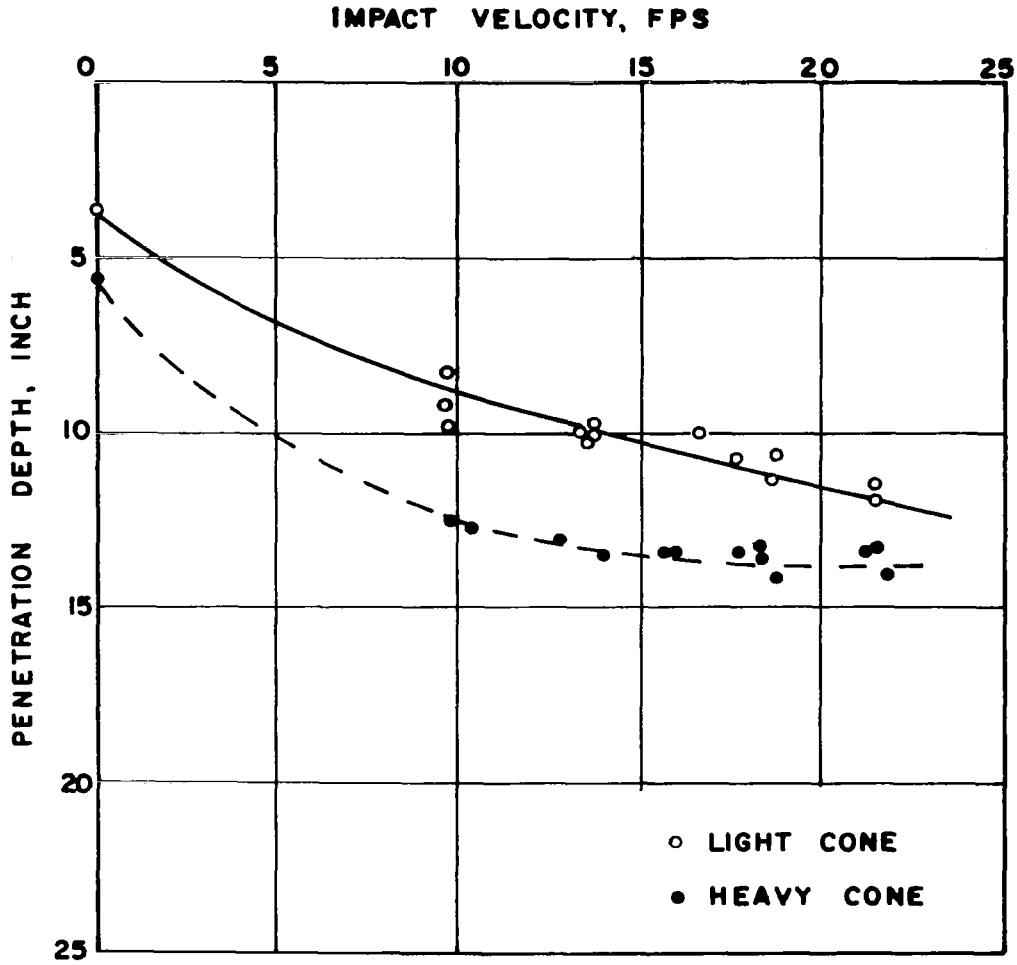

FIG. 3.13 PENETRATION VS. IMPACT VELOCITY
DRY-LOOSE COLORADO RIVER SAND

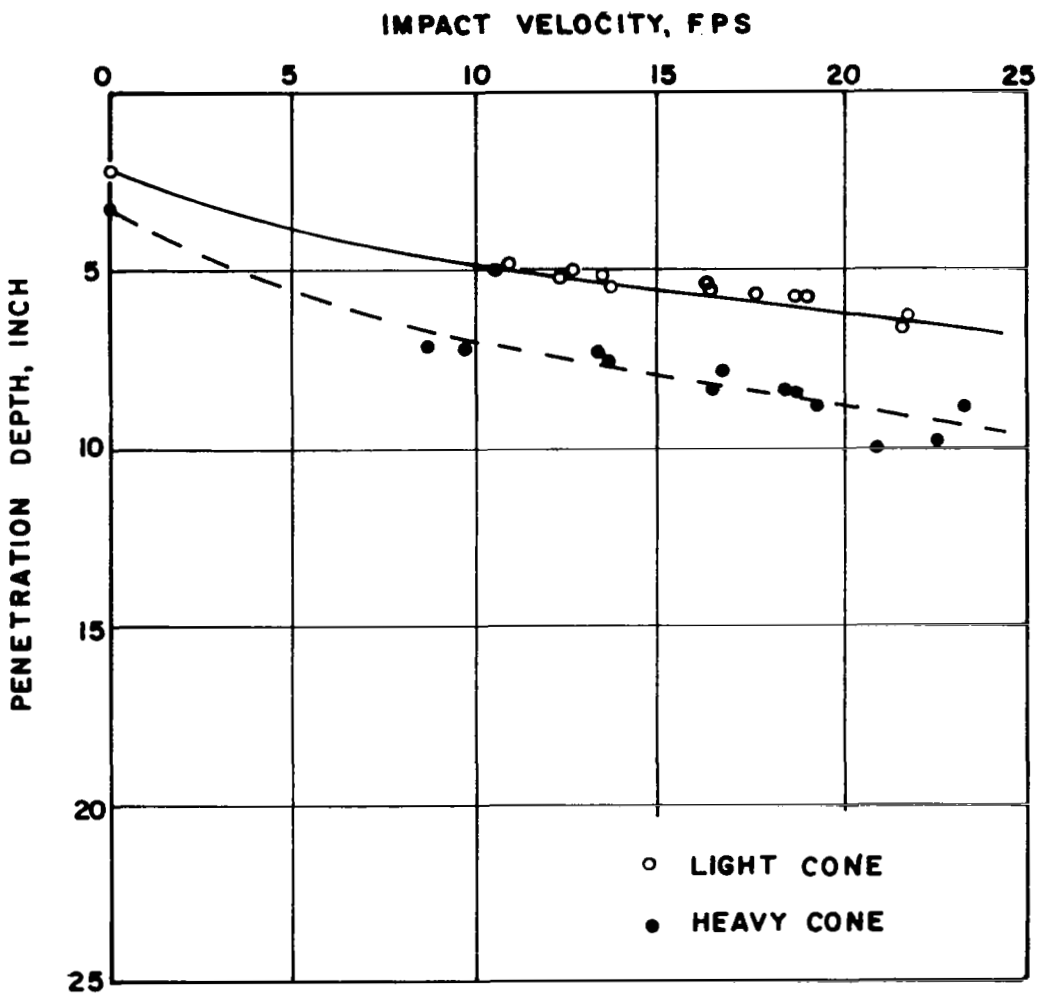

FIG. 3.14 PENETRATION VS. IMPACT VELOCITY DRY-DENSE COLORADO RIVER SAND

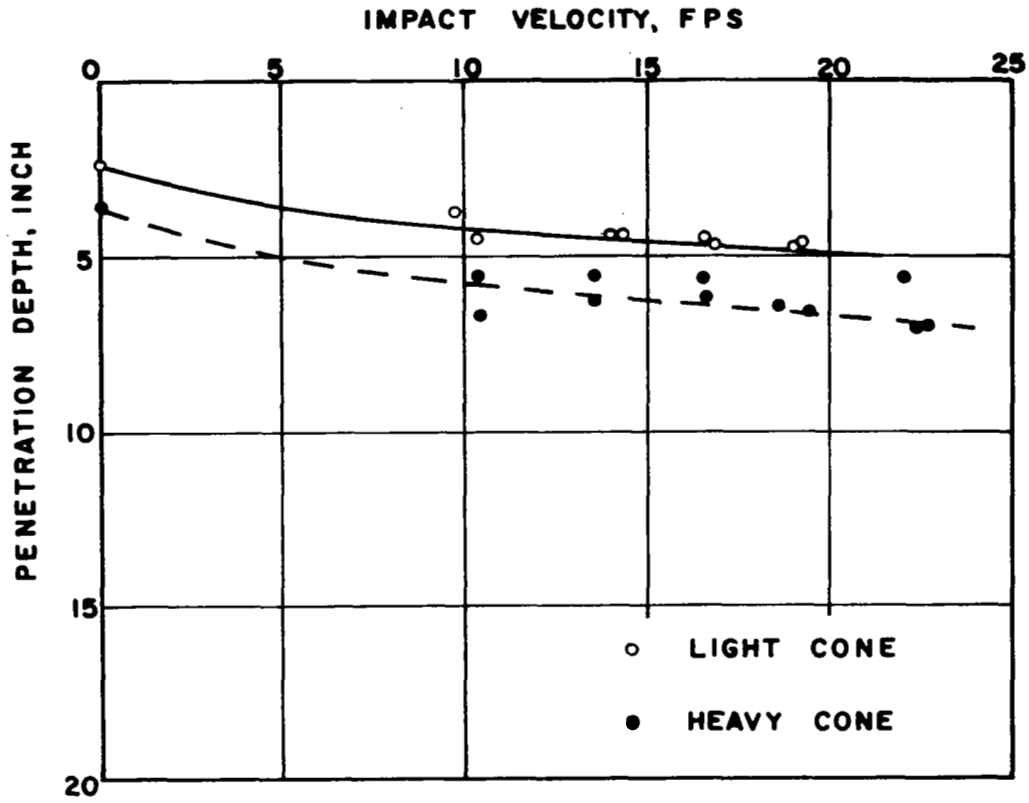

FIG. 3.15 PENETRATION VS. IMPACT VELOCITY SATURATED-DENSE COLORADO RIVER SAND

continuously with increasing impact velocity. This is attributed to the dense layer of sand underlying the one and a half ft of loose sand under the top layer.

Figures 3.16 through 3.21 show the relations of the impact velocity versus the maximum acceleration for each state of sands. The acceleration of a light cone is always higher than a heavy cone except for loose sands tests as shown in Figs. 3.16 and 3.19.

The results of tests in loose sands have been excluded from the further analysis, since the heavy model is affected by the dense layer under the loose sand.

3.6.2 Validity of Model Design

The validity of model design is proved if all the pertinent variables of a prototype and its model satisfy the relation developed in section 2.5.1. Among the variables, the angle of internal friction of a soil, ϕ, the mass density of a soil, ρ, the degree of saturation of a soil, S, and the apex angle of a cone, θ, satisfy automatically the required relationship between a prototype and its model. The mass of a prototype cone and the mass of a model cone have fixed values. The ratio of these two masses controls a number of scale factors. The impact velocity, v, is the operational variable of the test. The maximum acceleration, a, the penetration depth, d, and the rise time, t, of the impact are the variables that predict the prototype behavior from the model test.

Four variables, v, a, d, and t, were considered in the test program.

Impact Velocity vs. Penetration

The scale factor for velocity is 1.20. The scale factor for the penetration is 1.44. Prediction by the model is obtained by multiplying the

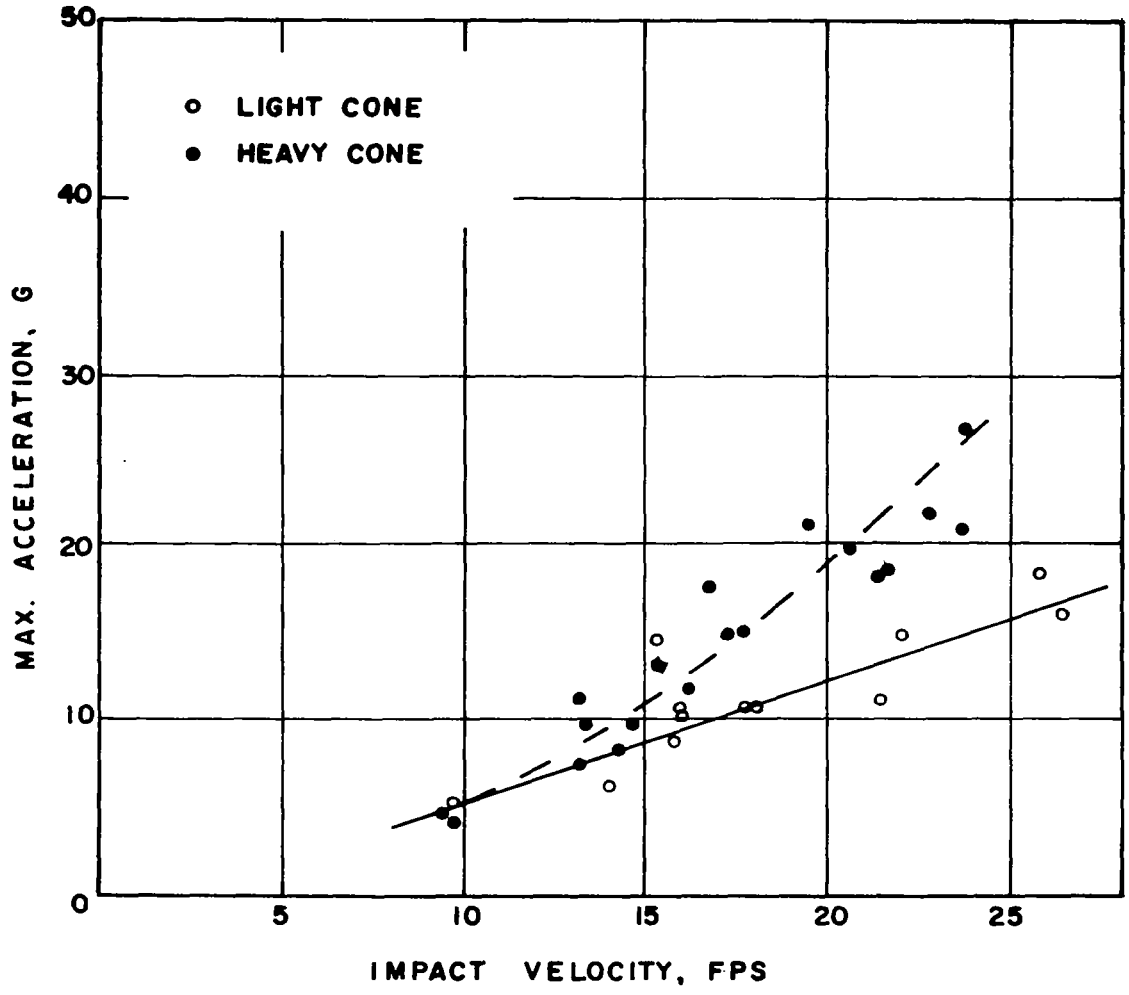

FIG. 3.16 MAX. ACCELERATION VS. IMPACT VELOCITY DRY-LOOSE OTTAWA SAND

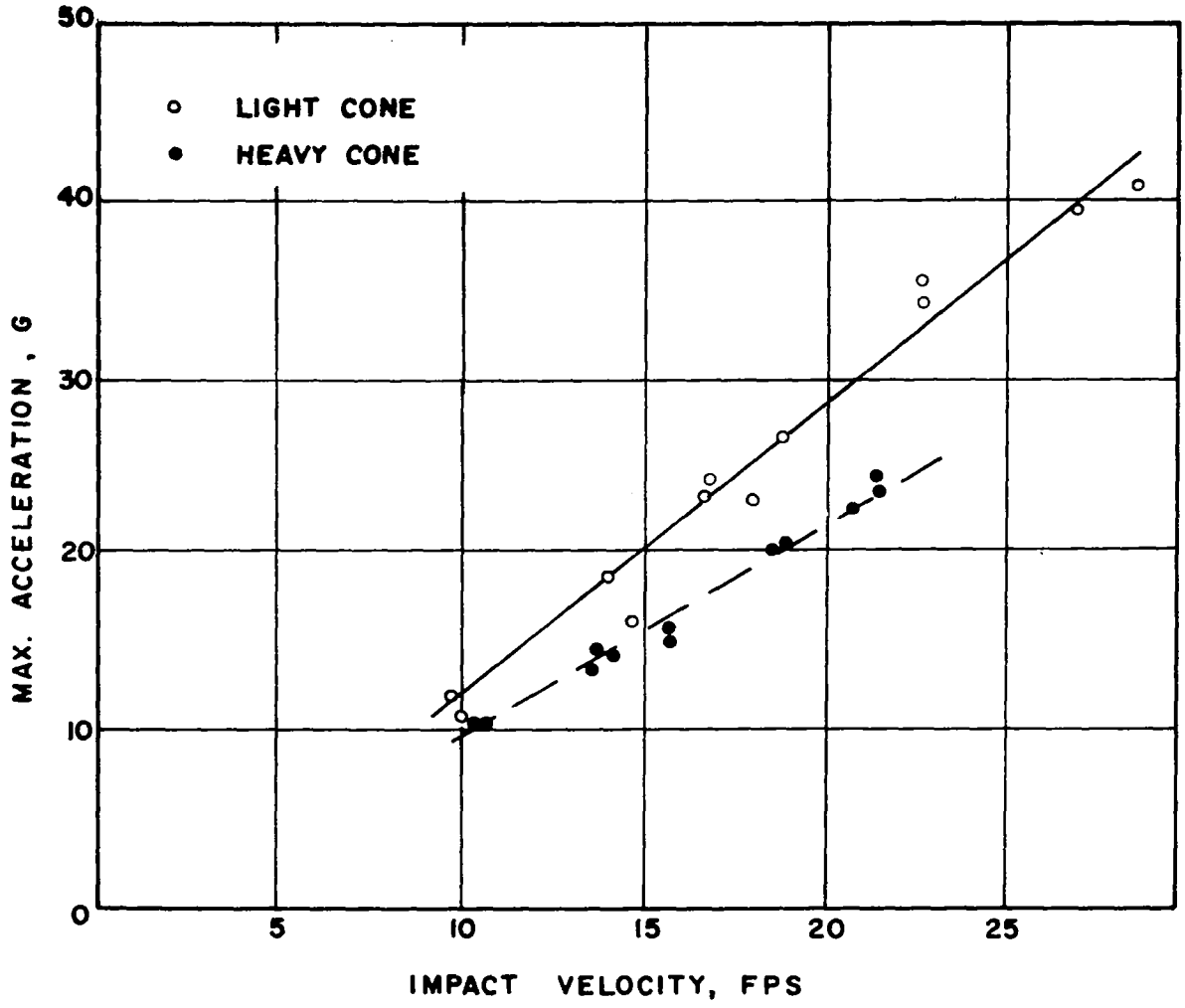

FIG. 3.17 MAX. ACCELERATION VS. IMPACT VELOCITY DRY-DENSE OTTAWA SAND

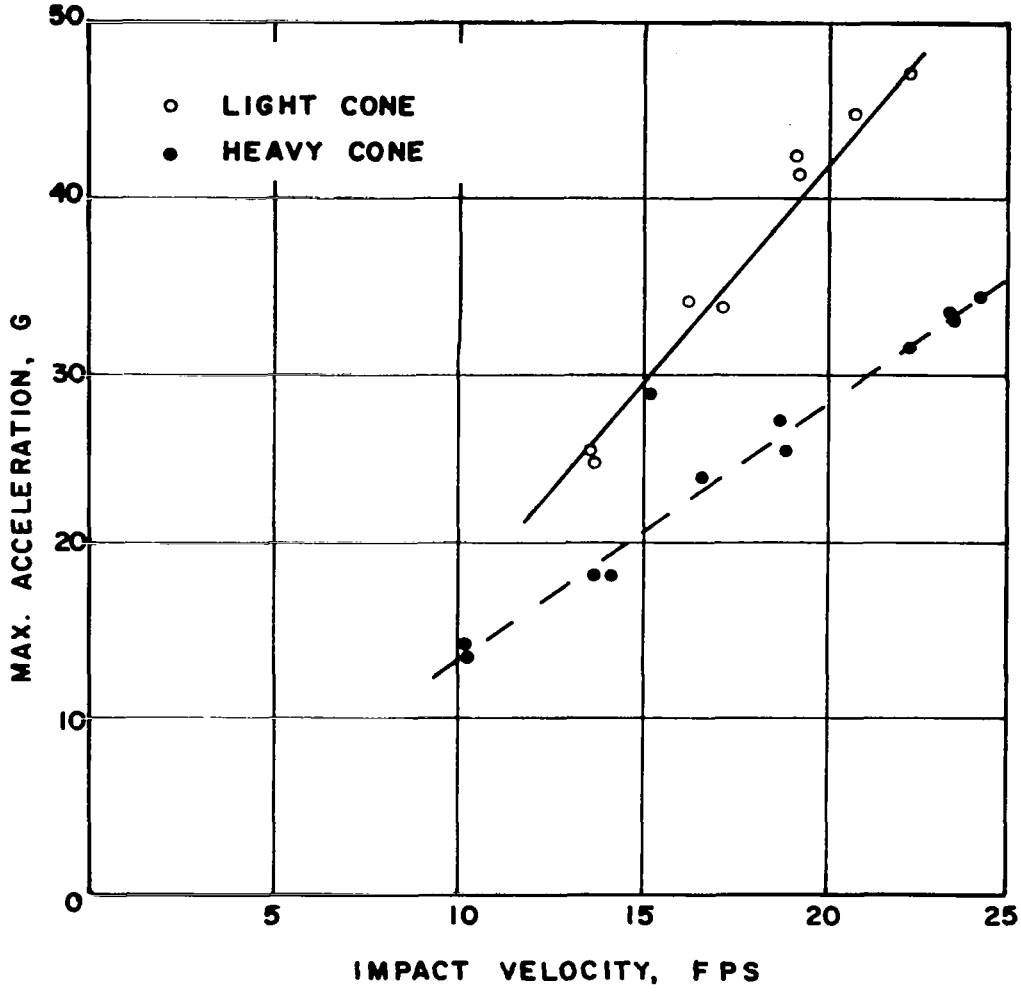

FIG. 3.18 MAX. ACCELERATION VS. IMPACT VELOCITY SATURATED-DENSE OTTAWA SAND

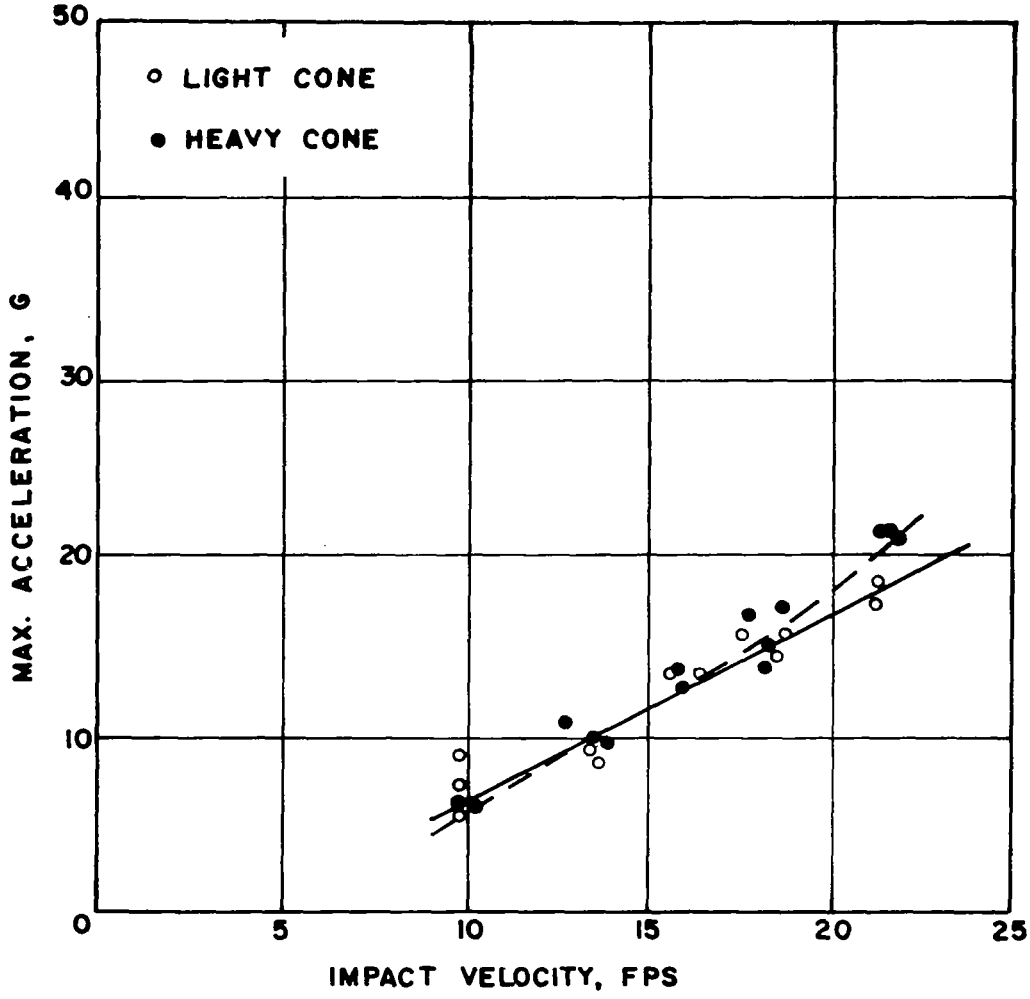

FIG. 3.19 MAX. ACCELERATION VS. IMPACT VELOCITY DRY-LOOSE COLORADO RIVER SAND

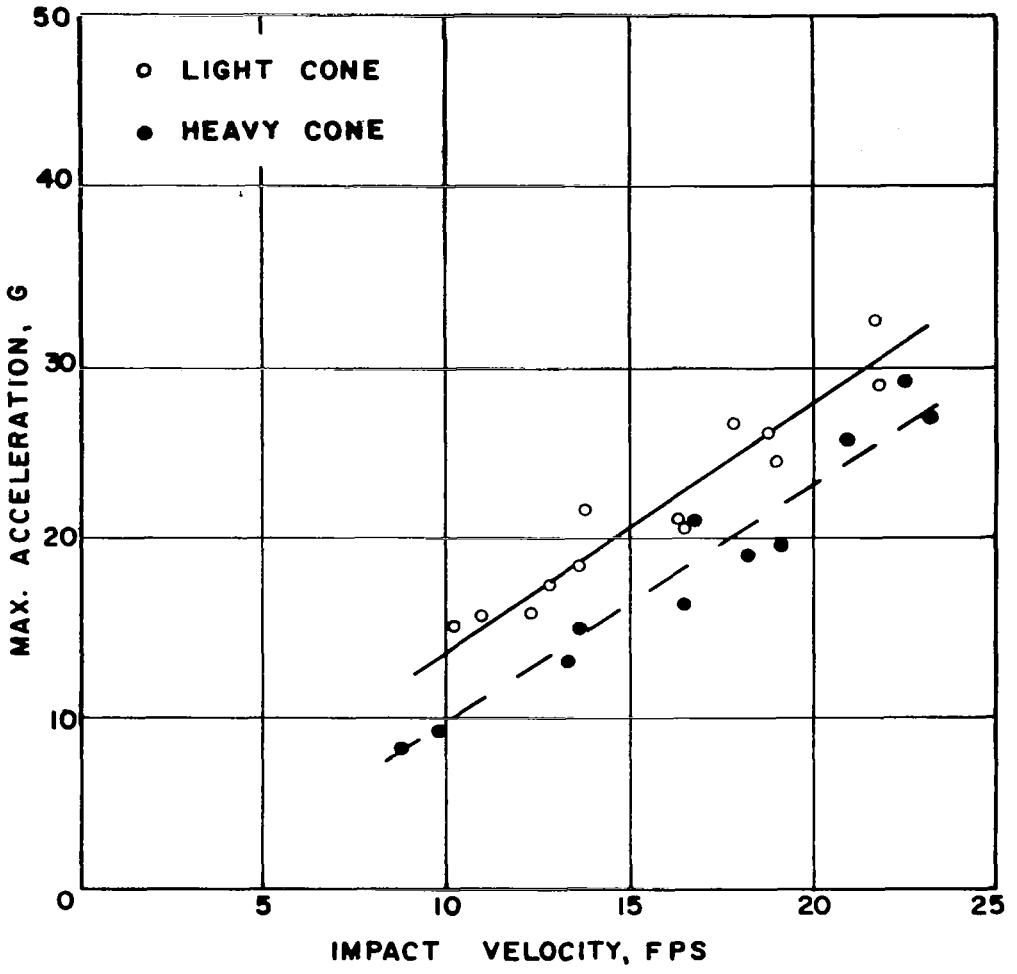

FIG. 3.20 MAX. ACCELERATION VS. IMPACT VELOCITY DRY-DENSE COLORADO RIVER SAND

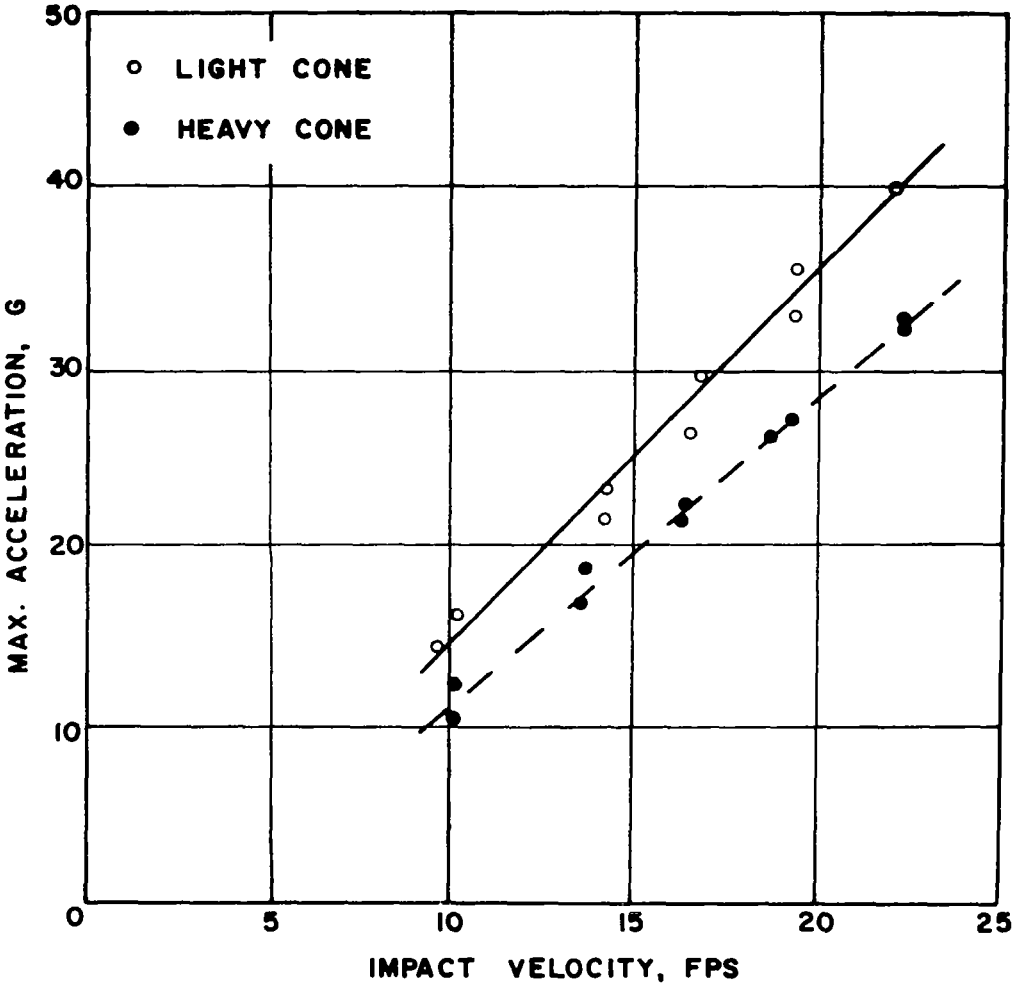

FIG. 3.21 MAX. ACCELERATION VS. IMPACT VELOCITY SATURATED-DENSE COLORADO RIVER SAND

model velocity by 1.20 and the model penetration by 1.44. The scale factors for the prototype velocity and penetration are unity. Figures 3.22 through 3.25 show the measured velocity versus penetration of the prototype compared with that predicted from its model.

Considering the errors in the original data, the prediction by a model agrees quite well with the prototype behavior.

Impact Velocity vs. Maximum Acceleration

The scale factor for the velocity is 1.20. The scale factor for the maximum acceleration is 1.00. When the model velocity is multiplied by 1.20, its maximum acceleration should coincide with that of the prototype. The scale factors for the prototype velocity and maximum acceleration are taken as unity. Figures 3.26 through 3.29 show the measured impact velocity versus maximum acceleration of a prototype compared with the prediction from its model. The values of maximum acceleration are the corrected values. The agreement between the prototype and the prediction by a model is good, except for the saturated-dense Ottawa Sand test, Fig. 3.27. In the saturated-dense Ottawa Sand, the disparity between the model and the prototype increases gradually with increasing impact velocity.

Impact Velocity vs. Rise Time of Impact

The scale factor for the impact velocity is 1.20. The scale factor for the rise time of impact is also 1.20. Then, if both the impact velocity and the rise time of the model are multiplied with 1.20, they give the prediction of its prototype.

Figures 3.30 through 3.33 show the measured rise time versus impact velocity of the prototype compared with the prediction by its model. Although there is scattering of the plots, both the prototype and the prediction of its model are in general agreement.

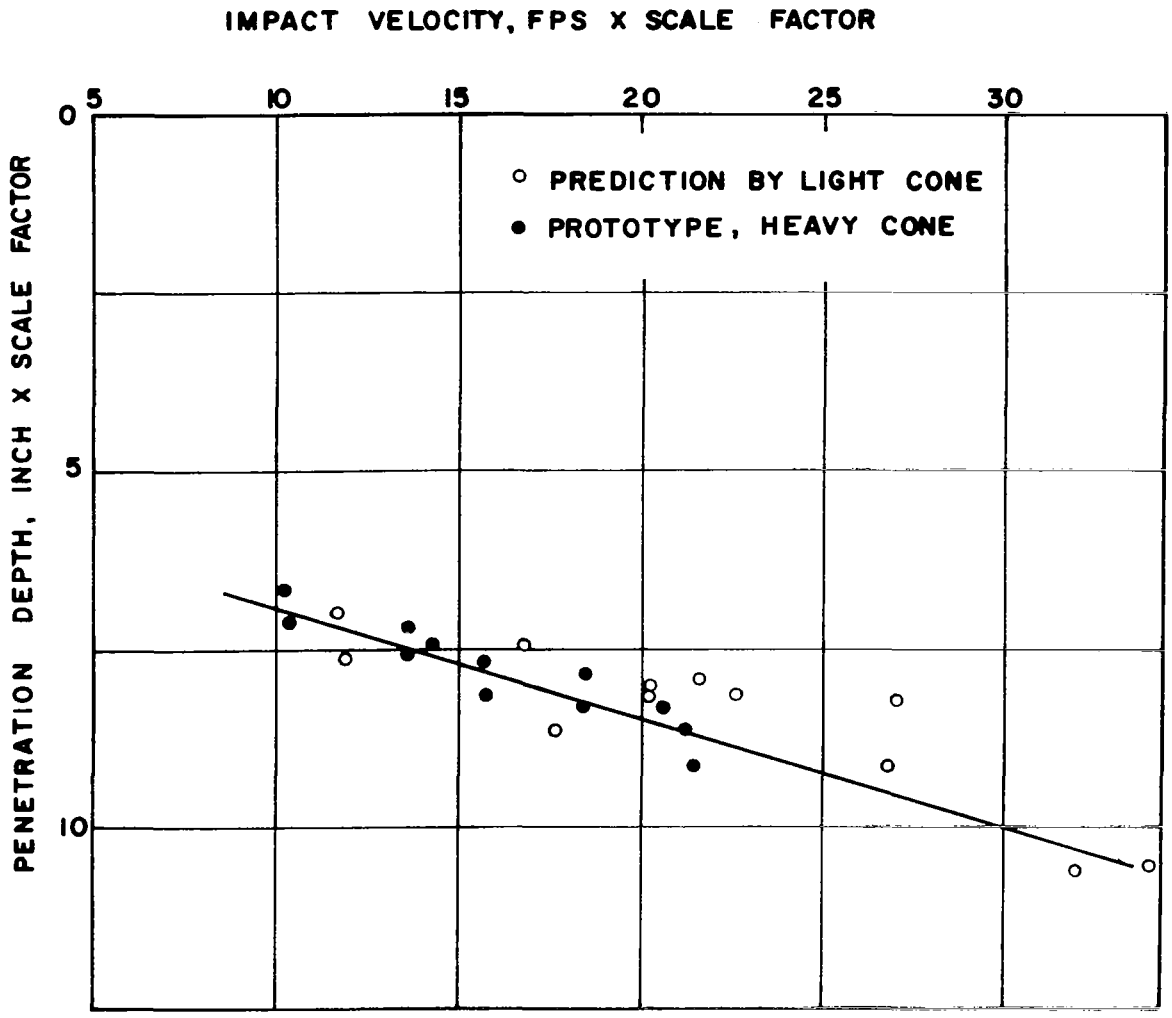

FIG. 3.22 PENETRATION VS. IMPACT VELOCITY PROTOTYPE AND PREDICTION BY MODEL DRY-DENSE OTTAWA SAND

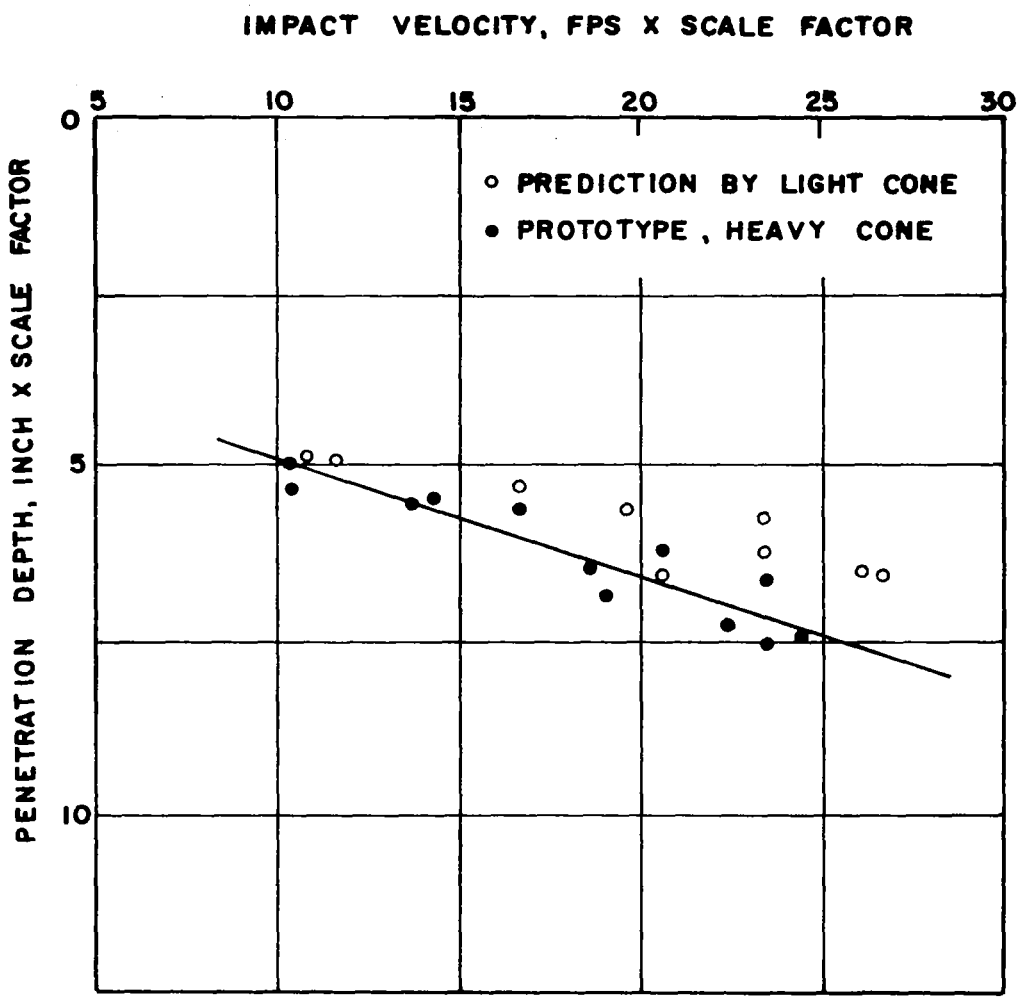

FIG. 3.23 PENETRATION VS. IMPACT VELOCITY PROTOTYPE AND PREDICATION BY MODEL SATURATED-DENSE OTTAWA SAND

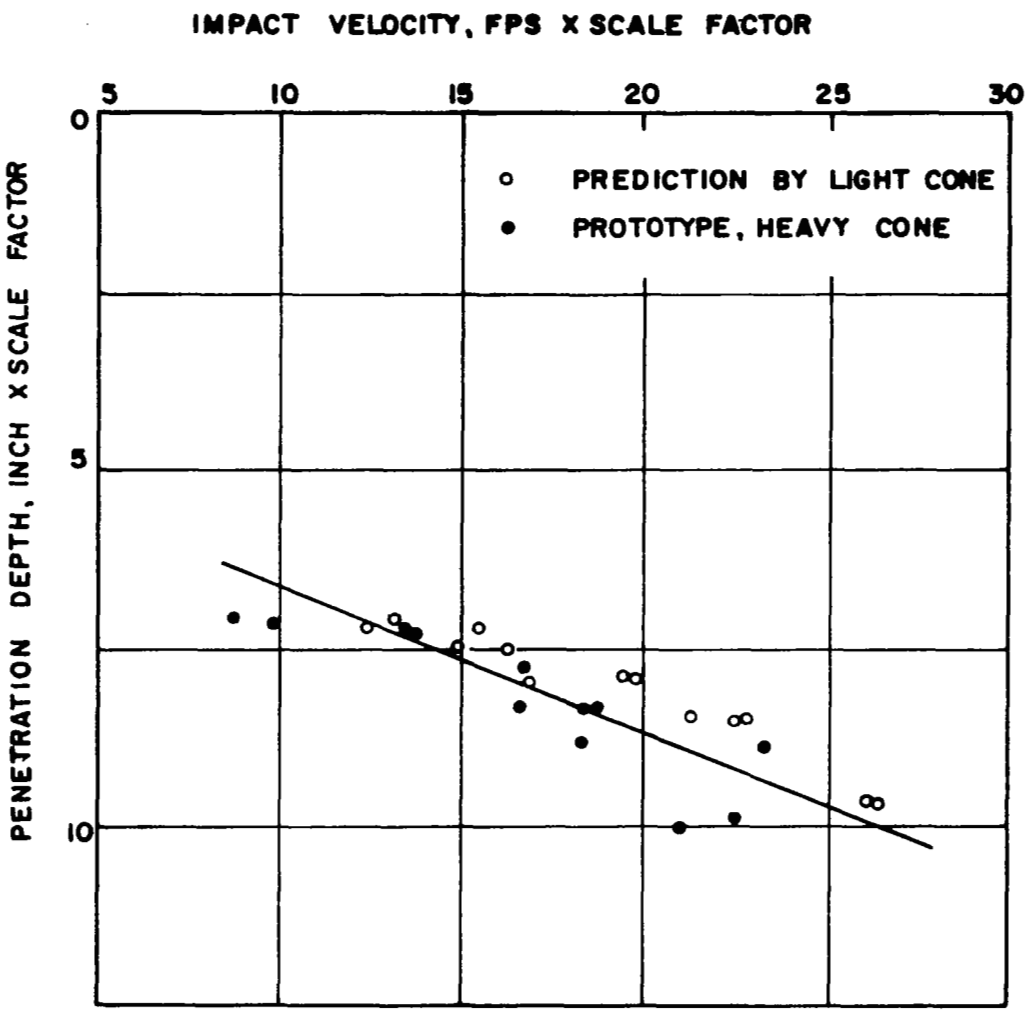

FIG. 3.24 PENETRATION VS. IMPACT VELOCITY PROTOTYPE AND PREDICTION BY MODEL DRY-DENSE COLORADO RIVER SAND

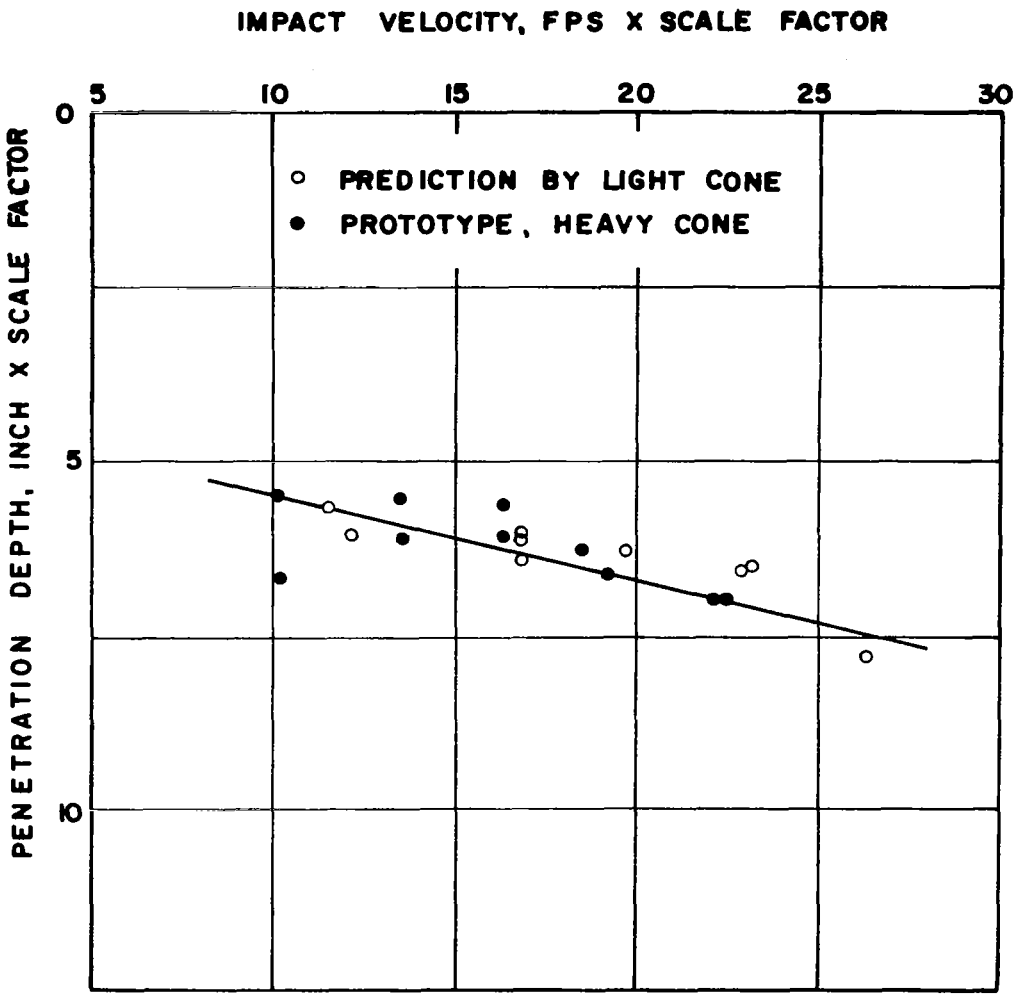

FIG. 3.25 PENETRATION VS. IMPACT VELOCITY PROTOTYPE AND PREDICTION BY MODEL SATURATED-DENSE COLORADO RIVER SAND

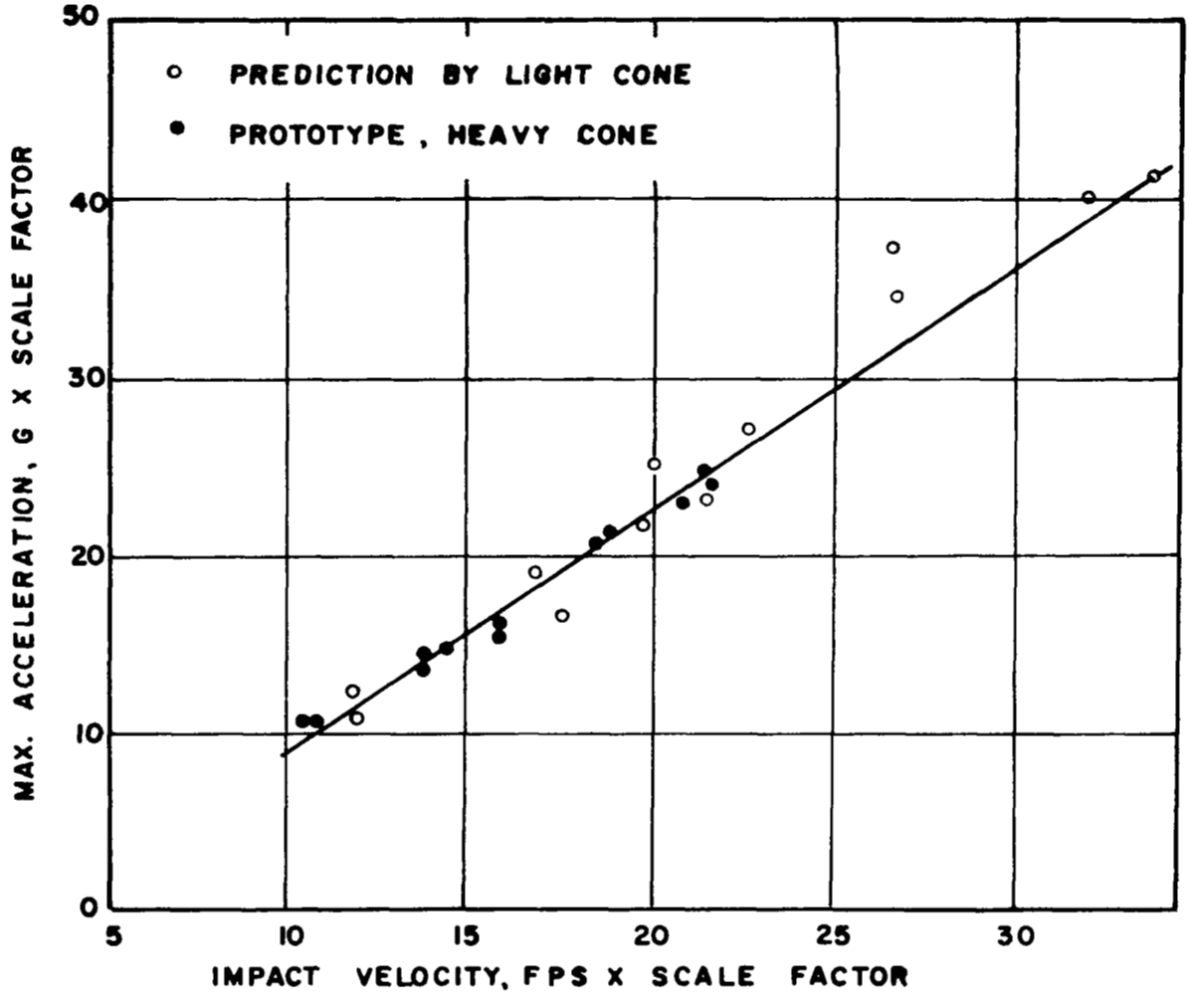

FIG. 3.26 MAX. ACCELERATION VS. IMPACT VELOCITY PROTOTYPE AND PREDICTION BY MODEL DRY-DENSE OTTAWA SAND

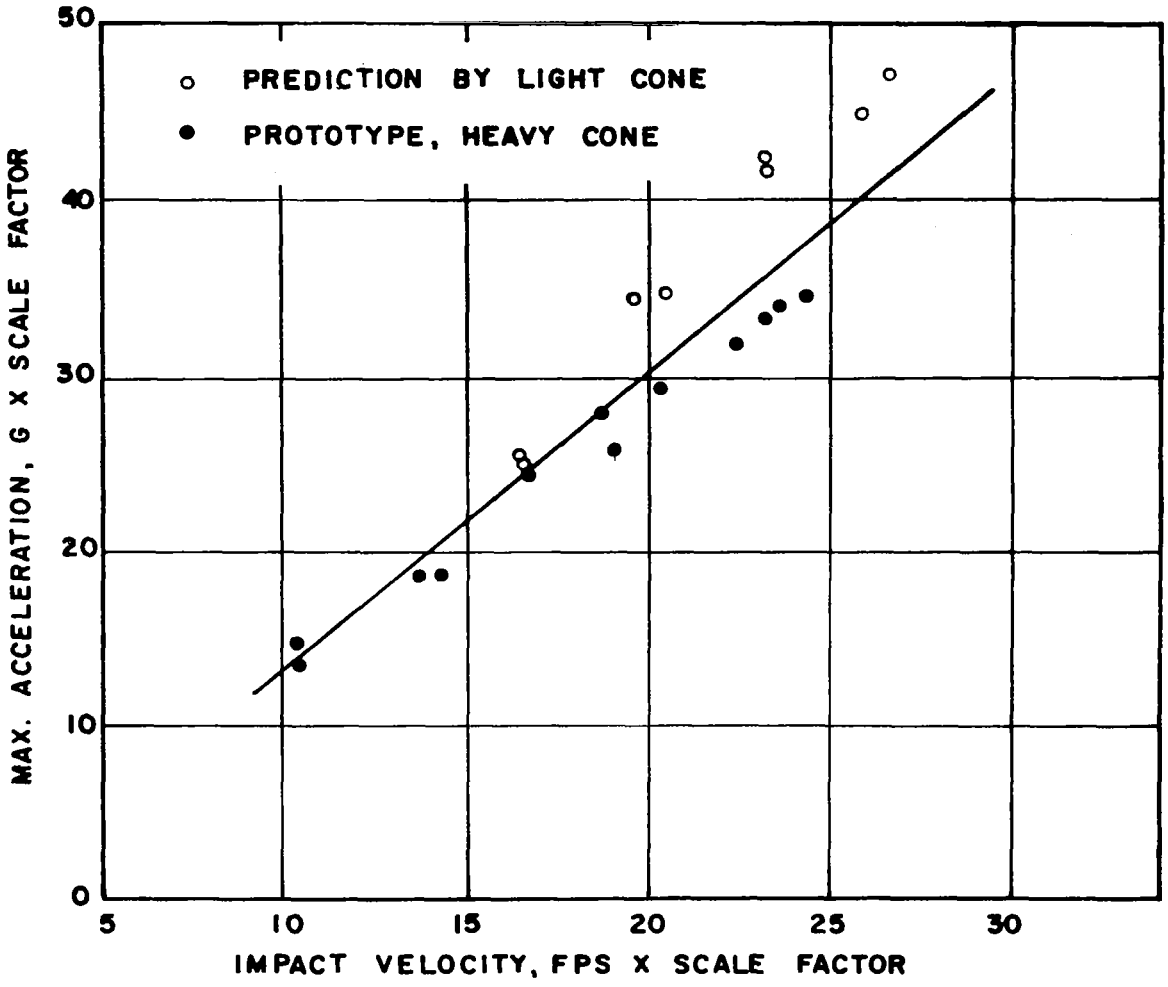

FIG. 3.27 MAX. ACCELERATION VS. IMPACT VELOCITY PROTOTYPE AND PREDICTION BY MODEL SATURATED-DENSE OTTAWA SAND

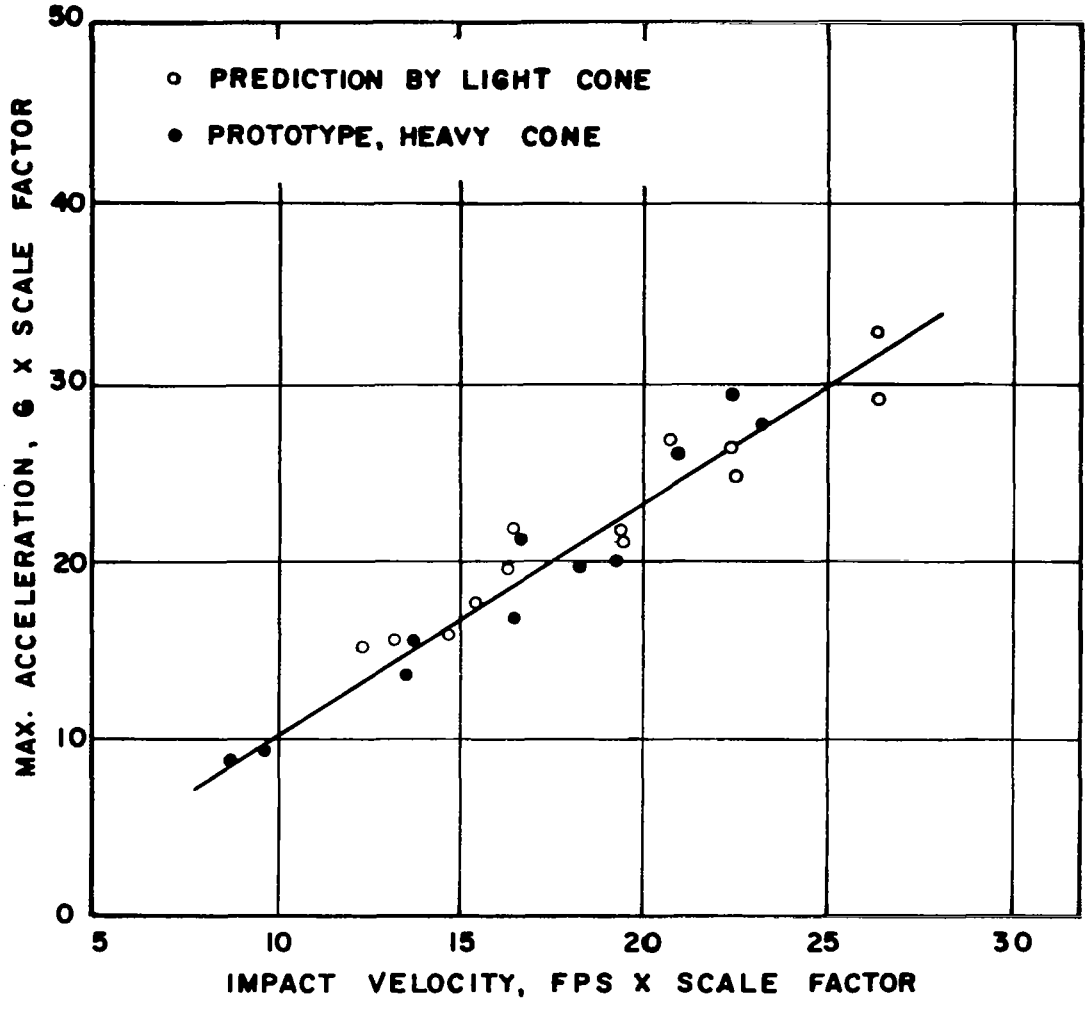

FIG. 3.28 MAX. ACCELERATION VS. IMPACT VELOCITY PROTOTYPE AND PREDICTION BY MODEL DRY-DENSE COLORADO RIVER SAND

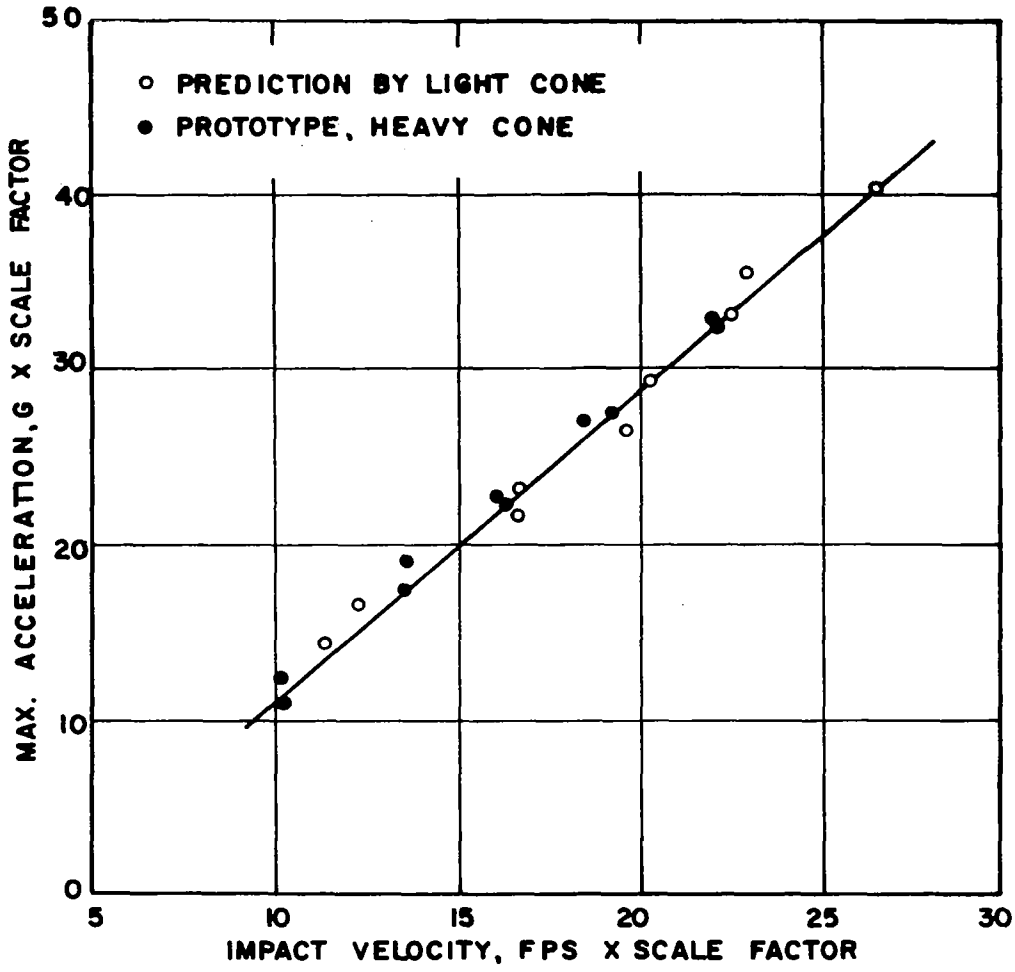

FIG. 3.29 MAX. ACCELERATION VS. IMPACT VELOCITY PROTOTYPE AND PREDICTION BY MODEL SATURATED-DENSE COLORADO RIVER SAND

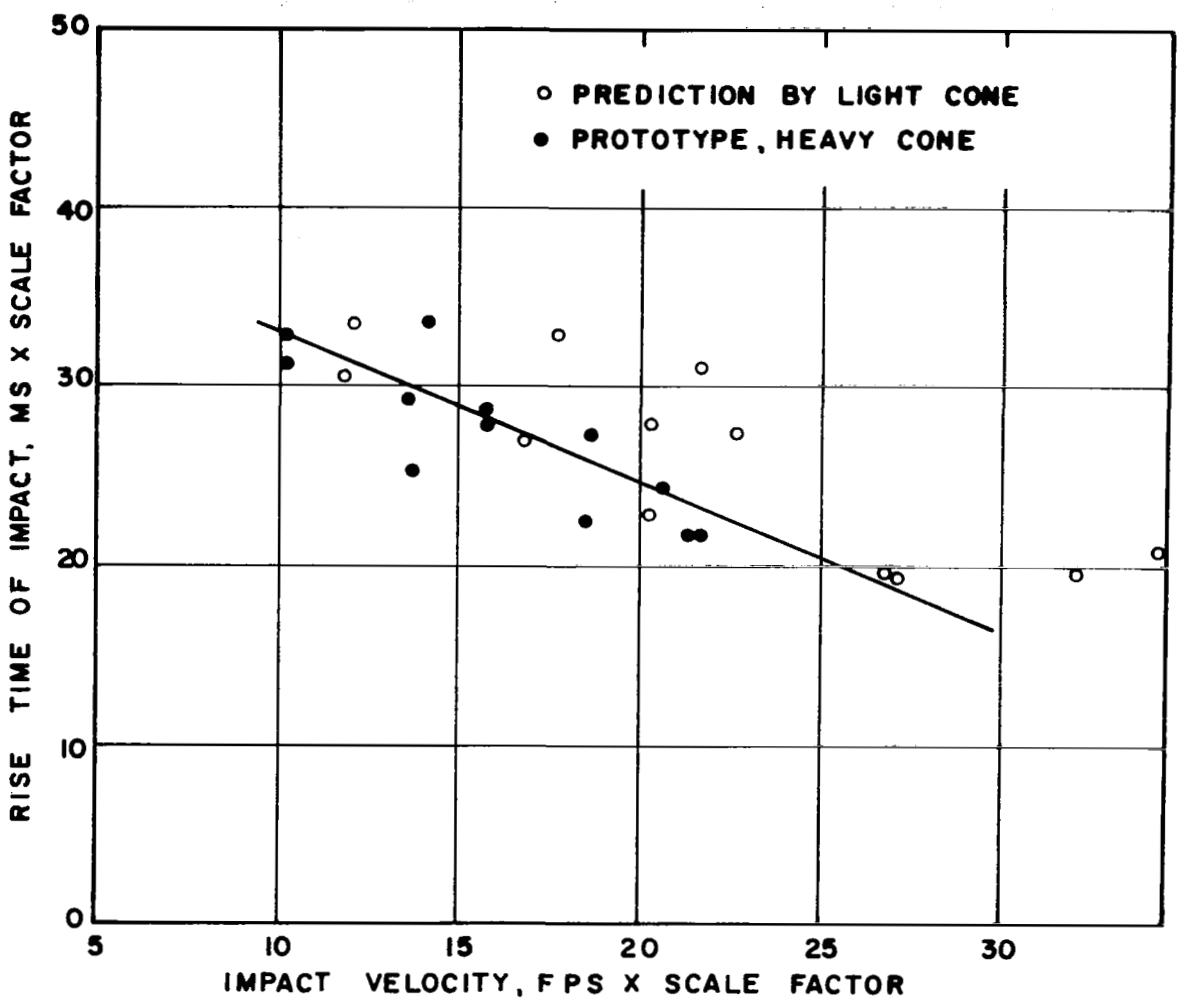

FIG.3.30 RISE TIME OF IMPACT VS. IMPACT VELOCITY PROTOTYPE AND PREDICTION BY MODEL DRY-DENSE OTTAWA SAND

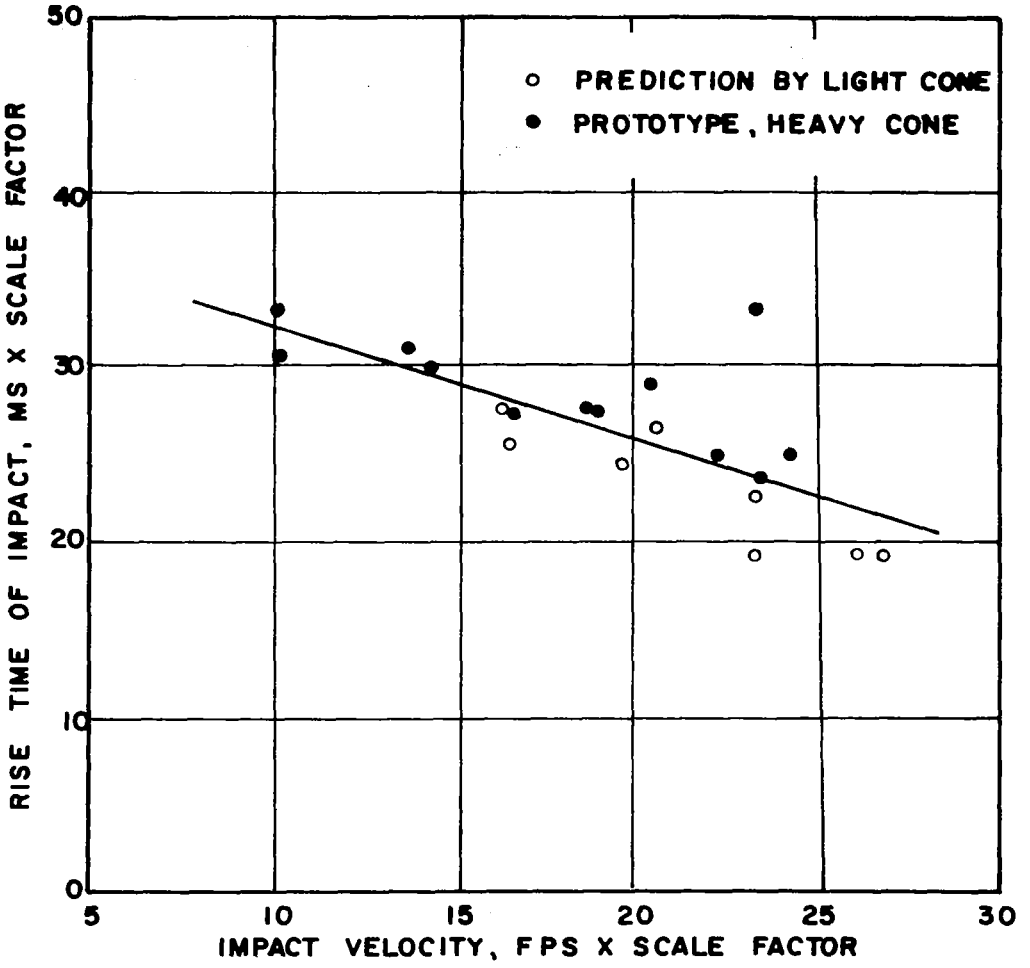

FIG. 3.31 RISE TIME OF IMPACT VS. IMPACT VELOCITY PROTOTYPE AND PREDICTION BY MODEL SATURATED-DENSE OTTAWA SAND

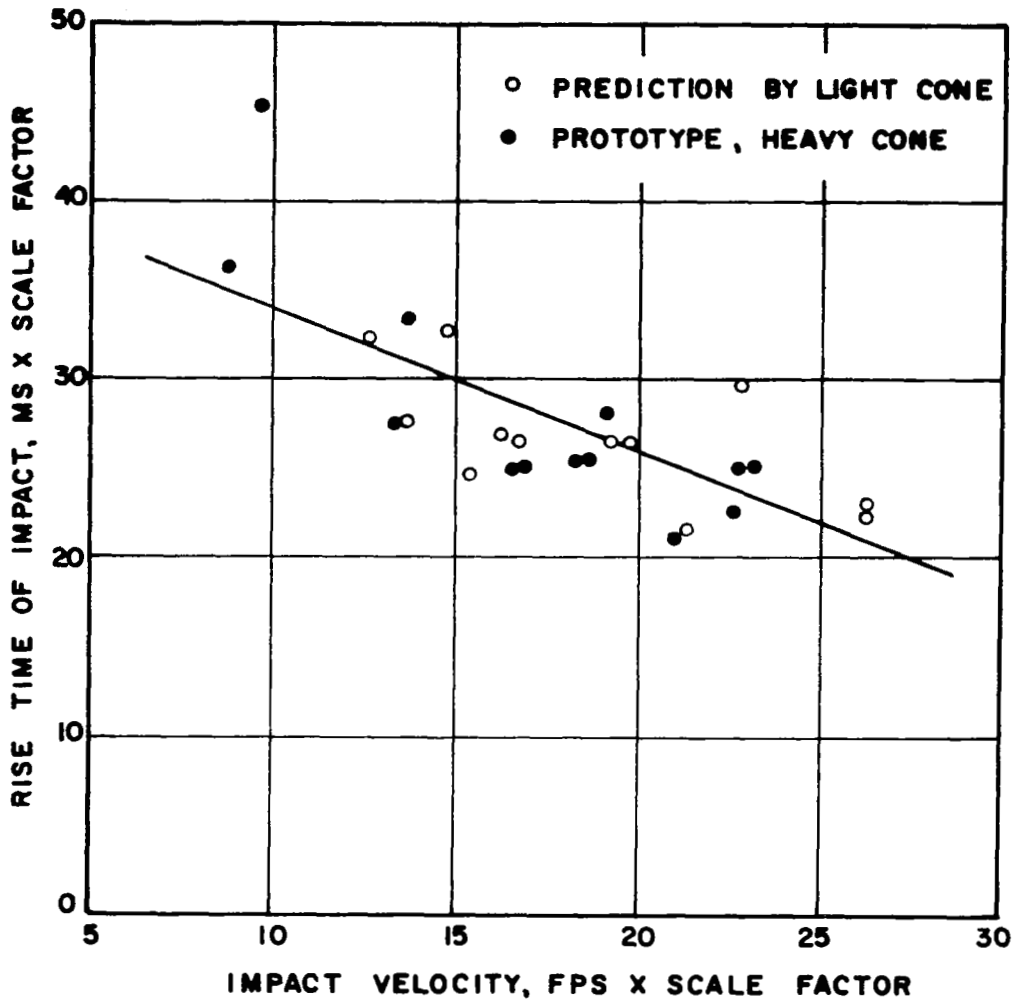

FIG. 3.32 RISE TIME OF IMPACT VS. IMPACT VELOCITY PROTOTYPE AND PREDICTION BY MODEL DRY-DENSE COLORADO RIVER SAND

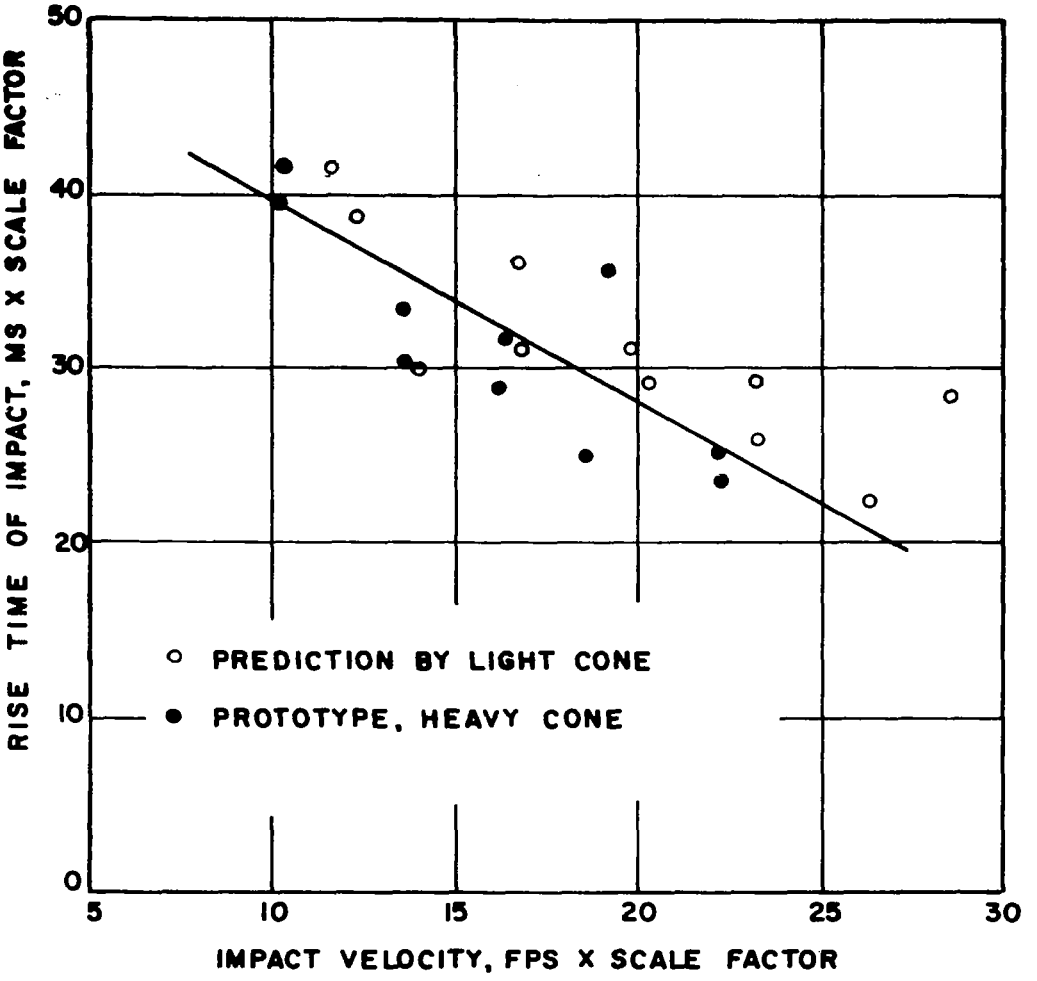

FIG. 3.33 RISE TIME OF IMPACT VS. IMPACT VELOCITY PROTOTYPE AND PREDICTION BY MODEL SATURATED-DENSE COLORADO RIVER SAND

Summary

Comparisons were made between the test results of a prototype and the prediction from its model. The heavy cone was regarded as a prototype and the light cone was regarded as its model.

The identical soil and soil conditions were used for both the prototype and the model. Analysis was carried out for four different kinds of sand beds, namely, the dry-dense Ottawa Sand, the saturated-dense Ottawa Sand, the dry-dense Colorado River Sand and the saturated-dense Colorado River Sand.

The test variables include the penetration depth of a cone, d, maximum acceleration on a cone, a, and the rise time of impact, t. The impact velocity, v, was varied as an operational variable to obtain several sets of data. The agreement between the variables of a prototype and the predictions from its model was good. It can be concluded that the model design law for vertical impact of a cone on dense and saturated sands is valid.

3.7 PREDICTION OF FULL-SCALE MODEL BEHAVIOR

All the scale factors were derived from the ratio of the mass of prototype to the mass of model. The mass ratio in this test was 3.01. The conceived prototype is estimated to weigh about 13,000 lbs.

Assuming the use of light cone (43.0 lbs) to predict the behavior of a full-scale cone weighing 13,000 lbs, the predicted variables are calculated from a test, for instance by the test No. 91, as follows.

Variable	Scale Factor	Light Cone	Full-Scale Cone
Penetration depth of a model, d	n = 6.70	12.0 in.	80.5 in.
Mass of a model, m	n^3 = 302	43.0 lbs	13,000 lbs

Variable	Scale Factor	Light Cone	Full-Scale Cone
Impact velocity of a model, v	$\sqrt{n} = 2.58$	21.3 fps	55.0 fps
Max. acceleration of a model, a	1	18.8 g	18.8 g
Rise time of impact, t	$\sqrt{n} = 2.58$	32.2 msec	83.0 msec

CHAPTER IV

TEST ON CLAYS

4.1 GENERAL

Poor[15] has conducted on clays a series of vertical impact tests of projectiles with various geometric shapes. The feasibility of modeling for impacting projectiles on clays was tested by making use of Poor's test results.

Poor has tested circular plates, cones and spheres. Each type of shape of model has two series of models that have the length scale of 2 and the mass scale of 8. The models were dropped free in the vertical direction to attain an impact velocity of up to about 30 fps.

An oscilloscope was used to record the acceleration time history generated by the same kind of accelerometer as that used in the sand test. The checking of the terminal velocity which was calculated from the acceleration curves, also showed the necessity of correcting the acceleration record. However, the uncorrected record was used by Poor and is used in the analysis here.

4.2 TEST DATA

4.2.1 Soil

The test site was in Austin, Texas. The area was generally composed of an alluvial flood plain of the Colorado River. The soil was classified as a lean clay (CL) of low plasticity. The soil was fairly homogeneous and isotropic to the depth of 7 or 8 ft. The triaxial compression test indicated an apparent cohesion as 5.8 psi and an apparent angle of internal friction of 27 degrees. The liquid limit (LL) of the clay was about 30 percent and the

plastic limit (PL) was about 20 percent. The natural moisture content of the clay was kept constant at about 18 percent by flooding the test site.

4.2.2 Models

The dimensions and weights of all test models are shown in Table 4.1.

TABLE 4.1

MODELS OF VARIOUS GEOMETRIC SHAPES

	Plate		Cone		Sphere	
	Model	Prototype	Model	Prototype	Model	Prototype
Diameter or Radius, in.	10	20			10	20
Apex Angle, deg			60	60		
Weight, lb						
Series A	8.0	64.0	8.0	64.0	8.0	64.0
Series B	16.0	128.0	16.0	128.0	16.0	128.0

As was mentioned at the beginning of this chapter, the smaller model and the larger model (prototype) satisfy the length scale of 2 and the mass scale of 8.

4.3 MODEL LAW

The maximum acceleration of the projectile and the penetration are expressed by the following two equations.

$$\frac{a}{g} = f\left(\frac{c}{\rho v^2}, \left(\frac{\rho}{m}\right)^{1/3} d, \frac{gd}{v^2}, \frac{gt}{v}, \frac{d}{\ell_1}, \frac{\ell_2}{\ell_1}, S, \theta\right) \qquad (5.12)$$

$$\frac{gd}{v^2} = f\left(\frac{c}{\rho v^2}, \left(\frac{\rho}{m}\right)^{1/3} d, \frac{gt}{v}, \frac{a}{g}, \frac{d}{\ell_1}, \frac{\ell_2}{\ell_1}, S, \theta\right) \qquad (5.13)$$

Referring to the section 2.5.2, the distortion of model takes place due to the inability to satisfy the model design condition of the term $\frac{c}{\rho v^2}$. Denoting the prediction factor of the variable $\frac{a}{g}$ as δ_1 and the prediction

factor of the variable $\frac{gd}{v^2}$ as δ_2, the prediction equations for the maximum acceleration and the penetration depth are derived.

$$\delta_1 = \frac{\frac{a_p}{g_p}}{\frac{a_m}{g_m}}$$

$$\frac{a_p}{a_m} = \delta_1 \cdot \left(\frac{g_p}{g_m}\right) = \delta_1 \cdot 1 = \delta_1$$

and

$$\delta_2 = \frac{\left(\frac{gd}{v^2}\right)_p}{\left(\frac{gd}{v^2}\right)_m}$$

$$\frac{d_p}{d_m} = \delta_2 \cdot \left(\frac{g_m}{g_p}\right) \cdot \left(\frac{v_p}{v_m}\right)^2 = \delta_2 \cdot 1 \cdot (\sqrt{n})^2 = \delta_2 \cdot n$$

The scale factors of all the variables are summarized as follows.

Variables	Scale Factors
Cohesion of a soil, c	1
Wet mass density of a soil, ρ	1
Degree of saturation of a soil, S	1
Characteristic length, ℓ_1 and ℓ_2	n = 2.0
Penetration Depth, d	$\delta_2 \cdot n = 2.0\ \delta_2$
Mass of a cone, m	$n^3 = 8.0$
Impact velocity of a cone, v	$\sqrt{n} = 1.41$
Maximum acceleration during impact, a	δ_1

Variables	Scale Factors
Gravitational acceleration, g	1
Rise time of impact, t	$\sqrt{n} = 1.41$

4.4 TEST RESULT AND ANALYSIS

Figures 4.1, 4.2 and 4.3 show the maximum acceleration of a prototype and its model in terms of the impact velocity. Figures 4.4, 4.5 and 4.6 show the impact velocity versus the penetration depth relation of a prototype and the prediction by its model. The prediction of the maximum acceleration was obtained by multiplying the model impact velocity with $\sqrt{n} = 1.41$ and the model maximum acceleration with 1.0. The prediction of the penetration depth was obtained also by multiplying the model impact velocity with $\sqrt{n} = 1.41$ and the model penetration depth with $n = 2.0$. If there is no effect of model distortion on the $\frac{a}{g}$ term and the $\frac{gd}{v^2}$ term, both prediction factors, δ_1 and δ_2, are unity. In this case the plots of a series A test and the series B test must each be a continuous curvilinear relationship. If there is any effect of model distortion, there results an offset of plots of prediction by a model from the curve of its prototype.

There are a few problems in making an analysis of the feasibility of the model law.

One problem is the scattering of the record. Together with this, the scarce number of observations made it difficult to draw certain general relationships out of the test results.

Another problem is the range in impact velocities of test for the model and the prototype. Both the model and the prototype, that is the larger model, were tested in the same impact velocity range of 20 - 30 fps. In order to see the prediction by the model, model impact velocity has to be multiplied by a scale factor of 1.41. As a result the model predicts the

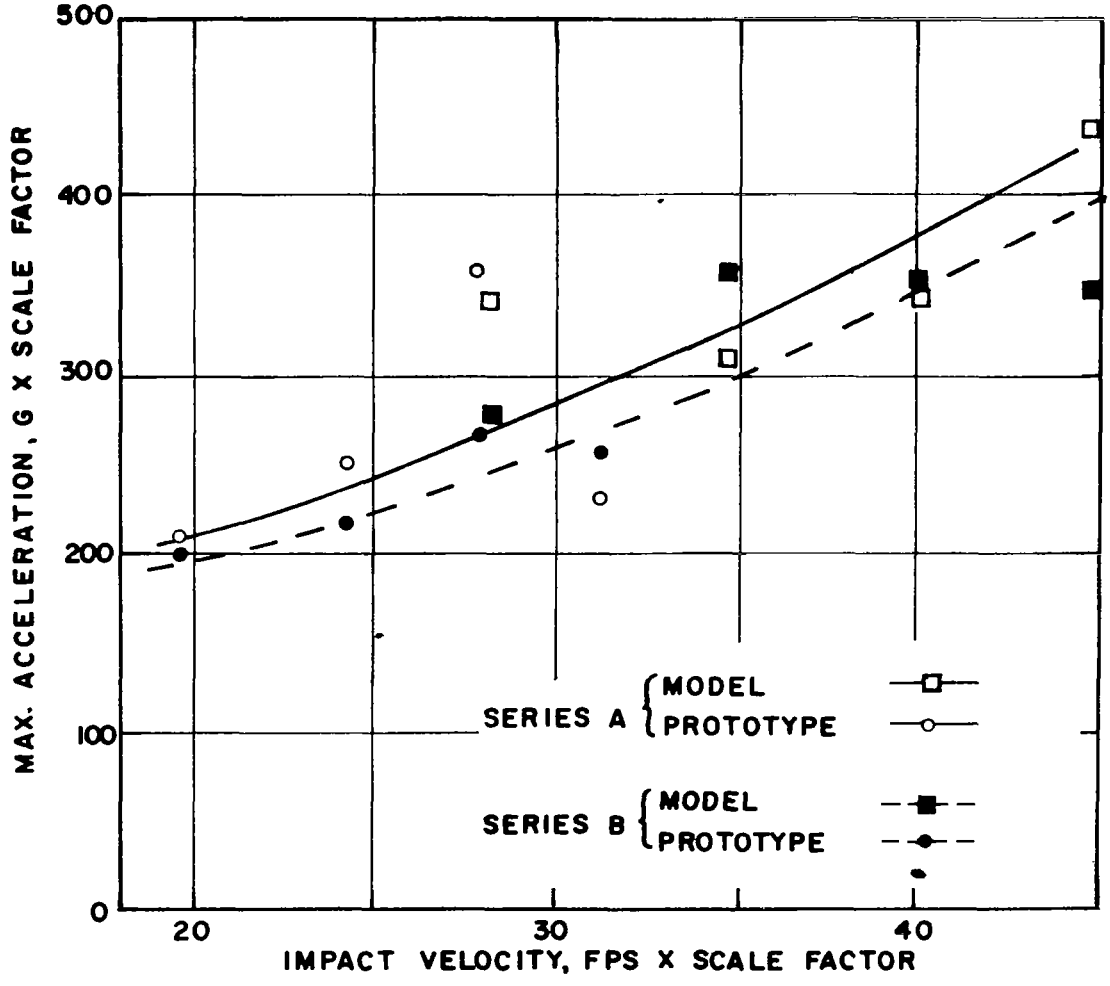

FIG. 4.1 MAX. ACCELERATION VS. IMPACT VELOCITY PROTOTYPE AND PREDICTION BY MODEL CIRCULAR PLATES ON CLAY

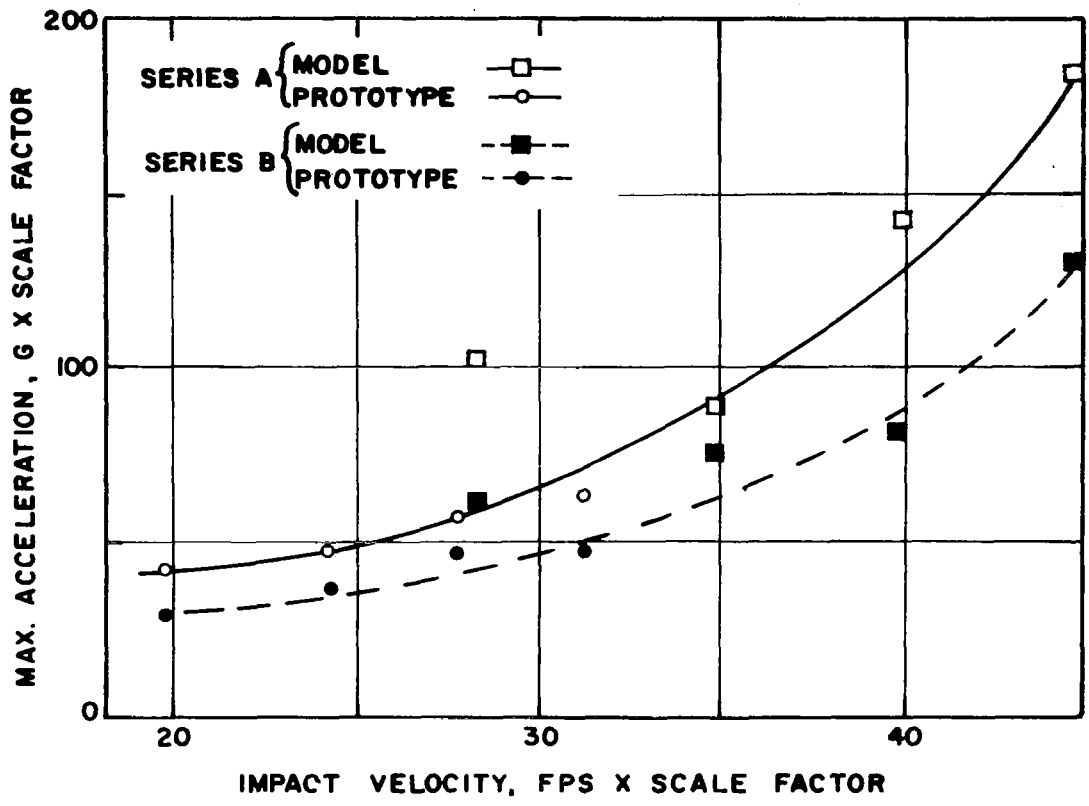

FIG. 4.2 MAX. ACCELERATION VS. IMPACT VELOCITY PROTOTYPE AND PREDICTION BY MODEL CONES ON CLAY

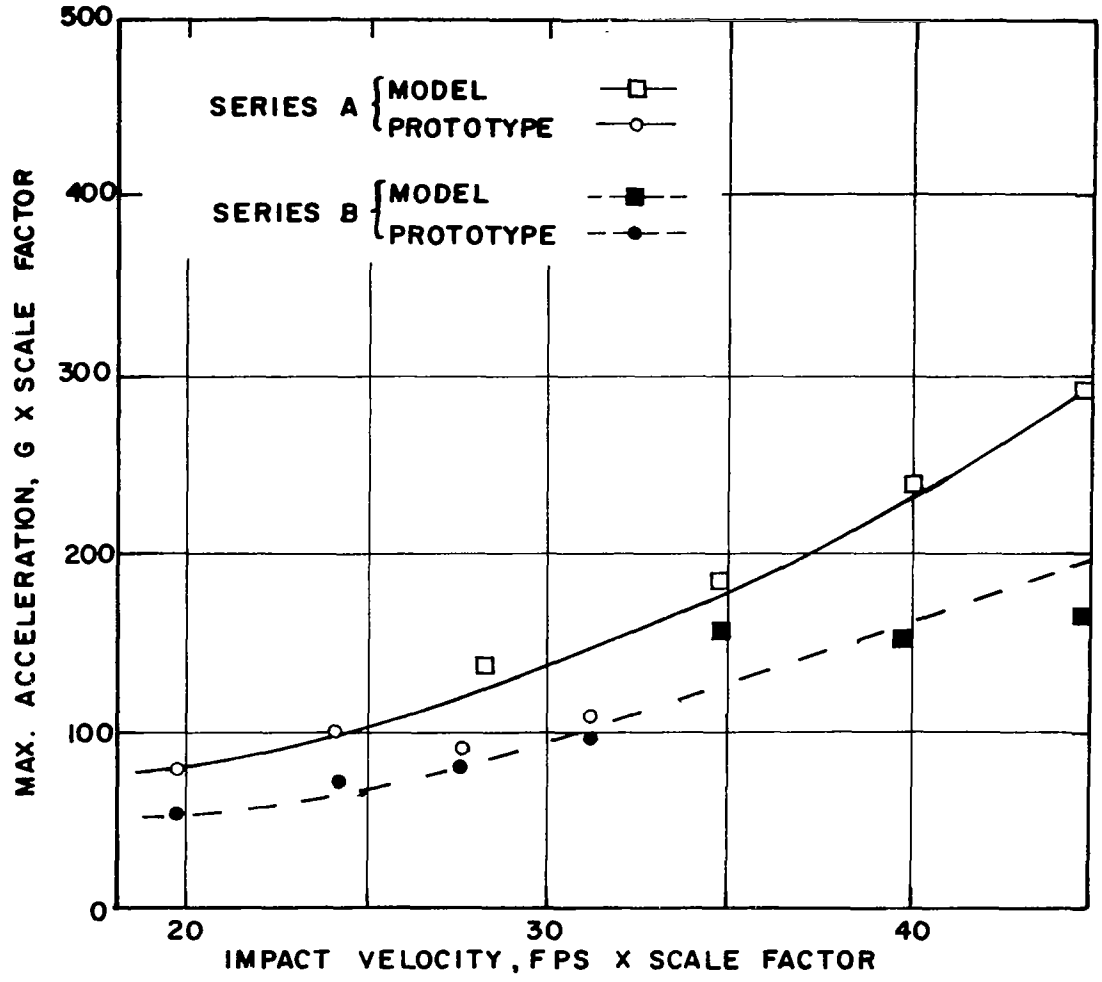

FIG. 4.3 MAX. ACCELERATION VS. IMPACT VELOCITY PROTOTYPE AND PREDICTION BY MODEL SPHERES ON CLAY

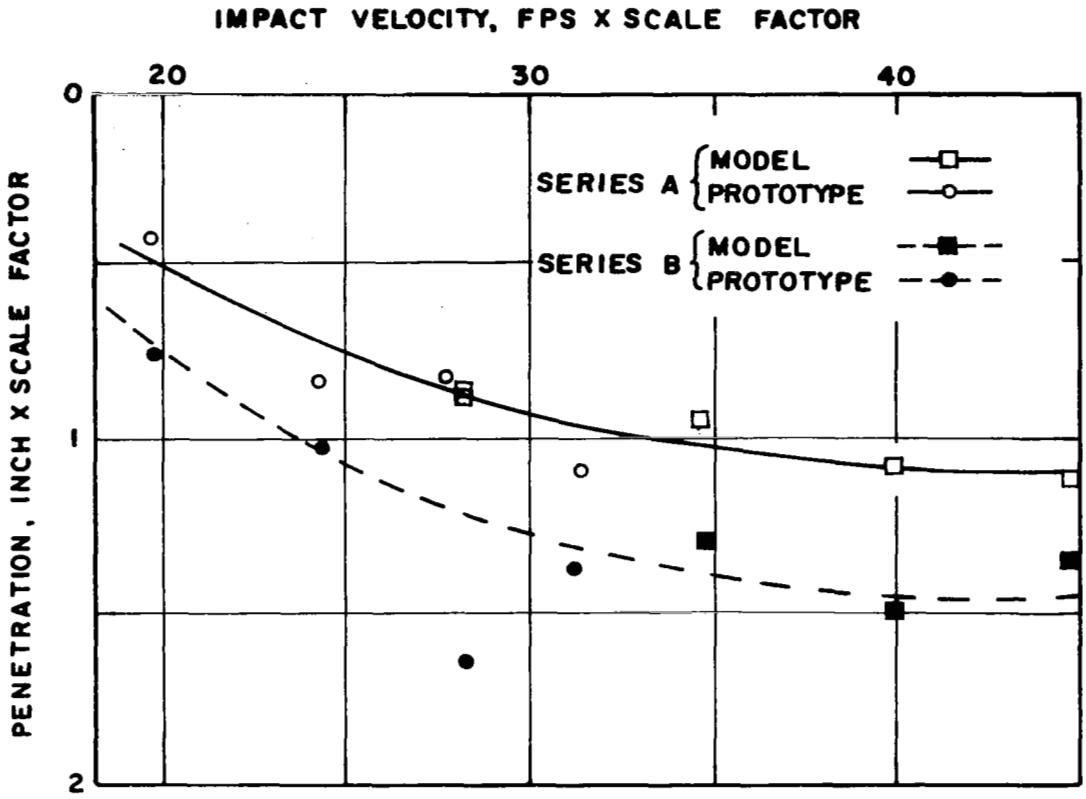

FIG. 4.4 PENETRATION VS. IMPACT VELOCITY PROTOTYPE AND PREDICTION BY MODEL CIRCULAR PLATES ON CLAY

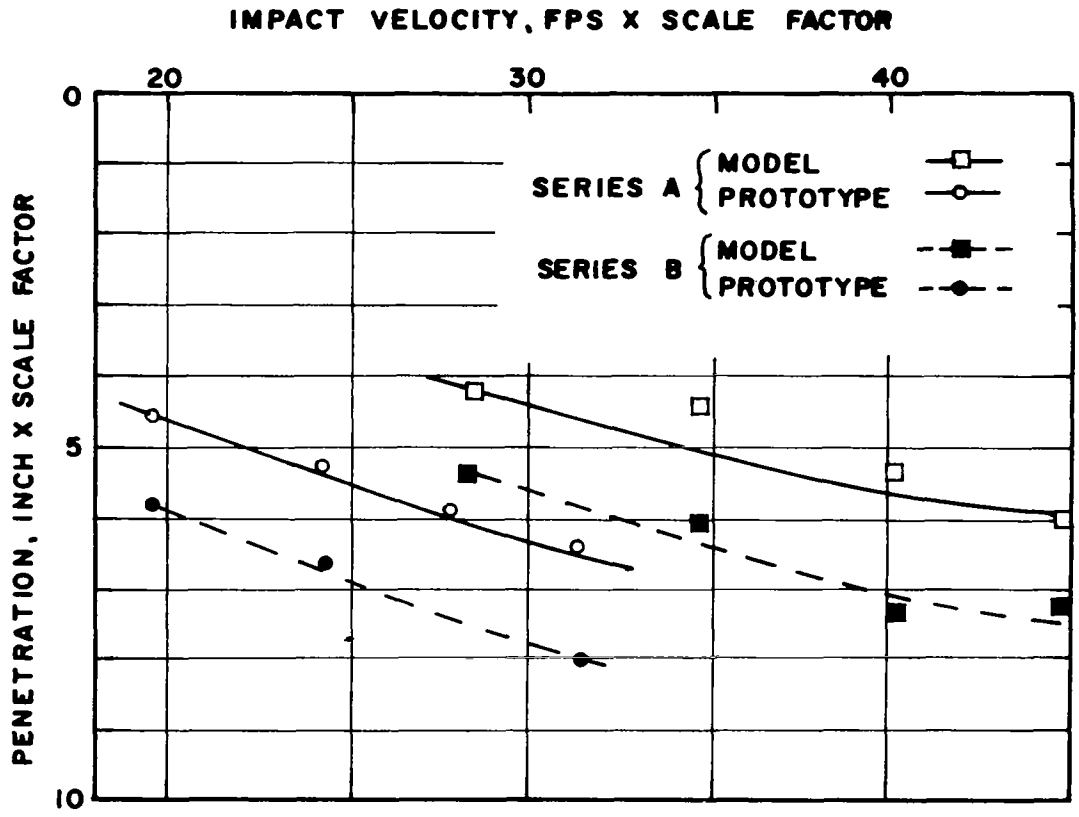

FIG. 4.5 PENETRATION VS. IMPACT VELOCITY PROTOTYPE AND PREDICTION BY MODEL CONES ON CLAY

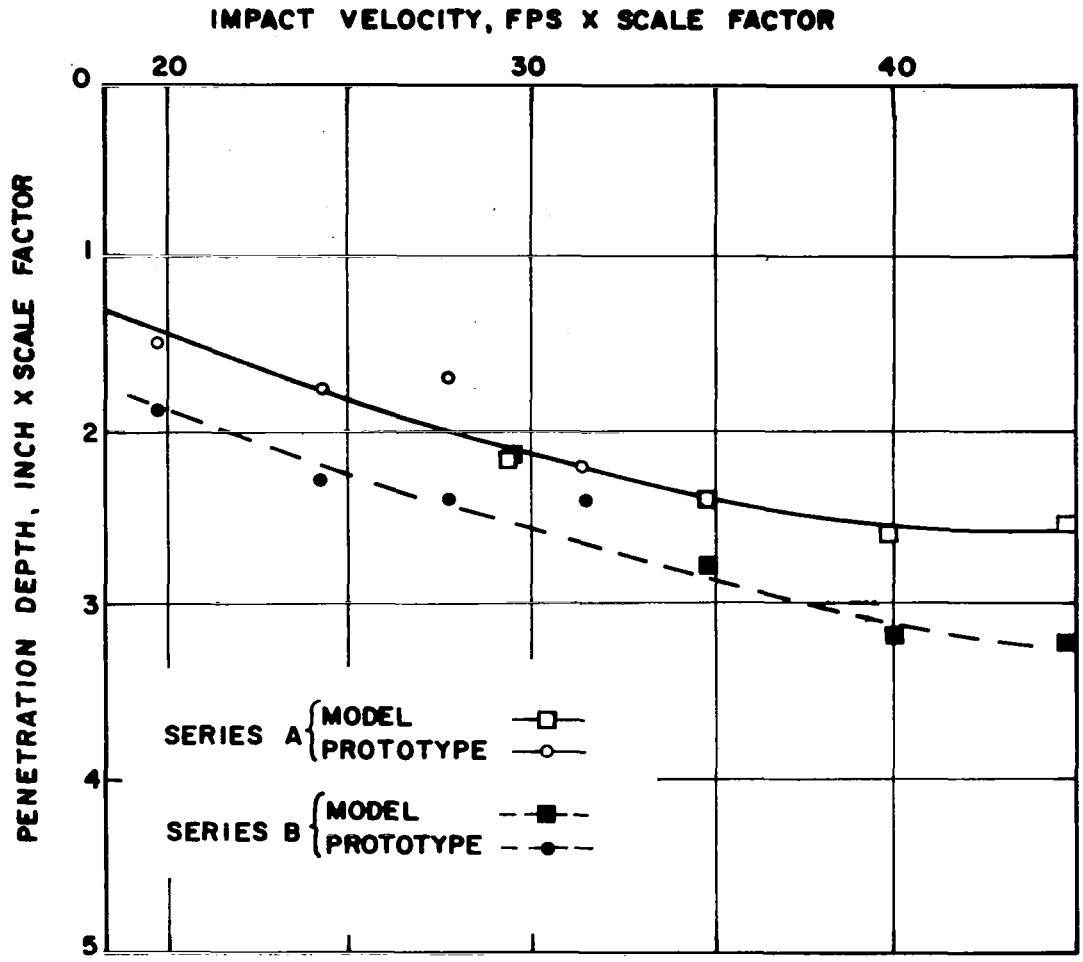

FIG. 4.6 PENETRATION VS. IMPACT VELOCITY PROTOTYPE AND PREDICTION BY MODEL SPHERES ON CLAY

prototype in the impact velocity range of 28 - 42 fps. Then the real correspondence is only checked at the prototype impact velocity of 30 fps. For the rest of the impact velocity range, the agreement between the prototype and the prediction by the model is only checked by extrapolation.

In Figs. 4.1 through 4.6, the solid lines and the broken lines were drawn intuitively just to indicate the tendencies between the plottings.

These plottings may be too scattered to draw any conclusions about the feasibility of the model design law. However, the general tendencies observed in the plottings encourage the fruitful application of dimensional model design method to the vertical impact of projectiles with various geometric shapes on clays.

CHAPTER V

SUMMARY AND CONCLUSIONS

5.1 PROCEDURE OF MODEL DESIGN BY SIMILITUDE

5.1.1 Pertinent Variables

There are many variables involved in the phenomenon of a projectile-soil impact. In a study of the response of impact, it is desirable to select only those variables which are believed to have significant influence on the response.

The selections of pertinent variables for this study were guided by the following assumptions:

a. projectile is a rigid body,

b. elastic properties of a soil do not influence the dynamic behavior,

c. static strength is expressed in terms of angle of internal friction, ϕ, and cohesion, c, and

d. failure mechanism of a soil is analogous to the classical failure mechanism described by Prandtl.

5.1.2 General Procedures

The procedures used in this study for model design by similitude can be summarized as follows:

Step 1 Select the pertinent variables

1. Cohesion of a soil (FL^{-2}), c
2. Angle of internal friction of a soil (dimensionless), ϕ
3. Wet mass density of a soil ($FL^{-4}T^{2}$), ρ
4. Degree of saturation of a soil (dimensionless), S
5. Apex angle of a projectile (dimensionless), θ

6. First characteristic length of a projectile (L), ℓ_1
7. Second characteristic length of a projectile (L), ℓ_2
8. Mass of a projectile ($FL^{-1}T^2$), m
9. Penetration depth of a projectile (L), d
10. Impact velocity of a projectile (LT^{-1}), v
11. Maximum acceleration on a projectile (LT^{-2}), a
12. Gravitational acceleration (LT^{-2}), g
13. Rise time of impact (T), t

Step 2 Form dimensionless products by means of Buckingham π Theorem.

There are several choices available for combinations of π terms. One combination of π terms is given as,

$$\pi_1 = \frac{c}{\rho v^2}, \quad \pi_2 = \left(\frac{\rho}{m}\right)^{1/3} d, \quad \pi_3 = \frac{gd}{v^2}, \quad \pi_4 = \frac{gt}{v}$$

$$\pi_5 = \frac{a}{g}, \quad \pi_6 = \frac{d}{\ell_1}, \quad \pi_7 = \frac{\ell_2}{\ell_1}, \quad \pi_8 = \phi$$

$$\pi_9 = S, \quad \text{and} \quad \pi_{10} = \theta$$

Upon formation of π terms, the whole system is expressed in the most general form by an equation,

$$f(\pi_1, \pi_2, \ldots, \pi_{10}) = 0$$

or

$$f\left(\frac{c}{\rho v^2}, \left(\frac{\rho}{m}\right)^{1/3} d, \frac{gd}{v^2}, \frac{gt}{v}, \frac{a}{g}, \frac{d}{\ell_1}, \frac{\ell_2}{\ell_1}, \phi, S, \theta\right) = 0 \qquad (5.1)$$

Step 3 Select the necessary π Terms.

The soil condition and the geometry of projectile may indicate that certain π terms have little significance and may be eliminated from Eq 5.1.

Sand Neglect $\pi_1 = \frac{c}{\rho v^2}$.

Clay Neglect $\pi_8 = \phi$.

Cone Neglect $\pi_6 = \frac{d}{\ell_1}$ and $\pi_7 = \frac{\ell_2}{\ell_1}$.

Circular Plate Neglect $\pi_7 = \frac{\ell_2}{\ell_1}$ and $\pi_{10} = \theta$.

Define ℓ_1 = radius of plate.

Rectangular Plate Neglect $\pi_{10} = \theta$.

Define ℓ_1 = width of plate

ℓ_2 = length of plate.

Wedge Neglect $\pi_7 = \frac{\ell_2}{\ell_1}$.

Define ℓ_1 = width of wedge.

Sphere Neglect $\pi_7 = \frac{\ell_2}{\ell_1}$ and $\pi_{10} = \theta$.

Define ℓ_1 = radius of curvature of sphere.

Step 4 Derive Scale Factors of Pertinent Variables.

The scale factors of pertinent variables are derived from the π terms by using the following conditions:

a. the same gravitational acceleration (on earth)

b. the same soil.

Sand For example, the scale factors for the test of a sphere on a sand are as follows.

Pertinent Variables	Scale Factor
1. Angle of internal friction of a sand, ϕ	1
2. Wet mass density of a sand, ρ	1
3. Degree of saturation of a sand, S	1
4. Radius of curvature of a sphere, ℓ_1	n
5. Mass of a sphere, m	n^3
6. Penetration depth of a sphere, d	n
7. Impact velocity of a sphere, v	$\sqrt{n}$
8. Max. acceleration on a sphere, a	1
9. Gravitational acceleration, g	1
10. Rise time of impact, t	$\sqrt{n}$

where n = the length scale.

Clay The condition of the same mass density will force distortion of the term $\pi_1 = \frac{c}{\rho v^2}$. In order to correct the effect of the distortion, a prediction factor, which can be obtained experimentally, has to be used for the variables that predict the prototype behavior.

The scale factors for a test of a sphere on a clay are shown below,

Pertinent Variables	Scale Factor
1. Cohesion of a clay, c	1
2. Wet mass density of a clay, ρ	1
3. Degree of saturation of a clay, S	1
4. Radius of curvature of a sphere, ℓ_1	n
5. Mass of a sphere, m	n^3
6. Penetration depth of a sphere, d	δ_1 n
7. Impact velocity of a sphere, v	$\sqrt{n}$

Pertinent Variables	Scale Factor
8. Max. acceleration on a sphere, a	δ_2
9. Gravitational acceleration, g	1
10. Rise time of impact, t	$\delta_3 \sqrt{n}$

where n = length scale, δ_1, δ_2 and δ_3 are prediction factors.

Step 5 Determine the Dimensions of Model.

Once the dimensions of a prototype is given, the weight and the configurations of its model are obtained by dividing the prototype dimensions with the appropriate scale factors.

Step 6 Prediction by Model

Prediction of model behaviors, such as the maximum acceleration, penetration depth and rise time of impact, are obtained by multiplying the model behaviors with the appropriate scale factors.

5.1.3 Model Design

Projectile

There is little difficulty in designing a rigid model of a projectile since the rigid model only has to satisfy the specified mass scale factor and the length scale factor at the contacting surface.

Soil

If it is attempted to model the prototype soil with a different material, it will be difficult to find a model soil which satisfies the scale factors for such properties as mass density, cohesion, degree of saturation and angle of internal friction.

If the identical soil is used for both the prototype and its model, the scale factors are automatically satisfied for the dimensionless soil

properties, such as the degree of saturation and the angle of internal friction.

There is a disadvantage in the use of the identical soil. Clayey soils cause distortion of the model and the test results require corrections to get the true prediction of the prototype. These corrections, or prediction factors, can be determined experimentally. Since the prediction factor is a function of the distortion factor and all of the soil properties, the prediction factor has to be determined for each particular soil. This disadvantage is not sufficient to discourage use of the same soil in model and prototype tests.

5.2 VALIDITY OF MODEL DESIGN

5.2.1 Method of Checking the Validity of Model Design

The validity of model design was tested by means of comparing the prototype behavior and the prediction by its model. If the model design were right, both the prototype behavior and the prediction by its model should agree.

The judgment of agreement was done by inspecting the plottings of pertinent variables. For a more rigorous check, an analytical method such as regression analysis, may be used to test if there is significant difference between the behavior of the prototype and the prediction by its model.

For the purpose of checking the validity of model design, it is desirable to test the full-scale prototype. If it is impractical to test a full-scale prototype, a hypothetical prototype can be used. The hypothetical prototype is another scaled model. The hypothetical prototype should be as close in size to the full-scale prototype as possible.

In this study the hypothetical prototypes, in the shapes of cone, circular plate and sphere, weighed from 64.0 to 129.5 lbs. Assuming the

weight of a full-scale prototype as 13,000 lbs, these hypothetical prototypes were scaled down in weight or mass by factors from 203 to 100. This is equivalent to a scaling down in length by factors from 5.9 to 4.6. In this study the mass scale factors of models to the hypothetical prototypes were 3.0 and 8.0, which correspond to length scales of 1.44 and 2.0. A comparison of these scale factors will indicate that even a few drop tests of a full-scale prototype would contribute a great deal for checking the validity of model design procedures.

The pertinent variables used for the comparisons are the penetration depth, maximum acceleration, rise time of impact, and impact velocity of the projectile. For each set of comparisons, only the impact velocity was varied to see the response of projectile. All the soil properties and the geometry and mass of projectile were held constant.

5.2.2 Sand

In sand the disparity between the plottings of prototype and that of model before the application of scale factors is evident in Figs. 3.10 through 3.21. After the application of scale factors to the model variables, the plottings of both the prototype and the model are seen in Figs. 3.22 through 3.33 to center around a common line and it can be said that the agreement is good.

From details of these plottings, it is observed that plottings may be represented by straight lines. The scattering of plotting is small for the penetration and the maximum acceleration. The scattering in the plottings of rise time of impact are somewhat greater.

5.2.3 Clay

Due to lack of adequate data, a conclusive analysis was not possible

of drop tests in clay. However, the usefulness of modeling by similitude in clay soils may be proven in future experiments.

5.3 PREDICTION EQUATION

Once the validity of modeling is verified, a model can be used to predict prototype behavior without aid of a mathematical model or a form of function expressing the phenomenon. The prediction of prototype behavior by its model is made in one-to-one correspondence. In other words, the π terms of the prototype and its model are the same in value. Therefore, a model has to be designed for each set of values of prototype terms and the prediction by a model is restricted to a single state of the prototype.

In order to develop a more general prediction method, the effects of π terms or combinations of π terms must be known to determine the form of Eq 5.1. In the present study, for instance, the cone test on sands is expressed by an equation,

$$f\left(\left(\frac{\rho}{m}\right)^{1/3} d,\ \frac{gd}{v^2},\ \frac{gt}{v},\ \frac{a}{g},\ \phi,\ S,\ \theta\right) = 0 \qquad (5.2)$$

The experiment was carried out keeping constant the π term related to the apex angle of cone, θ. The π terms related to the angle of internal friction of soil, ϕ, and the degree of saturation of soil, S, were varied in two stages. If the form of Eq 5.2 is determined, a generality of the equation exists only on the conditions of constant θ, ϕ and S. If a number of tests are carried out with systematically planned combinations of values of all π terms, the generality of Eq 5.2 is broadened.

5.4 EXPERIMENTAL TECHNIQUE

5.4.1 Soil

Sand Bed

In these tests there was a significant variation of density in the sand beds. The degree of density variation was the greatest for dry-loose sands. Better control of the state of sands would be desirable in any future testing. The procedure for preparing the sand beds must remain practical and should not be time-consuming.

5.4.2 Launching Device

The launching device used in this experiment had previously been designed and used for a projectile-soil impact study which involved wide ranges of launch angle and impact velocity. The device had great mobility and versatility.

The device had certain characteristics which were undesirable for the vertical drop tests in this study. The deflection of the track and the bouncing of the whole system gave a disturbing effect on the test conditions. The mechanism of jaws that hold the model failed to provide a smooth release and this caused a slight rotational movement of the model.

For tests involving only vertical drops a simpler and more stable launching device could be used.

5.4.3 Instrumentation

Accelerometer

The accelerometer record is essential for the test, and yet the acceleration record involved an irregular deviation. Additional work is required to determine the reason for the deviation in the accelerometer record.

Velocity Detector

The velocity detector itself functioned perfectly. Only the bouncing of the launching device on which the velocity detector pickup was mounted disturbed the velocity measurements.

APPENDIX I - TEST DATA

TABLE 1-A

TEST RESULTS IN DRY-LOOSE OTTAWA SAND

No.	Model Type	Nominal Velocity fps	Measured Velocity fps	Pene-tration Inch	Max. Force kip	Max. Acc. g	Wet Unit Wt. of Soil pcf	Dry Unit Wt. of Soil pcf	Water Content %	Rise Time ms	Correction Factor for Acc. and Force
1	L	10	9.8	10.0	0.24	5.5	93.2	91.8	1.65	50.7	1.25
2	L	10	9.9	9.9	0.22	5.1	82.9	81.6	1.57	54.9	1.18
3	L	14	15.4	12.8	0.21	4.8	94.4	93.2	1.37	22.2	1.00
4	L	14	14.0	12.0	0.29	6.7	90.5	89.7	0.83	55.6	1.35
5	L	15	16.0	11.6	0.44	10.3	96.9	94.1	2.95	44.0	1.41
6	L	15	15.8	11.2	0.38	8.9	90.5	89.1	1.56	33.8	1.54
7	L	15	16.0	12.5	0.46	10.6	92.7	91.2	1.65	46.5	1.41
8	L	19	18.0	12.7	0.46	10.7	98.7	97.9	0.87	36.2	1.70
9	L	19	17.8	12.0	0.47	11.0	91.7	89.9	2.01	40.3	1.61
10	L	23	21.5	13.8	0.49	11.3	93.2	91.5	1.86	32.7	1.28
11	L	23	22.0	13.9	0.64	14.9	89.4	88.0	1.64	48.7	1.62
12	L	30	26.4	15.6	0.70	16.3	90.2	88.8	1.56	48.6	1.33
13	L	30	25.9	14.2	0.79	18.3	81.3	79.6	2.14	45.2	1.24
14	H	10	9.8	14.4	0.63	4.9	92.0	91.1	0.94	77.8	1.23
15	H	10	9.7	14.5	0.67	5.1	88.8	87.8	1.01	78.3	1.28
16	H	13	13.2	16.3	0.98	7.5	89.3	88.4	1.03	69.1	1.17
17	H	14	13.3	13.0	1.27	9.8	89.3	88.4	1.01	63.3	1.38
18	H	14	13.1	15.8	1.45	11.3	86.9	85.5	1.60	69.1	1.34
19	H	14	14.2	19.4	1.10	8.5	92.4	91.6	0.83	67.1	1.40
20	H	17	14.7	16.5	1.29	10.0	86.6	85.6	1.09	76.4	1.46
21	H	17	15.4	15.8	1.71	13.3	86.0	85.1	1.10	50.4	1.59
22	H	17	16.1	16.0	1.54	11.9	85.7	84.9	1.00	61.5	1.49
23	H	19	17.9	16.4	2.09	16.2	88.7	87.8	1.09	46.5	1.27
24	H	19	16.8	15.6	2.17	17.8	90.1	89.2	1.05	50.0	1.20
25	H	19	17.2	15.6	1.93	14.9	83.5	82.4	1.34	50.7	1.23
26	H	23	21.2	15.3	2.36	18.2	91.7	90.9	0.83	51.3	1.33

TABLE 1-A (CONT.)

No.	Model Type	Nominal Velocity fps	Measured Velocity fps	Pene-tration Inch	Max. Force kip	Max. Acc. g	Wet Unit Wt. of Soil pcf	Dry Unit Wt. of Soil pcf	Water Content %	Rise Time ms	Correction Factor for Acc. and Force
27	H	23	19.6	16.1	2.77	21.3	86.7	86.0	0.84	44.6	1.20
28	H	23	21.3	16.0	2.41	18.6	89.3	88.3	1.10	55.6	1.25
29	H	23	20.5	16.1	2.50	19.9	90.4	88.5	0.97	44.8	1.26
30	H	30	22.8	18.9	2.85	22.0	93.1	92.0	1.13	44.4	1.14
31	H	30	23.7	17.2	2.71	21.0	88.3	87.3	1.17	46.5	1.25
32	H	30	23.8	16.7	3.52	27.1	86.2	85.3	1.05	42.0	1.17

Weight of Model Type L 43.0 lbs
Type H 129.5 lbs

TABLE 1-B

TEST RESULTS IN DRY-DENSE OTTAWA SAND

No.	Model Type	Nominal Velocity vps	Measured Velocity fps	Pene-tration Inch	Max. Force kip	Max. Acc. g	Wet Unit Wt. of Soil pcf	Dry Unit Wt. of Soil pcf	Water Content %	Rise Time ms	Correction Factor for Acc. and Force
33	L	10	9.9	4.8	0.52	12.1	105.2	103.8	1.33	25.4	1.05
34	L	10	10.0	5.2	0.47	10.8	103.6	102.4	1.14	27.9	1.04
35	L	14	14.0	5.1	0.81	19.0	104.7	103.9	0.72	22.4	1.17
36	L	14	14.7	5.9	0.70	16.2	106.2	105.4	0.81	27.3	1.19
37	L	15	16.7	5.6	1.00	23.2	101.8	100.4	1.38	23.2	1.08
38	L	15	16.8	5.5	1.06	24.8	100.2	99.1	1.07	19.0	1.15
39	L	19	18.0	5.4	0.99	23.1	104.7	103.3	1.34	25.7	1.04
40	L	19	18.9	5.6	1.16	26.9	101.9	100.9	0.95	22.6	1.23
41	L	23	22.5	5.7	1.59	36.9	107.5	105.1	2.29	15.9	1.27
42	L	23	22.4	6.3	1.48	34.5	106.6	104.7	1.79	16.3	1.25
43	L	30	28.5	7.2	1.76	40.9	106.8	105.0	1.73	16.9	1.15
44	L	30	26.8	7.4	1.70	39.6	101.3	99.7	1.63	16.1	1.16
45	H	10	10.2	6.6	1.34	10.4	101.6	100.7	0.85	32.9	1.10
46	H	10	10.2	7.1	1.35	10.4	103.2	102.2	1.00	31.0	1.12
47	H	14	13.8	7.1	1.75	13.5	102.4	101.5	0.80	29.2	1.23
48	H	14	13.9	7.6	1.90	14.6	103.6	102.6	1.00	25.0	1.18
49	H	14	14.1	7.4	1.87	14.5	105.9	105.0	0.92	33.6	1.24
50	H	15	15.8	8.1	1.96	15.2	108.3	106.2	1.99	28.4	0.96
51	H	15	15.8	7.7	2.06	15.9	102.6	101.9	0.69	27.4	1.05
52	H	19	18.5	8.3	2.63	20.4	96.5	95.7	0.77	22.1	1.18
53	H	19	18.8	7.8	2.68	20.7	103.8	103.3	0.52	27.2	1.19
54	H	23	20.7	8.3	2.95	22.7	105.2	104.7	0.52	24.3	1.20
55	H	23	21.2	8.6	3.20	24.6	103.9	103.4	0.45	21.6	1.23
56	H	23	21.5	9.1	3.09	23.9	105.7	105.2	0.47	21.6	1.19

TABLE 1-C

TEST RESULTS IN SATURATED-DENSE OTTAWA SAND

No.	Model Type	Nominal Velocity fps	Measured Velocity fps	Pene-tration Inch	Max. Force kip	Max. Acc. g	Wet Unit Wt. of Soil pcf	Dry Unit Wt. of Soil pcf	Water Content %	Rise Time ms	Correction Factor for Acc. and Force
57	L	10	9.7	3.4	0.98	22.8	138	115	19.16	47.5	1.00
58	L	10	9.1	3.3	0.89	20.7	136	114	19.88	47.5	1.00
59	L	14	13.7		0.92	25.5	140	116	20.27	23.0	1.11
60	L	14	13.8	3.7	1.11	25.5	136	114	18.99	21.4	1.12
61	L	17	17.1	4.6	1.52	35.4	135	112	19.81	21.7	1.04
62	L	17	16.4	3.9	1.48	34.2	135	113	19.25	20.1	1.17
63	L	19	19.4	4.0	1.78	41.4	134	112	19.50	15.7	1.02
64	L	19	19.4	4.3	1.82	42.3	139	117	18.65	18.7	1.05
65	L	23	22.3	4.6	2.02	47.0	135	113	18.85	15.8	1.13
66	L	23	21.7	4.5	1.93	45.0	132	111	18.70	15.8	1.12
67	H	10	10.1	5.3	1.87	14.4	141	119	18.50	33.3	1.02
68	H	10	10.3	5.0	1.75	13.5	141	118	19.31	30.8	0.99
69	H	14	14.1	5.5	2.38	18.4	142	118	19.94	30.0	0.89
70	H	14	13.9	5.6	2.41	18.7	132	111	19.71	30.8	0.97
71	H	17	20.4	6.3	3.78	29.0	135	114	19.10	29.2	1.25
72	H	17	16.8	5.6	3.14	24.2	135	114	19.24	27.3	1.14
73	H	19	19.0	6.8	3.32	25.7	135	114	18.70	27.3	1.06
74	H	19	18.8	6.5	3.52	27.4	138	116	19.71	27.3	1.15
75	H	23	23.5	6.7	4.37	33.8	133	112	18.75	23.6	1.14
76	H	23	24.2	7.5	4.45	34.2	138	116	19.07	25.0	1.16
77	H	23	22.3	7.3	4.06	31.4	136	114	19.27	25.0	1.17
78	H	23	23.3	7.6	4.28	33.2	132	110	20.01	33.3	1.24

TABLE 1-D

TEST RESULTS IN DRY-LOOSE COLORADO RIVER SAND

No.	Model Type	Nominal Velocity fps	Measured Velocity fps	Pene-tration Inch	Max. Force kip	Max. Acc. g	Wet Unit Wt. of Soil pcf	Dry Unit Wt. of Soil pcf	Water Content %	Rise Time ms	Correction Factor for Acc. and Force
79	L	10	9.7	8.2	0.29	6.7	95.8	93.9	1.99	33.6	0.97
80	L	10	9.6	9.3	0.37	8.5	94.3	92.5	1.91	50.7	1.11
81	L	10	9.8	9.7	0.23	5.4	95.0	93.2	1.95	56.4	1.14
82	L	14	13.5	10.4	0.39	9.0	96.3	94.3	2.11	44.0	1.03
83	L	14	13.6	10.2	0.40	9.2	94.4	92.4	2.07	52.4	1.31
84	L	14	13.6	10.0	0.35	8.3	91.7	89.3	2.70	64.9	1.30
85	L	17	15.6	10.2	0.57	13.3	94.5	92.6	2.10	32.2	1.50
86	L	17	16.4	10.0	0.57	13.2	95.1	93.4	1.86	48.3	1.46
87	L	19	18.7	10.8	0.67	15.5	91.7	90.1	1.80	40.0	1.47
88	L	19	17.5	10.9	0.67	15.7	94.0	91.5	2.93	32.0	1.52
89	L	19	18.5	11.3	0.61	14.2	95.9	94.0	2.00	36.2	1.69
90	L	23	21.3	11.4	0.74	17.3	92.2	90.6	1.80	34.9	1.39
91	L	23	21.3	12.0	0.70	18.8	97.1	95.4	1.78	32.2	1.36
92	H	10	10.1	12.7	0.76	5.9	97.6	96.2	1.44	64.4	1.00
93	H	10	9.9	12.6	0.81	6.3	99.2	98.0	1.31	64.4	1.14
94	H	14	14.0	13.4	1.22	9.4	96.5	95.1	1.45	53.7	1.34
95	H	14	12.8	13.0	1.34	10.3	95.7	94.3	1.47	48.3	1.41
96	H	17	15.9	13.3	1.75	13.5	95.3	94.1	1.24	52.4	1.44
97	H	17	16.0	13.4	1.63	12.6	95.9	94.6	1.41	52.4	1.44
98	H	19	18.4	13.7	1.94	15.0	96.1	95.0	1.24	48.0	1.25
99	H	19	18.1	13.3	1.79	13.8	96.7	95.5	1.28	40.0	1.26
100	H	19	18.8	14.1	2.22	17.3	95.8	94.7	1.23	43.0	1.45
101	H	19	17.8	13.3	2.01	16.2	99.1	97.9	1.19	45.3	1.46
102	H	23	21.7	13.2	2.74	21.1	98.6	97.4	1.20	37.5	1.23
103	H	23	21.4	13.4	2.73	21.1	100.8	99.6	1.17	46.2	1.31
104	H	23	21.9	14.0	2.68	20.7	104.2	102.4	1.77	41.7	1.21

TABLE 1-E

TEST RESULTS IN DRY-DENSE COLORADO RIVER SAND

No.	Model Type	Nominal Velocity fps	Measured Velocity fps	Pene-tration Inch	Max. Force kip	Max. Acc. g	Wet Unit Wt. of Soil pcf	Dry Unit Wt. of Soil pcf	Water Content %	Rise Time ms	Correction Factor for Acc. and Force
105	L	10	10.3	5.0	0.64	15.0	104.5	103.6	0.90	27.1	1.14
106	L	10	11.0	4.9	0.68	15.7	105.9	104.9	1.03	22.9	1.24
107	L	14	12.8	5.0	0.74	17.3	104.3	102.9	1.32	20.6	1.45
108	L	14	12.4	5.2	0.67	15.8	104.9	103.6	1.32	27.4	1.32
109	L	14	13.9	5.4	0.93	21.7	105.6	104.4	1.14	21.9	1.28
110	L	14	13.5	5.2	0.80	18.6	103.4	102.5	0.84	22.4	1.14
111	L	17	17.6	5.8	1.15	26.6	100.9	99.8	1.02	18.0	1.57
112	L	17	16.1	5.4	0.91	21.1	108.0	106.8	1.10	21.9	1.13
113	L	17	16.4	5.5	0.90	20.8	106.7	105.6	0.99	21.9	1.20
114	L	19	19.0	5.9	1.05	24.4	101.3	99.1	2.22	24.7	1.28
115	L	19	18.8	5.9	1.12	26.0	105.1	103.7	1.34	20.6	1.23
116	L	23	21.9	6.7	1.24	28.8	105.3	103.8	1.57	18.5	1.20
117	L	23	21.9	6.7	1.41	32.7	104.1	102.8	1.31	19.1	1.29
118	H	10	8.8	7.1	1.04	8.0	108.2	106.7	1.37	36.1	1.00
119	H	10	9.8	7.2	1.20	9.2	109.6	108.8	1.19	45.5	1.16
120	H	14	13.4	7.2	1.68	13.0	106.6	105.0	1.49	27.6	1.42
121	H	14	13.7	7.6	1.96	15.1	106.9	105.6	1.28	33.1	1.35
122	H	17	16.5	8.4	2.09	16.2	108.4	106.9	1.41	25.0	1.31
123	H	17	16.7	7.8	2.72	21.0	109.0	107.3	1.60	25.0	1.54
124	H	19	19.1	8.9	2.52	19.5	102.3	100.3	1.95	28.0	1.17
125	H	19	18.3	8.4	2.48	19.2	106.5	103.9	2.57	25.2	1.29
126	H	19	18.7	8.4	2.25	17.3	102.5	99.6	2.88	25.2	1.00
127	H	23	21.0	10.0	3.35	25.8	111.3	110.6	0.65	21.0	1.26
128	H	23	23.2	8.9	3.52	27.2	105.3	102.6	2.56	25.0	1.31
129	H	23	22.6	9.9	3.77	29.1	104.3	102.1	2.16	22.4	1.32

TABLE 1-F

TEST RESULTS IN SATURATED-DENSE COLORADO RIVER SAND

No.	Model Type	Nominal Velocity fps	Measured Velocity fps	Pene-tration Inch	Max. Force kip	Max. Acc. g	Wet Unit Wt. of Soil pcf	Dry Unit Wt. of Soil pcf	Water Content %	Rise Time ms	Correction Factor for Acc. and Force
130	L	10	9.7	3.9	0.62	14.4	129	111	16.12	34.3	1.06
131	L	10	10.2	4.5	0.70	16.2	132	114	15.87	32.1	1.00
132	L	14	14.1	4.3	1.01	23.4	136	118	15.88	25.7	1.00
133	L	14	14.0	4.2	0.94	21.9	127	109	16.24	30.0	1.15
134	L	17	16.5	4.4	1.13	26.4	187	118	17.29	25.9	1.13
135	L	17	16.9	4.5	1.27	29.6	137	118	16.32	24.3	1.03
136	L	19	19.3	4.5	1.53	35.5	128	110	16.75	21.4	1.08
137	L	19	19.2	4.6	1.42	33.0	131	123	16.37	24.3	1.21
138	L	23	23.9				129	112	15.42	23.6	1.30
139	L	23	22.0	5.5	1.74	40.5	136	118	15.01	18.6	1.21
140	H	10	10.2	6.7	1.38	10.7	128	110	15.73	41.4	1.00
141	H	10	10.2	5.5	1.57	12.2	134	115	16.35	39.6	1.00
142	H	14	13.6	5.5	2.24	17.3	126	108	16.70	33.3	1.08
143	H	14	13.8	6.1	2.44	18.8	134	116	15.36	30.4	1.00
144	H	17	16.4	5.6	2.92	22.5	129	112	15.35	29.0	1.54
145	H	17	16.4	6.1	2.83	21.9	135	117	15.57	31.3	1.07
146	H	19	18.6	6.3	3.47	26.8	121	105	15.27	25.0	1.14
147	H	19	19.2	6.6	3.53	27.3	130	112	16.26	35.4	1.14
148	H	23	22.2	7.0	4.17	32.2	123	106	15.63	23.6	1.17
149	H	23	22.2	7.0	4.19	32.4	129	111	16.44	25.0	1.16

REFERENCES

1. Baker, Wilfred E., Westine, Peter S., Garza, Luis R., Hunter, Percy A., "Water Impact Studies of Model Appollo Command Module," Southwest Research Institute, San Antonio, Texas, Aug. 1965.

2. Barkan, D. D., Dynamics of Bases and Foundations, McGraw-Hill, New York, 1962.

3. Colp, John L., "An Experimental Investigation on the Continuous Penetration of a Blunt Body into a Simulated Cohesionless Soil," SC-RR-65-260 Sandia Corp., 1965.

4. Focken, Charles M., Dimensional Methods and Their Applications, Edward Arnold, London, 1953.

5. Ghazzaly, Osman I. and Cox, William R., "Load-Settlement Behavior of Geometric Shapes on Silty Clay," a report from Department of Civil Engineering, The University of Texas, to National Aeronautics and Space Administration, Langley Research Center, Hampton, Virginia, August 1967. (NASA CR-66483 - N67-39060)

6. Gukhman, A. A., Introduction to the Theory of Similarity, Academic Press, 1965.

7. Heller, L. W., "Failure Modes of Impact-Loaded Footings on Dense Sand," U. S. Naval Civil Engineering Laboratory Technical Report R-281, 27 Jan. 1964.

8. Jackson, J. G., Jr., and Hadala, P. F., "Dynamic Bearing Capacity of Soils," (The Application of Similitude to Small-Scale Footing Tests), Technical Report No. 3-599, U. S. Army Engineer Waterways Experiment Station, Corps of Engineers, Vicksburg, Mississippi, December 1964.

9. Jumikis, A. R., Soil Mechanics, Van Nostrand, 1962.

10. Langhaar, Henry L., Dimensional Analysis and Theory of Modeling, John Wiley and Sons, New York, 1951.

11. McCarty, John L., Beswick, Alfred G., Brooks, George W., "Application of Penetrometers to the Study of Physical Properties of Lunar and Planetary Surfaces," NASA Technical Note, NASA TN D-2413, Langley Research Center, August, 1964.

12. Murphy, Glen, Similitude in Engineering, The Ronald Press, New York, 1950.

13. Nevill, Gale E., Jr., "Modeling Studies of the Response of Weapon Foundations in Soils," Southwest Research Institute, San Antonio, Texas, June 1963.

14. Newmark, N. M., "Failure Hypothesis for Soils," Proc. ASCE Research Conference on Soil Mechanics and Foundation Engineering, Vol. 1, 1960.

15. Poor, Arthur R., Cox, William R., and Reese, Lymon C., "Behavior of a Sandy Clay Under Vertical Impact of Geometric Shapes," a report from Department of Civil Engineering, The University of Texas, to National Aeronautics and Space Administration, Langley Research Center, Hampton, Virginia, May 1965.

16. Reese, Lymon C., Dawson, Raymond F., Coyle, Harry M., Baker, William E., Ghazzaly, Osman I., and Smith, Robert E., "Investigation of the Effects of Soil Conditions on the Landing of a Manned Spacecraft," a report from Structural Mechanics Research Laboratory, The University of Texas, to National Aeronautics and Space Administration, Manned Spacecraft Center, Houston, Texas, March 1964.

17. Reichmuth, D. R., Stagg, R. P., Womack, D. P., and Cox, W. R., "A Study of Soil-Spacecraft Interaction during Impact," a report from Department of Civil Engineering, The University of Texas, to National Aeronautics and Space Administration, Manned Spacecraft Center, Houston, Texas, December 1966.

18. Sedov, L. I., Similarity and Dimensional Methods in Mechanics, Academic Press, New York and London, 1959.

19. Soper, W. G., "Wedge Penetration in a Thick Target," Behavior of Materials under Dynamic Loading, ASME, Nov. 1965.

20. Tener, Robert K., "The Application of Similitude to Protective Construction Research," Proc. of the Symposium on Soil-Structure Interaction, University of Arizona, Tucson, Arizona, September 1964.

21. Thompson, L. J., and Colp, J. L., "Preliminary Evaluation of Earth Targets for Use in Impact Effects Studies," SC-DR 316-63, Sandia Corporation, Albuquerque, New Mexico.

22. Westine, Peter S., "Replica Modeling in Soil Dynamics," Jour. of the Soil Mechanics and Foundations Div., Proc. of ASCE, November 1966, SM 6, pp. 169-187.

23. Whitman, Robert V., Healy, Kent A., "Shearing Resistance of Sands During Rapid Loadings," R62-113, Massachusetts Institute of Technology, May 1962.

24. Womack, David P., and Cox, William R., "Measurement of Dynamic Characteristics of Soils with Penetrometers," NASA Contractor Report NASA CR-849, prepared by the Department of Civil Engineering, The University of Texas, for National Aeronautics and Space Administration, August 1967.

25. Young, Donald F., and Murphy, Glenn, "Similarity Requirements for Underground Structures," Proc. of the Symposium on Soil-Structure Interaction, University of Arizona, Tucson, Arizona, September 1964.

26. Young, D. F., and Murphy, G., "Dynamic Similitude of Underground Structures," Jour. of Engineering Mechanics, Proc. of ASCE, EM, June 1964, pp. 111-133.